NATIONAL ADVISORY COMMITTEE FOR AERONAUTICS

TECHNICAL NOTE 3780

INCOMPRESSIBLE FLUTTER CHARACTERISTICS OF REPRESENTATIVE AIRCRAFT WINGS

By C. H. Wilts

California Institute of Technology

Washington
April 1957

G

NATIONAL ADVISORY COMMITTEE FOR AERONAUT

TECHNICAL NOTE 3780

INCOMPRESSIBLE FLUTTER CHARACTERISTICS OF REPRESENTATIVE AIRCRAFT WINGS

By C. H. Wilts

SUMMARY

The present report gives the results of a detailed study of the flutter characteristics of four representative aircraft wings. This study was made using the electric analog computer at the California Institute of Technology. During the course of this investigation eight important parameters of each wing were varied and, in addition, the effects of mass, inertia, pitching spring, and location of a concentrated mass were investigated for all four wings and several sweepback angles.

The introduction of this report discusses in general terms the flutter characteristics of airplanes. The second section contains a discussion of the electric-analog principles that made a study of this magnitude feasible. The third section contains a discussion of the aerodynamic and structural approximations made for simplifying the flutter analysis of a wing. The fourth section gives information relating to the errors introduced by the finite-difference approximations to continuous aeroelastic systems. In addition, data are given pertaining to the flutter characteristics of a swept-wing wind-tunnel model and the results of computations based on two assumptions regarding aerodynamic forces on a swept wing. The fifth section lists all pertinent data relating to the four representative aircraft wings and the sixth section contains the computed flutter characteristics of the four wings.

INTRODUCTION

Flutter is a phenomenon which is observed in the transient or unforced response of an aerodynamic system. Mathematically speaking, it is observed in the solution of the homogeneous differential equation describing the behavior of an airplane in flight through still nonturbulent air. An airplane wing which is considered to be a continuous beamlike or platelike structure has an infinite number of degrees of freedom, and the characteristic equation which describes the transient response has an infinite number of roots. Experience has shown that only the roots of lower magnitude (frequency) exhibit the problem of instability or flutter.

It is this fact which makes it possible to predict flutter using an analog computer which represents only the lower frequency modes of the structure or using a few normal modes in either digital or analog computation.

The exponents in the transient response of a linear system are the roots of the characteristic equation. Since the characteristic equation involves real parameters, the roots are real or occur as complex conjugate pairs. The latter roots are the ones of interest here. The real part of a conjugate pair is the reciprocal of the time constant in the transient response and the (positive) imaginary part is the frequency of oscillation. This is illustrated in figure 1. Mathematical description of the transient term is

$$y = A_1 e^{(\sigma+i\omega)t} + A_2 e^{(\sigma-i\omega)t}$$

or in terms of real functions

$$y = Ae^{\sigma t}\cos(\omega t + \phi)$$

If the real part of the pair of roots σ is negative the "transient" dies out and the root is said to be stable. If the real part is positive the transient grows exponentially until limited by nonlinearities or destruction, and the root is said to flutter. The terminology is not strictly correct, but it is common practice to refer to the exponents of the transient response as flutter roots, since they are numerically equal to the roots of the characteristic equation. Throughout this report such terminology will be used.

Damping of flutter roots may be measured by two dimensionless numbers ζ and g, which differ from each other by a factor of 2. The former is generally used by control-system engineers; the latter, by flutter analysts. They can be defined by the equation for the particular term in the transient response given earlier

$$y = Ae^{\sigma t}\cos(\omega t + \phi) = Ae^{-\zeta\omega_n t}\cos\left[\sqrt{\left(1 - \zeta^2\right)}\,\omega_n t + \phi\right]$$

$$= Ae^{-\frac{g\omega_n t}{2}}\cos\left\{\sqrt{\left[1 - \left(g^2/4\right)\right]}\,\omega_n t + \phi\right\}$$

Flutter computations are usually centered around regions where the value of g lies in the range $-0.2 < g < 0.2$. In such cases the factor $\sqrt{1 - \zeta^2}$ differs from unity by less than 0.5 percent. For this reason it is customary to omit this factor in the trigonometric term giving the following approximation:

$$y = Ae^{-\frac{g\omega_n t}{2}} \cos(\omega_n t + \phi)$$

This practice will be followed in this report. For damping which is small, an approximate rule of thumb is that the damping factor g is nearly equal to the per unit decrement per cycle divided by π. If percent decrement per cycle δ is used, there results the convenient approximation

$$g \approx \frac{\delta}{100\pi}$$

The flutter roots of an airplane are complex functions of all geometrical, structural, and inertial properties of the airframe as well as of the airspeed and air density. With all other properties held constant, the lowest airspeed at which the flutter root exhibits neutral stability is called the flutter speed. If g is plotted as a function of velocity, the abscissa (speed) at which the curve first crosses the axis $g = 0$ is the flutter speed. In this study such curves were used to determine the flutter speed, but such curves are used in this report only to illustrate the behavior of some unusual flutter roots. A tabulation of flutter speeds does not always give a good picture of the flutter characteristics. An example is shown in figure 2, where the damping of two roots is shown. One root becomes unstable at a speed of about 300 miles per hour and the other, at a speed of about 600 miles per hour. If a parameter variation increases the damping g of both roots by 0.03, one flutter speed is raised to 350 miles per hour, a 17-percent increase, and the other is raised to 603 miles per hour, a 0.5-percent increase. A further increase in g of 0.02 will raise the second flutter speed 0.4 percent, to 605 miles per hour, while the first root will now exhibit no flutter. It should be emphasized that even though a design speed of, say, 500 miles per hour has been surpassed, the system may still be regarded as unsatisfactory. A system so close to flutter at a speed of 360 miles per hour might actually flutter because of weight (fuel) variations or minor differences in stiffness resulting from variations within the manufacturing tolerances. From the standpoint of this report, all three of the sets of roots discussed above will be regarded as having essentially the same "flutter characteristics," even though they exhibit radically different theoretical flutter speeds. Emphasis is given to this point because remarks to be made later in this report may be misunderstood without a clear conception of this viewpoint.

This investigation was conducted at the California Institute of Technology under the sponsorship and with the financial assistance of the National Advisory Committee for Aeronautics.

SYMBOLS

A, A_1, A_2	constants
b	half chord
b_r	half chord at root
b_x	half chord at tip
$C\left(\frac{bp}{V_n}\right)$	symbolic representation of circulatory component of lift force due to angle of attack
C_{L_α}	lift coefficient
d	wing station from root, in.
E	Young's modulus of elasticity
EI	equivalent beam flexural rigidity, (lb)(sq in.)
e	experimental; used as a subscript
f_f	flutter frequency, cps
f_n	normal mode frequency of cantilevered engine and nacelle, cps
f_∞	flutter frequency for continuous structure
G	shear modulus
GJ	equivalent beam torsional rigidity, (lb)(sq in.)
g	damping factor of a damped sinusoid, $e^{-\frac{gn_n t}{2}} \cos \omega t$
h	vertical deflection, positive down, in.
I	moment of inertia per unit length, $lb\text{-}sec^2$
J	torsional stiffness
j	increase in stiffness, percent
k	radius of gyration, in.
l	semispan of wing

M, M_1, M_2 twisting moment about elastic axis per unit length of wing, positive nose up, lb

m mass per unit length, lb-sec^2/sq in.

m_c mass of concentrated mass

m_f fuselage mass

m_w total wing mass, lb-sec^2/in.

m_{wf} total wing mass outside of fuselage

$\bar{m}$ lumped mass

P, P_1, P_2 lift force per unit length of wing, positive nose down, lb/in.

p Laplace transformation variable

q_n dynamic pressure based on normal component of velocity, $(1/2)\rho v_n^2$, lb/sq in.

t time, sec

v airstream velocity, in./sec

v_b flutter velocity of airplane with bare wing

v_f airstream velocity at which flutter occurs, in./sec

v_n component of airstream velocity perpendicular to elastic axis, $v \cos \Lambda$, in./sec

v_o reference velocity, in./sec

v_∞ flutter velocity for continuous wing

w distance measured along wing

x_o distance from midchord aft to elastic axis, in.

x_1 distance from quarter chord aft to elastic axis, $x_o + (b/2)$, in.

x_2 distance from three-fourths chord forward to elastic axis, $b - x_1$, in.

x_3 distance from elastic axis aft to center of mass, in.

y general variable

Δy cell size for finite-difference structure

α absolute pitch angle about elastic axis, positive nose up, radians

δ percent decrement per cycle

ζ per unit critical damping

θ slope of elastic axis or roll about horizontal axis normal to elastic axis, positive tip down, radians

Λ sweepback angle of elastic axis, deg

ρ air density, lb-sec^2/in.^{4}

τ wing twisting gradient, $\partial\alpha/\partial w$

σ real part of pair of roots

ω angular frequency, radians/sec

ω_n undamped natural frequency, radians/sec

ELECTRIC-ANALOG METHODS OF FLUTTER ANALYSIS

The use of electrical analogs for the solution of aeroelastic problems has been discussed in detail in reference 1. The purpose of the present section is to summarize the principles briefly. For purposes of flutter analysis, the structural system is assumed to be linear, and a linear electrical network is constructed whose electrical behavior approximates the dynamic behavior of the linearized structure. For this purpose, capacitors are ordinarily used to represent concentrated or lumped inertia properties, inductors are used to represent lumped flexibility properties, and transformers are used to represent the geometrical properties of the structure (refs. 1 and 2). In such electrical analogs, voltages throughout the network represent velocities in the structure and currents represent forces. Electronic equipment is used to produce currents which depend on voltages in the electrical system in the same manner in which aerodynamic forces depend upon the velocities of the airfoil.

The composite electrical structure can be regarded as an electrical model of the aircraft in the same manner that a wind-tunnel model would be regarded as a structural model. The advantage of this approach lies in the relative ease with which one can alter the properties of the model, thus performing flutter "computations" with great rapidity. It should be emphasized that the normal modes of the structure are not used as tools or elements in the analysis. The analysis consists, in fact, in observing the behavior of an electrical model of an aircraft in flight.

That behavior which is most readily observed is the transient response to a sudden disturbance. This method is therefore similar to the testing technique which is ordinarily used for wind-tunnel models. An advantage of the electrical method is that tuned pulses may be used, so that separation of two or more nearly unstable or slightly unstable modes of oscillation is more readily accomplished. Basic recorded data consist of the logarithmic decrement of the response and the frequency of oscillation. Flutter speed and frequency for any configuration are ordinarily found by computing the damping g and frequency f for specific values of velocity and interpolating to find the frequency and speed at which g is zero.

APPROXIMATIONS FOR SIMPLIFYING FLUTTER ANALYSIS

Structural Representation

For dynamic analysis of airplane wings of large aspect ratio, it is customary to treat the wing as a beamlike structure in both vertical bending and torsion. It is usually assumed for simplicity that an elastic axis exists. For an unswept wing, this is a straight line which undergoes no vertical displacement when the wing is subjected to a pure torque parallel to this axis and along which no twisting gradient exists when vertical loads are applied anywhere along this line. For an unswept wing of conventional construction, this simplification is usually quite accurate. For a swept wing an elastic axis may be defined as a straight line which assumes a constant slope over its entire length when a twisting moment is applied parallel to this line and which has no twisting gradient when vertical loads are applied anywhere along this line. For aspect ratios greater than 5 or 6 and for conventional wing construction, a line can be found on the structure which satisfies this definition reasonably well except near the root. It is not uncommon to find an equivalent elastic axis at about the 35 or 40 percent chord, a line located aft of the leading edge a distance equal to 35 or 40 percent of the local chord.

The assumption of an elastic axis involves the tacit assumption that chordwise bending of the wing is negligible. It follows, then, that the motion of the wing at any spanwise coordinate can be described by two coordinates, the vertical displacement of some point on the chord, and the

angle of twist of the chord. If wing motion is described in terms of vertical motion of the elastic axis and twisting motion about this line, then these motions are not coupled through the action of elastic forces in the wing except in the root region for a swept wing.

The root region of a swept wing is necessarily a relatively complicated structure. However, for aeroelastic problems an equivalent simple structure can be found which is completely satisfactory for wings of large aspect ratio. This can be demonstrated by the following reasoning. The outer sections of a wing exhibit definite beamlike properties, but in the region of the root considerable warping of the wing surface must take place. The aerodynamic forces near the root of the wing are therefore not adequately described by strip theory. In addition, the inertia effects of this section are not readily computed. However, the effects of the aerodynamic forces on the root section are insignificant for ordinary flutter computations. This has been demonstrated many times with the analog computer by removing the aerodynamic forces on the inboard cell of the finite-difference structure. The inertia forces are also insignificant compared with the elastic forces transmitted by the root section, and it is therefore possible to replace this section for purposes of analysis by a set of "influence coefficients" relating transmitted forces to relative displacement of an outer section of the wing relative to the fuselage. It has been found that in some cases these influence coefficients resemble coefficients for a simple beam extending straight into the fuselage and attaching there in some simple way. The wing structural axis then consists of a short section which may be perpendicular to the fuselage center line and which is simply attached to a swept-back elastic axis which extends to the wing tip.

Methods for determining the equivalent structure are outside the scope of this report. Since this structure varies greatly with the particular wing construction used, it was necessary to choose a simple though typical root structure for this study. That chosen is illustrated in figure 3 where the elastic axes are shown by dotted lines. The break in the elastic axis is assumed to be at the edge of the fuselage, and the axis inside the fuselage is assumed to be straight and perpendicular to the airplane center line. The wing is assumed to be pinned at the side of the fuselage. Consequently, all twisting moment is removed at this point and it is not necessary to make any assumptions regarding twisting rigidity inside the fuselage. Bending rigidity inside the fuselage is, however, important for symmetric motion. During the past 6 years, extensive flutter computations have been made with the electric-analog computer for commercial and military aircraft as well as for wind-tunnel models including those described in references 3 and 4. In all cases investigated, it has been found that relatively large variations in root conditions have a negligible effect on the flutter characteristics (in the sense described in the Introduction). Observed changes in damping were usually in the range $0 < |\Delta g| < 0.05$, which has very small effect on

flutter speed unless the curve of g against velocity is very flat, near zero values of g. Needless to say, both symmetric and antisymmetric motion of the airplane must be permitted since the flutter characteristics for the two types of motion may be quite different.

Fuselage stiffness and inertia properties usually have such values that an assumption of a rigid fuselage for symmetric motion alters the flutter characteristics little. For fighter planes, the error introduced is negligible. For large bombers, the change in flutter speed may be appreciable, but it does not alter the trends to be observed upon variation of wing properties. It has therefore been assumed in this study that the airplane fuselage is rigid. Tail-surface flexibility does not significantly affect wing flutter problems. A rigid tail surface with sufficient area to provide satisfactory static stability has therefore been assumed.

Aerodynamic Forces

For all the flutter computations given in this report, the aerodynamic forces have been simplified by two important assumptions:

(1) The air flow is incompressible.

(2) If the airfoil is divided into strips perpendicular to the elastic axis, then the forces on each strip can be computed as a function of the normal component of the airstream velocity and the motion of that strip independently of the motion of adjacent strips.

The first assumption is not required by analog methods in general, but its use greatly increases the rapidity with which data can be obtained. Since the purpose of the study is not to obtain specific accurate flutter speeds but to study trends in flutter characteristics, this assumption does not seem unreasonable. With regard to the use of strip theory, two assumptions are often found in the literature. In using the "airstream method" the wing is divided into strips parallel to the airstream, and the forces and moments on each strip are computed as though the wing were not swept and the air flow about the section were a two-dimensional incompressible flow. The aerodynamic coefficients may be taken to be the same as those for an unswept wing or may be modified by a factor $\cos \Lambda$. In applying the "normal-component method," the wing is divided into strips perpendicular to the elastic axis. The aerodynamic forces and moments are computed as though the effective air velocity were the normal component $v \cos \Lambda$, and the forces depend only on the motion of the individual strip and not upon the motion of adjacent strips (except that some small terms may be included which are proportional to the twisting gradient and therefore dependent upon the motion of the nearest strips). A critical discussion of the two alternatives is given in reference 5. This reference recommends use of the normal-component method.

Before adopting the second assumption, an effort was made to find some correlation with experimental results. Reference 3 contains experimental flutter speeds for a wind-tunnel model wing with sweepback angle equal to about 35°. This angle is sufficient to give an appreciable difference in results obtained with the various assumptions mentioned above. The section entitled "Finite-Difference Errors" in the present report contains the results of computations which show that the normal-component method gives results which are as satisfactory as those given by any other method used.

Equations for determining the aerodynamic forces by this method are given in reference 5. In the equations given there, several terms are found whose theoretical justification is not well established. These terms (grouped in special brackets on p. 16 of ref. 5) were found to have negligible effect on sample flutter computations. It seems reasonable, therefore, to omit these terms from computations involved in the present trend study. With these omissions and with obvious changes to conform to the symbols and notation used in the present report, the equations are:

$$P = P_1 + P_2 + P_3$$

$$M_\alpha = M_1 + M_2 + M_3 + M_4$$

$$P_1 = -2\pi(q_n)(2b)C\left(\frac{bp}{v_n}\right)\left[\frac{\dot{h}}{v_n} + (\alpha + \theta \tan\Lambda) + \frac{x_2}{v_n}(\dot{\alpha} + \dot{\theta}\tan\Lambda)\right]$$

$$P_2 = -2\pi(q_n)\left(\frac{b^2}{v_n}\right)(\dot{\alpha})$$

$$P_3 = -\pi\rho b^2(\ddot{h} - x_o\ddot{\alpha})$$

$$P_4 = -2\pi(q_n)(2b)\left[C\left(\frac{bp}{v_n}\right)\left(-\frac{x_2}{v_n}\dot{\theta} + x_2\tau\right) + \frac{b}{v_n}(\dot{\theta} - x_o\dot{\tau})\right]\tan\Lambda$$

$$M_1 = -x_1P_1$$

$$M_2 = -x_1P_2$$

$$M_3 = -2\pi(q_n)\left(\frac{b^3}{v_n}\right)(\dot{\alpha})$$

$$M_4 = -\pi\rho b^2\left[\left(\frac{b^2}{8} + x_o^2\right)\ddot{\alpha} - x_o\ddot{h}\right]$$

$$M_5 = 2\pi(q_n)(b^2)\left[2\left(\frac{x_1}{b}\right)C\left(\frac{bp}{v_n}\right)\left(-\frac{x_2}{v_n}\dot{\theta} + x_2\tau\right) + \frac{b}{2}\tau + \frac{x_o}{v_n}\dot{\theta} - \left(\frac{b^2}{8} + x_o^2\right)\frac{\dot{\tau}}{v_n}\right]\tan\Lambda$$

The terms are grouped in the order shown for convenience in establishing analog circuits. The last term in P_1 is not found in the corresponding equation of reference 5. This term is removed (mathematically) by insertion of an equal but opposite term in P_4 and a similar term in M_5. It is added to P_1 here because the circuits which generate the term $\alpha + \theta \tan\Lambda$ also provide the term $(x_2/v_n)(\dot{\alpha} + \dot{\theta}\tan\Lambda)$, the last part of which is not found in reference 5. As is pointed out below, this term has a negligible effect so that its inclusion is of no importance, but it is indicated in the expression for P_1 for the sake of completeness. It should be emphasized that the dynamic pressure q_n is based on v_n, where v_n is the velocity component normal to the elastic axis. The coordinates α and θ are both measured in elastic-axis coordinates. The symbolism $C(bp/v_n)$ is used to represent the Theodorsen or Wagner function. A short discussion of the interpretation of this symbolic representation can be found in reference 6.

All terms found above can be represented by simple analog circuits with the exception of P_4 and M_5. Examination of equations 6 and 7 of reference 5 shows that each term in P_4 and M_5 is similar to (if not equal to) a term found in the special brackets. Since the latter terms have been omitted, there seems to be no logical reason for retaining P_4 and M_5. Inasmuch as their inclusion greatly complicates the analog circuits, these terms were also omitted.

In addition to the finite-difference approximations and those contained in the assumptions of incompressible flow and strip theory, three other aerodynamic approximations should be mentioned. The first of these is the failure to modify aerodynamic forces at the wing tip. The delay in the growth of lift forces as described by the Wagner or Theodorsen functions for two-dimensional flow cannot apply near the tip. Indeed, both the delay in lift and the magnitude of the lift must go to zero at the tip. The extent of the error introduced depends upon the importance of tip forces in flutter computations. Insofar as their location is concerned, these forces are quite important, but, because of wing taper, the magnitude of the total force per unit length diminishes near the tip. Since wings of considerable taper are involved in this investigation, it is to be expected that the error will be relatively small. The second approximation is failure to compute aerodynamic forces properly at the root of a swept wing. As stated earlier, the error introduced by this

approximation is negligible, since the aerodynamic force for a large section of the wing root can be omitted entirely without an appreciable change in flutter speed. The third approximation is introduced by the necessity of computing the Wagner function (or the Theodorsen function) electrically. This function is computed using networks shown in reference 1 with an error no greater than 2 percent over the frequency range or time interval of interest.

FINITE-DIFFERENCE ERRORS

Finite-Difference Structures

No practical methods have been devised for representing general continuous structures with continuous electrical systems. The electric-analog computer utilizes lumped electrical elements which can, in principle, be used only to construct analogs for lumped mechanical systems. However, as pointed out in references 1 and 2, it is possible to represent the dynamic characteristics of beamlike structures by a lumped structure based upon finite-difference approximations to partial differential equations. It is convenient to call this lumped system a finite-difference structure, whether it is a mechanical model or an electrical analog. These references outline the process by which inertia and stiffness properties and aerodynamic forces are averaged or replaced by single concentrated inertias, springs, or forces in the finite-difference structure.

It should be remarked, at this point, that the assumption of a finite-difference structure insures a finite number of flutter roots or exponential functions in the transient response, whereas the continuous structure has, in principle, an infinite number. Since the higher frequency roots have high damping, it is only the lower frequency roots that are of interest. Two or three of these may, however, show essentially zero damping simultaneously at a given velocity, and it is sometimes necessary to determine the characteristics of several flutter roots. There is obviously a lower limit to the number of cells that must be used to obtain satisfactory accuracy, since each cell adds roughly two roots to the system.

There is little information in the literature which pertains to the accuracy with which such structures represent the continuous system. Reference 7 gives data for static-deflection and normal-mode characteristics of certain finite-difference structures but no information about accuracy of flutter computations. It is the purpose of this section to summarize work at the Analysis Laboratory of the California Institute of Technology which was carried out to determine finite-difference errors in flutter computations for several specific structures.

Using equations for aerodynamic forces based on two-dimensional strip theory and linear incompressible fluid flow, several "exact solutions" have been obtained for flutter problems. Some of these are found in references 8 and 9. These solutions are exact in the sense that no further physical or mathematical simplifications are involved and the only errors are introduced by round-off errors in evaluating transcendental functions and infinite series. Solution of these same problems by use of finite-difference approximations to partial differential equations provides the most practical way of estimating finite-difference errors for other configurations for which exact solutions are not obtainable. It is true that, in all cases mentioned above, the airfoil has been assumed to have uniform spanwise properties and that in most practical cases the airfoil has a significant taper. On the other hand, reference 7 contains a study of the finite-difference errors in the deflection characteristics and normal-mode properties of both uniform and tapered beams. This study showed no unusual differences in these properties, and so it is assumed that the results obtained for flutter of uniform airfoils are typical of results that would be obtained for flutter of tapered airfoils.

Although much of the work reported in this section was not done in the present investigation, it is included here since most of it does not appear in any readily available publication.

Uniform Airfoil With Pinned Ends

A uniform beam with pinned ends will support only sinusoidal modes in both bending and torsion. Flutter modes are also of sinusoidal shape and it is therefore possible to reduce the flutter problem to an eigenvalue problem which can be solved with a high degree of numerical accuracy. The finite-difference analogs for a pinned-pinned beam likewise will support only sinusoidal modes. It is possible therefore to get exact solutions for the finite-difference approximations to the continuous airfoil.

The airfoil chosen for this analysis is described in table I. For the continuous wing, the flutter speed and frequency were found to be $v_f = 692$ miles per hour and $f_f = 12.72$ cycles per second, respectively. Analysis of the finite-difference structure was carried out using eight-, four-, and two-cell divisions between the pinned ends. Results are given in table II and figure 4. For this particular case it is necessary to use more than four cells if flutter speed is to be obtained with error less than 2 percent. By use of symmetry conditions at the center of the beam, it is necessary to use only half this number of cells with an electric analog computer. Thus, use of two analog cells gives a theoretical error of about 2.2 percent, and four analog cells would give an error of only 0.6 percent.

Uniform Cantilever Wing With Concentrated Mass

Analytical determination of the flutter speed of a cantilever wing is much more difficult than that for a beam with pinned ends. However, other investigators have obtained accurate numerical solutions for a few configurations. The most important of these is described in reference 9. This case is of importance for two reasons: It involves several spanwise positions of a large eccentric concentrated mass which has a great effect upon the flutter speed; and, for some positions, at least two completely different flutter roots can be found.

Table III presents the physical characteristics of the airfoil analyzed in reference 9. In this reference, the flutter speed and flutter frequency were computed for seven mass locations, data for which are reproduced in table IV. Since the location of a concentrated mass may be important in flutter analysis, and since all points on a finite-difference beam are not equally suitable as an attachment point for a concentrated mass, it was believed that a comparison of the above data with finite-difference solutions was quite important. Unfortunately, similar accurate solutions for a finite-difference structure are not readily obtained, so it was necessary to use the electric-analog computer to obtain these solutions. The resulting comparison therefore contains both finite-difference and analog-computer errors. Previous work has indicated that the latter are probably not greater than 1 percent if the Theodorsen function is represented accurately.

In this analysis, two slightly different beam analogs were used. In both, the beamlike properties were represented by a system of levers (transformers), but in one group the lumped forces were applied at the junctions of the levers and in the second group the forces were applied at the midpoints of the levers. The analog of the second group was once thought to give a better approximation since it resembles the Russell beam analog discussed in reference 7. Recent investigation has shown that this belief is without foundation, and the second analog is now preferred only as a matter of convenience for sweptback wings since it provides the wing slope directly at the force stations where it is needed for computation of aerodynamic forces. In both cases the cantilever condition at the root was provided by a half cell at the root, and the forces nearest the tip were applied one half cell from the tip. Thus the first group involved an integral number of cells, and the second group involved a half integral (integer plus one-half) number of cells. Five cases were investigated; 2, $2\frac{1}{2}$, 4, $5\frac{1}{2}$, and 6 cells. Since it was shown in the previous section that less than 4 cells was of no interest for present purposes, only the results of 4, $5\frac{1}{2}$, and 6 cells are presented in this report.

In view of the simplicity of the flutter curves shown in reference 9, it was expected that data would be taken at only a few spanwise mass locations. However, it was soon found that the flutter characteristics were much more complicated than anticipated, and data were taken at 24 mass locations in the 6-cell case. The flutter characteristics of the wing with variable location of the concentrated mass are sketched in figure 5(a). As the concentrated mass is moved outward from the root, the flutter speed drops slightly. At a distance about 16 percent of the total span from the root a minimum is reached, and beyond the 25-percent position the flutter speed rises very rapidly. At the 30-percent position the flutter speed for this root has become equal to the flutter speed of a completely different root. The flutter speed for this second root drops with increasing spanwise position of the mass making it impossible to determine with the analog computer the speed for the original root beyond the 30-percent position. The flutter speed for the second root reaches a minimum with the mass at the 45-percent position, then rises to a very high value as the mass is moved toward the 75-percent position. A flutter root which is probably the second is observed for mass positions near the tip, the lowest flutter speed occurring with mass at the tip. It was also observed that divergence of the wing occurred whenever the flutter speed exceeded about 5,000 inches per second. Because of divergence, it was not possible to measure with accuracy flutter speeds which exceeded divergence speed by more than about 50 percent. As a result, flutter speeds with mass near the 75-percent span could not be measured.

The flutter characteristics for the 4-, $5\frac{1}{2}$ -, and 6-cell structures are shown in table V and figure 5(b). Data for the seven positions analyzed in reference 9 are also plotted in the figure. Inspection of these curves shows that many more accurate numerical solutions are required to determine the finite-difference errors for all mass positions. In spite of the inadequate numerical data, an attempt was made to draw a smooth curve through the known points taken from reference 9. In doing this the $5\frac{1}{2}$- and 6-cell analog data were used as a guide in determining the shape of the curve. This curve, shown in figure 5(a), has already been discussed. It is realized that a significant error of as much as 2 or 3 percent may exist in this curve for some mass positions, but there was no other method for obtaining estimated errors for the finite-difference structures. With the understanding that the comparison data may be in error in some regions, figure 6 was prepared showing the percentage error in flutter speed for the various analogs as functions of the mass location. For $5\frac{1}{2}$- and 6-cell structures the average errors are about 2 percent. It can be readily seen that, although a 4-cell analog gives very satisfactory results for the bare wing (mass position 0), it is necessary to use more than 4 cells if errors less than 5 percent are required at other mass locations. A further discussion of this investigation will be found in reference 10.

As a result of this analysis, it was decided that all flutter computations made in this trend study would be made using $6\frac{1}{2}$ cells to represent one-half of the airplane wing.

Experimental Correlation

Wind-tunnel tests have been made of many model structures. It is difficult, however, to find unclassified data in which the structure is completely and accurately described. In the course of this investigation, two cases were found in which a correlation between experimental and computed characteristics could be attempted. The first of these is the uniform unswept cantilever wing discussed in the preceding section. The flutter speed and frequency observed in a wind tunnel are reported in reference 9 and a companion report, reference 11. These data are summarized in table IV, which also contains the computed values of reference 9. A better understanding of the correlation is obtained if the experimental data are plotted with the assumed analytic solution. Figure 5(a) shows such a comparison. The correlation for this case seems unusually good.

Flutter Speed of a Swept-Wing Model

Reference 3 gives results of wind-tunnel tests to determine the flutter speed of a model wing with sweepback angle equal to 34.5°. This wing had two concentrated masses attached at approximately the 30- and 80-percent span positions. In an effort to compare the airstream and normal-component aerodynamics for flutter computations, an electrical analog was constructed for this wing. For any sweepback angle, it is to be expected that the two methods will give flutter speeds differing by a factor of approximately $(\cos \Lambda)^{1/2}$, unless the aerodynamic coefficients are modified by the factor $\cos \Lambda$ in the airstream method, in which case the two methods should give similar results. The principal difficulty encountered was determination of the properties of the concentrated masses on the wing, since reference 3 does not give complete information about these masses and their geometrical location. The best data that could be deduced from this report are given in table VI. Since the masses are alined with the airstream but are represented in elastic-axis coordinates, a product of inertia between roll and pitch exists. Since no such information was available, the product of inertia was omitted from computations, and the rolling inertia about a chord line was assumed to be one-half as large as the pitching inertia about the elastic axis. It is believed that these approximations and simplifications will affect the results by less than 1 percent.

A comparison of observed and computed characteristics is given in table VII. The first three normal-mode frequencies show satisfactory

agreement, with differences of 1, 5, and 3 percent, respectively. The flutter speed computed with either representation of aerodynamic forces is lower than the wind-tunnel value. In the case of the airstream method, the discrepancy is 19 percent, or, if the aerodynamic coefficients are modified, 11 percent. Using the normal-component method, the discrepancy is 12 percent. Flutter frequency is in error about 20 percent in all cases. Although the observed differences are relatively large in all cases, it is concluded that the normal-component method recommended in reference 5 is satisfactory for this model.

CHARACTERISTICS OF FOUR REPRESENTATIVE AIRCRAFT

Plan forms and stiffness and inertia data were chosen after surveying the various fighter, bomber, and transport planes developed in recent years. Four representative airplanes were chosen, two fighters and two large bombers. Smaller attack bombers and transports were not included because of lack of time. The airplanes chosen are not similar in all respects to any particular set of four airplanes, but they do have stiffness and inertia properties which resemble four specific aircraft. Plan form, sweepback angle, elastic-axis location, and concentrated-mass locations were, however, chosen more arbitrarily so that this report could remain unclassified. The four basic plan forms are shown in figure 3. The basic fighter A has a bare unswept wing with span of about 500 inches, taper ratio of 2.0, and aspect ratio 6. The basic fighter B has a wing sweepback angle of 30°, a span of about 400 inches, and a taper ratio of 2.0. The two basic wings have the same length measured along the elastic axis and the same chords measured perpendicular to the elastic axis.

The basic bomber A has an unswept wing with span of about 1,700 inches, taper ratio of 2.5, and aspect ratio 12. It has a concentrated mass representing an engine nacelle at the 0.46-span position with center of mass about one-half chord forward of the elastic axis. The basic bomber B has a wing sweepback angle of 30°, a span of about 1,500 inches, and a taper ratio of 2.4. It also has a concentrated mass representing an engine nacelle at the same relative position as for bomber A. The two basic wings have the same length measured along the elastic axis and approximately equal chords when measured parallel to the airstream.

Mass per unit length, pitch inertia per unit length, bending rigidity, and torsional rigidity were drawn as smooth curves approximating the characteristics of some typical modern aircraft. As described in reference 2, these data must be collected or lumped over distances corresponding to the cell length of the analog finite-difference structure. The assumed curves and the lumped values are shown in figure 7. The lumped values

are also listed in tables VIII to XI, which give all pertinent characteristics of the basic airplanes.

Eight important parameters of the basic airplane wings were varied in an effort to find similar features in the flutter characteristics of the various wings. The quantities varied and the extent of their variation is summarized as follows:

Quantity varied	Minimum value	Maximum value
Wing mass density, per unit basic	0.5	2.0
Wing pitch inertia, per unit basic . . .	0.5	2.0
Bending rigidity, per unit basic	0.67	1.5
Torsional rigidity, per unit basic	0.67	1.5
Center-of-mass location, percent chord . .	25	60
Elastic-axis location, percent chord . . .	30	50
Chord, per unit basic	0.67	1.5
Sweepback angle, deg	0	45

With the exception of sweepback angle, these quantities were varied one at a time from their basic value. However, for all four basic airplanes, some or all of the parameters were varied for two or three values of sweepback angle. It is realized that the above variations do not constitute a comprehensive survey. However, to a considerable extent the changes in flutter speed due to several variations are additive if the variations are small and are made simultaneously. Another limitation is that the flutter characteristics are affected by the spanwise variation in the first seven quantities listed. The two fighters and two bombers constitute four changes in the spanwise variation of these quantities but unfortunately are cases in which four or five of them are varied simultaneously. Other quantities which were thought to have second-order effects were not considered. Among these are altitude (represented by ratio of air density to wing mass), fuselage mass and pitching inertia, and tail configuration. This does not imply that flutter velocity is independent of altitude, but with very minor variations the flutter velocity varies inversely as the square root of the air density. Sea-level air density was used throughout this study.

It is improbable that bombers of the plan form and size studied will be flown without engines on the wing. Consequently, the basic cases of interest are those in which a concentrated mass is located there. On the other hand, it is of some interest to compare the characteristics of the bare wing as well as those of a wing with concentrated mass. Both bombers A and B were studied with bare wing as well as with concentrated mass in the basic position on the wing.

For purpose of reference, it is necessary to assign a number to designate each particular case. The group discussed above comprises

175 cases. The assignment of case numbers is shown in table XII. This table shows most rapidly the various cases that were studied.

Concentrated masses on fighter wings usually consist of fuel tanks, bombs, or similar stores. It is impossible, therefore, to select a single value for mass and inertia which can be regarded as typical. For certain positions, many values for mass and inertia were chosen, although in most cases the number of values was restricted by the time available for computations. For reference purposes, the basic mass for fighter planes was arbitrarily chosen to be one-quarter of the mass of the entire wing (half of the mass of one side), the pitching radius of gyration was set equal to 30 inches, and the roll radius of gyration was assumed to be 15 inches or less. Specific data for the two fighters are listed in table XIII.

Concentrated masses for bomber airplanes are usually engine nacelles, with a mass which can be predicted within a factor of 2. Nevertheless, it is of some interest to study the effect of various mass values in these cases also. Basic mass value for both bombers was assumed to be 15 pound-seconds squared per inch, which corresponds to a weight of nearly 6,000 pounds. Pitching radius of gyration was assumed to be 35 inches. Basic mass position was assumed to be at the 0.46-span position and 60 inches in front of the elastic axis. These data are also tabulated in table XIII.

The concentrated-mass characteristics varied in this study are:

(1) Mass
(2) Pitching inertia about center of mass
(3) Spanwise location
(4) Chordwise location
(5) Pitching flexibility

The assignment of case numbers is more difficult for this phase of the study. Although specific spanwise positions were chosen, it was not possible to choose chordwise positions beforehand. The chordwise positions were chosen as the data were obtained. In some cases more than 20 positions were used for a given spanwise location. Consequently, one case number was assigned to all chordwise variations at a given spanwise location. A summary of all variations with the corresponding case numbers is given in table XIV.

Pitching flexibility of the concentrated mass was varied in six cases involving both bombers. In all cases, the chordwise location of the center of mass was basic (table XIII). In three cases the mass was in basic spanwise position and in three cases the mass was at the tip. Case numbers are given in table XIV.

TRENDS IN FLUTTER CHARACTERISTICS

Reference Quantities and Graphical Presentation

Results of the study of trends in flutter characteristics which are listed in table XV are given in miles per hour and in per unit values of a reference speed. The reference velocity chosen is

$$v_o = 10^4 \text{in./sec} = 568 \text{ mph}$$

Obviously a flutter speed of 1.5 would not represent a realistic value since this would correspond to supersonic speed with a Mach number of about 1.1. However, such a number still has useful significance for two reasons: (1) A major purpose of this study is to establish trends and to determine what configurations tend to be more or less stable than others, and (2) a change in stiffness is equivalent to a change in velocity, so that a structure with one-half the stiffness of another, but otherwise unchanged, would exhibit a flutter speed $1/\sqrt{2}$ times as great as that of the other, a value equal to 1.06 or 600 miles per hour in the case given above.

All geometrical, structural, and inertia quantities are given in per unit values. For example, distances are measured in units of the airplane semispan and masses, in terms of a basic value. For conversion to specific mechanical units, the reference quantities will be found in figure 3, which shows the plan forms, figure 7, which gives inertia per unit length and rigidity data for the wings, and tables VIII to XI, which list all pertinent characteristics of the four basic airplanes. The density of air at sea level was used throughout these computations. The value chosen is:

$$\rho = 1.146(10^{-7}) \text{ lb-sec}^2 \text{ in.}^{-4}$$

In presenting results graphically, flutter speeds have, in general, been reduced to dimensionless values by using as the velocity unit the flutter speed of the basic configuration. For example, when plotting antisymmetric flutter speed as a function of wing mass density for a particular wing such as that of fighter B with $\Lambda = 45^\circ$, the flutter speeds have been divided by the antisymmetric flutter speed of fighter B, $\Lambda = 45^\circ$, with basic wing mass. Symmetric and antisymmetric results are both presented, rather than choosing the one which gives lowest flutter speed. Where such results are presented in the same figure, symmetric results are generally indicated by solid lines, and antisymmetric results, by dotted lines. Specific numerical values for the flutter speeds and flutter frequencies are found in table XV.

Mass and Inertia Variations

In most practical configurations, the normal mode of vibration with lowest frequency is predominantly a bending mode and is usually called the first wing bending mode. In the absence of a large concentrated mass on the wing, a predominant torsional motion is usually observed in the third or fourth mode. Simple flutter can often be predicted with engineering accuracy using only these two modes as the normal coordinates of the structure. When a large concentrated mass is involved, the situation is much more complex. Two or more torsion modes as well as two or more bending modes become important in flutter computations, and several flutter roots may be observed which predominantly involve various ones of these modes. For eccentric masses it becomes, in fact, impossible to speak of bending and torsion modes since many modes will involve both large bending and torsion displacements.

In those cases in which flutter involves a bending mode and a higher frequency torsion mode, it can be said that a structural change which separates the frequencies of these modes ordinarily raises the flutter speed, and a change which makes the frequencies more nearly equal lowers the flutter speed. It will be observed below that this generalization is not always valid. A change in mass density without change in pitching inertia has greatest effect on first bending frequency even in cases with large sweepback. Consequently, increase in wing mass density would be expected to give an increase in flutter speed and decrease in mass density, a decrease in flutter speed. Changes in pitching inertia would normally be expected to have an opposite effect. Such variations were made for three fighter configurations, four bare-wing bomber configurations, and five bomber configurations with concentrated mass. The mass density and pitching inertia were separately changed by factors of 2.0 and 0.5, making a total of 48 configurations in addition to the 12 basic cases. Reference case numbers are given in table XII.

Tabulation of flutter speed and frequency for each case will be found in table XV. The results are also shown in figure 8. As mentioned earlier, the flutter speeds have been reduced to dimensionless values by using as the velocity unit the flutter speed of the basic wing for each basic configuration. The trends predicted above are found in most cases. In the case of bare-wing fighters the effect is very systematic. The average of all cases is given as follows:

Mass value	Pitch inertia value	Average change in V_f, percent
0.5	1.0	-12
2.0	1.0	6
1.0	.5	8
1.0	2.0	-9

The effect, though uniform, is quite small.

The results for bombers show much less consistency. For cases both with and without concentrated masses, the effect of wing-mass density variation is unpredictable. Nearly half of the cases show trends which are opposite to that predicted above. The addition of a concentrated mass at the 0.46-span position reversed the trend in several cases. On the other hand, change in wing pitching inertia did show a systematic trend for all bomber cases. On the average, a change in pitching inertia by a factor of two changed the flutter speed about 7 percent.

The following conclusions can be drawn:

(1) A change of wing pitching inertia shows a systematic trend for all wings, although the effect is small.

(2) A change of wing mass shows a definite trend for typical fighters, although the effect is small.

(3) Change of wing mass for typical large bombers with or without concentrated masses shows no systematic trend.

Stiffness Variations

It has been pointed out (e.g., ref. 1, p. 783) that when incompressible fluid flow is assumed, a change of stiffness is equivalent to a change of velocity insofar as transient response of an airfoil is concerned. Consequently, it can be said that a uniform increase in stiffness will raise the flutter speed by the square root of the factor by which stiffness is increased. In most airplanes, it is found that the increase in torsional rigidity is primarily responsible for the increase in flutter speed and that, in general, a change in bending rigidity over rather wide limits does not change the flutter speed significantly.

As shown in table XII, 12 configurations were studied to support this conclusion. Since both bending rigidity and torsional rigidity were separately changed by factors of 0.67 and 1.50, there are a total of 48 case numbers assigned to this group. The results of this study are listed in table XV and presented graphically in figure 9. For ease of comparison, flutter speeds are converted to dimensionless values, and flutter characteristics for changes in bending and torsional rigidity are plotted side by side. In general, it was found that change in torsional rigidity by a factor of 3/2 or 2/3 increased or decreased the flutter speed by 20 percent and that a similar change in bending rigidity had a negligible effect upon the flutter speed. Among the 12 configurations studied, the following exceptions to this trend were noted:

(1) Bomber A, $\Lambda = 0^\circ$: In the antisymmetric case both bending and torsional rigidity had roughly equal effects, flutter speed changing ±10 percent for the rigidity change given above.

(2) Bomber B, $\Lambda = 45^\circ$: Symmetric case same as case (1) above.

(3) Bomber A, concentrated mass at 0.46 span, $\Lambda = 0^{\circ}$: In the antisymmetric case, torsional rigidity had a 50 percent greater effect (±30-percent change in flutter speed) and bending rigidity had a negative effect (∓10-percent change in flutter speed).

(4) Bomber A, concentrated mass, $\Lambda = 30^{\circ}$: In the symmetric case, the trend was normal only for increase in torsional rigidity and decrease in bending rigidity.

These exceptions do not constitute a major deviation, and the trend is considered well established.

Local Stiffness Variations

It is not to be expected that the same effect will be observed if torsional rigidity is changed at various stations along the wing. In the absence of a concentrated tip mass, any effect on flutter speed must vanish for stations near the tip, and presumably the largest effect will be observed for stations near the fuselage. Because of the great ease with which these data could be obtained, the effect of local stiffness variation was obtained for several configurations.

The analog computer requires lumping or averaging of inertia and stiffness properties. Consequently, it is possible to determine readily only the effect of a stiffness variation which must be assumed to extend over the entire length of a cell in the finite-difference structure. The basic data consist therefore of step curves. To obtain an approximate value for the per unit change in flutter speed per unit change in stiffness per unit length at any point along the wing it is necessary to draw a smooth curve passing through this curve such that the areas under the two curves are approximately equal. It is believed more suitable to present the step curve and let the reader do any smoothing his application requires. The configurations studied are listed below:

(1) Fighter A, $\Lambda = 0^{\circ}$, symmetric and antisymmetric, case 10
(2) Fighter B, $\Lambda = 0^{\circ}$, symmetric and antisymmetric, case 32
(3) Bomber A, $\Lambda = 0^{\circ}$, bare wing, symmetric, case 93
(4) Bomber A, $\Lambda = 0^{\circ}$, concentrated mass at 0.46 span, symmetric, case 67

Results of this study are presented in figure 10. The abscissa of a curve is the spanwise station at which the bending or torsional rigidity variation is made. The ordinate is the per unit change in flutter speed per unit change in stiffness per unit length along the wing. If, for example, the stiffness is increased j percent over a distance w along a wing of semispan l between the stations $d - (w/2)$ and $d + (w/2)$, then the ordinate of the smoothed curve at the abscissa d/l when multiplied by $j(w/l)$ will give the approximate percent change in flutter speed.

Data for the two fighters show great similarity both for symmetric and antisymmetric conditions. The greatest effect is obtained by changing torsional rigidity near the midspan position, slightly outboard for fighter A and slightly inboard for fighter B. The effect of a bending-rigidity change was found to be small at all stations. In most cases a small negative effect was observed, the flutter speed dropping slightly as the bending rigidity was increased.

Bomber A without concentrated mass showed a similar trend with the following exceptions:

(1) Maximum improvement was obtained by changing torsional rigidity near the root of the wing (0.25-span position).

(2) Increase in bending rigidity was observed to decrease the flutter speed by an amount which was 5 to 10 times greater than that for fighter A.

Addition of a concentrated mass at spanwise station 0.46 has a great effect on this characteristic. The mass chosen is typical for an airplane engine, and is sufficiently large so that the wing is to a certain extent pinned at this point for the particular flutter root involved. Consequently, stiffness changes inboard of the engine have a negligible effect, and changes outboard have an effect very similar to that observed for a bare wing of reduced length.

It should be remarked at this point that the result discussed above is not to be regarded as a trend for all configurations. When the flutter is primarily an outer-wing bending-torsion flutter then this result is to be expected. Experience has shown, however, that occasionally an inner-panel torsion mode is involved in flutter, and change in torsional rigidity outboard of the nacelle has no significant effect. It is unfortunate that such a configuration was not investigated for this report.

Center-of-Mass Location

The location of the wing center of mass has a great effect upon flutter speed of an airplane wing. The general trend is that flutter speed increases as the center of mass moves forward. It is not generally true that the center of mass is at a constant chord location at all spanwise stations. However, for purposes of studying the trends, it is necessary to assume some basic position for the center of mass. Past experience has shown that a center-of-mass location near the elastic axis (usually slightly aft) is both realistic and typical. For this reason the basic position of the center of mass was assumed to be the elastic axis or 40 percent chord. Variation in center-of-mass location was between the 25- and 60-percent-chord points. Thirteen configurations were studied, the various center-of-mass locations comprising 53 cases listed in table XII.

The results are listed in table XV and are shown graphically in dimensionless form in figure 11. The general trend is that the flutter speed increases as the center of mass moves forward and decreases as the center of mass moves aft, except for center-of-mass locations far behind the elastic axis. For positions near the elastic axis, the flutter speed changes about 3 percent for a shift in center of mass equal to 1 percent of the chord. For the extreme aft positions (60 percent chord) most of the curves become quite flat, and in about four cases the flutter speed has started to rise slightly as the center of mass is moved farther aft. On the other hand, the curves become very steep for center-of-mass locations forward of the elastic axis. In most cases the increase in flutter speed was so great that data could not be obtained for the 25- and 32.5-percent-chord locations because the flutter speed greatly exceeded the divergence speed. The average percentage change in flutter speed for a shift in center of mass equal to 1 percent of the chord depends upon location of the center of mass as indicated below:

Center-of-mass location, percent chord	40	50	60
Change in flutter speed, percent	3.1	1.7	0.8

One unusual case was noted. The results for fighter B, $\Lambda = 45^\circ$, in figure 11(a) show an unusual behavior for aft center-of-mass location in the antisymmetric case. A study of the frequency of oscillation for each position tends to support the conclusion that two different flutter roots are involved. In any case the results are anomalous and could bear further investigation.

Fighter A, $\Lambda = 0^\circ$, shows another unusual characteristic in the antisymmetric case. One flutter root disappears as the center of mass is moved forward of the 46-percent-chord location. This result, shown in figure 11(a), is more easily understood by reference to figure 12 where the curves of g against v are plotted for this configuration. A similar case shown in figure 11(b) has two readily observable flutter roots, one with low and the other with high flutter frequency. Data for both cases are given in figure 11(b). It is true that only the one with lower flutter speed is of practical interest, but for purposes of studying trends both are equally important. A plot of g against v for this case is also shown in figure 12.

Elastic-Axis Location

A main component of the aerodynamic pressures on an airfoil is equivalent to a force applied at the quarter chord. Consequently, the elastic-axis location relative to the quarter chord determines the nature of the coupling between aerodynamic forces and the structure. If elastic-axis location alone were changed, both center of pressure and center of mass would change with respect to the assumed structural axis.

In order to separate the effects due to these two changes, the center of mass was moved with the elastic axis in the configurations discussed here. Aerodynamic coupling in which the center of pressure (quarter chord) is forward of the elastic axis may have a destabilizing influence while center of pressure aft of the elastic axis generally has a stabilizing effect.

Elastic-axis locations between the 30 and 50 percent chord were used in the 16 cases listed in table XII. Results are given in table XV and figure 13. In all cases the expected trend was observed. For an elastic axis near the 40 percent chord, the flutter speed changed 3.2 percent on the average for a shift in elastic axis equal to 1 percent of the chord. This effect is not linear over a wide range, however; the flutter speed increases more rapidly as the quarter chord is approached and decreases more slowly as the elastic axis is moved aft. For an elastic axis at the 50 percent chord, the corresponding change in flutter speed was only 1.8 percent.

Chord Variations

A change in chord of a wing is usually accompanied by significant changes in mass, inertia, and stiffness as well as changes in other characteristics. In an effort to assess the effect of aerodynamic pressures alone, variations were made in which mass, inertia, and stiffness were held constant while the chord length was changed. Location of the elastic axis was maintained at a constant per unit chord station so that the distance between quarter chord and elastic axis changed in proportion to the change in the chord length. Since the magnitude of the aerodynamic force increases with chord length and since the predominantly destabilizing lag of the Theodorsen function increases with chord length, it is to be expected that the flutter speed will decrease as the chord length is increased.

Four configurations were studied in which the chord length was changed by factors of 0.67 and 1.50. The eight cases and the configurations are listed in table XII. Flutter characteristics are given in table XV and figure 14. The results are remarkably uniform. On the average, a 7-percent change in flutter speed results from a 10-percent change in chord, smaller chords giving a higher flutter speed.

Sweepback

The effect of sweepback upon flutter speed depends upon many factors. In conventional wing design, the root structure varies greatly with sweepback angle, and the equivalent elastic axis may show considerable variation in position. For wings of large sweepback angle and low aspect ratio,

the concept of an elastic axis may not be useful in describing structural properties. From another point of view the problem is even more perplexing since there is not general agreement about the nature of the aerodynamic forces on a swept wing. In the section of this report entitled "Finite-Difference Errors," the results of three methods of computation were compared with results of wind-tunnel tests of a model wing which was swept-back 34.5°. Two methods were found to give similar results, which were significantly better than those of the third. Although the agreement was not entirely satisfactory, it was decided to use the aerodynamic forces recommended in reference 5. For the present investigation, the following assumptions were therefore made:

(1) Aerodynamic forces are as discussed in the section entitled "Finite-Difference Errors."

(2) To achieve a sweepback angle, the wing is rotated about a vertical axis through the intersection of the unswept elastic axis and the side of the fuselage. The tip is, however, terminated parallel to the airstream, so that only the span measured along the elastic axis is unchanged in length.

(3) Structural properties of the wing are unchanged by sweepback.

(4) The center of mass of the fuselage is moved aft as the sweepback angle is increased so that it coincides roughly with the center of pressure of the wing.

(5) No modifications were made for aerodynamic forces at the tip.

The five basic configurations are shown in table XII, which gives reference numbers for the 17 cases. The results are given in table XV and figure 15. Flutter characteristics of the two fighters show a reasonable correlation, and, in general, a decrease in flutter speed for sweepback angles other than zero. However, the bombers do not show a correlation with the fighters or with each other. It is significant that a substantial change in flutter speed with sweepback angle was observed. In one case, flutter speed increased more than 60 percent for a 45° sweepback, while other cases showed a 30-percent decrease for sweepback angle of about 25°.

In addition to the cases above, it is possible to crossplot the variation of flutter speed with sweepback angle for the following parameter variations of bomber B: Wing mass density, wing pitching inertia, bending rigidity, torsional rigidity, and center-of-mass location. Most of these are plotted in figure 16. It is interesting to note that the general trend for bomber B is to a great extent independent of these variations.

Concentrated-Mass Pitching Flexibility

The engines on present-day bombers are sometimes mounted in nacelles on pylons some distance below the wing. Because of the inherent flexibility in such a structure and its fastening to the wing, the dynamic characteristics of the engine are altered. Because of the symmetry of the structure, it is possible to write two sets of equations for the nacelle, one involving pitching, vertical, and fore and aft motion and the other involving lateral, rolling, and yawing motion. These sets are uncoupled except through interactions with the wing. The characteristics represented by the equations involving pitch have a greater effect on flutter characteristics, or, stated in another way, the assumption of a rigid pylon for lateral motion has not ordinarily been observed to introduce great differences in flutter characteristics. This assumption becomes less valid for wings with large sweepback. On the other hand, a significant variation may be observed as the pitching flexibilities are varied. For pitching motion it is usually quite accurate to assume an effective center of rotation at some point in front of and below the elastic axis. Unless a specific case is to be considered, however, it is just as satisfactory to assume this center of rotation at the elastic axis, since variation in the location of this point has only a second-order effect. Consequently, in this study the center of rotation for pitching motion was established at the elastic axis and the pylon was assumed rigid for lateral motion.

Six cases shown in table XII were investigated:

(1) Bomber A, $\Lambda = 0^\circ$, mass at 0.46 span, case 176
(2) Bomber A, $\Lambda = 0^\circ$, mass at tip, case 179
(3) Bomber B, $\Lambda = 0^\circ$, mass at 0.46 span, case 177
(4) Bomber B, $\Lambda = 0^\circ$, mass at tip, case 180
(5) Bomber B, $\Lambda = 30^\circ$, mass at 0.46 span, case 178
(6) Bomber B, $\Lambda = 30^\circ$, mass at tip, case 181

In all of these cases the chordwise position of the mass was basic, 60 inches forward of the elastic axis.

In presenting the results, an effort has been made to put the data in dimensionless form. Thus, the flutter speed is given as a per unit value of the flutter speed with rigid connection. This basic flutter speed can be found in table XIV. The flexibility is conveniently measured by the normal-mode vibration frequency of the nacelle with the wing held rigid in pitch. However, instead of using the value of frequency in cycles per second, this frequency is measured in per unit value of the flutter frequency with rigid connection. Values for the flutter frequency with rigid connection can also be found in table XIV. There are two frequencies of the nacelle which might be regarded as significant. One of these is the cantilever frequency in which the wing is held rigid

in both pitch and plunge. However, for large bombers, the wing has such great flexibility in vertical bending that greater significance might be attached to the frequency when pitching motion is constrained and vertical motion is completely unrestrained. Because of the location chosen for the basic mass, the difference in these frequencies is a factor of 2, the frequency with vertical motion unrestrained being higher. For presentation of data, this higher value of frequency was chosen, because in those cases where a "tuning" effect was observed the maximum effect occurred when this frequency was equal to the flutter frequency for the basic rigid mass. One exception to this is observed in the discussion below.

Results are plotted in figure 17. Nine of the twelve cases show a predominant decrease in flutter speed as the rigidity is reduced from an infinite value. Seven of these cases show a minimum flutter speed when the nacelle frequency is nearly equal to the rigid flutter frequency. This decrease varies between 7 and 37 percent with an average value of 18 percent. Two cases show a decrease in flutter speed, but no tuning effect. The maximum rate of decrease occurs, in fact, when the nacelle frequency is far below the rigid flutter frequency. In both cases the flutter speed drops to an asymptotic value about six-tenths of the basic value.

Three of the twelve cases show an increase in flutter speed as the rigidity is reduced from an infinite value. In two cases increase takes place in the region where nacelle frequency is roughly equal to the flutter frequency. In both cases the flutter speed increases more than 50 percent. The last anomalous case shows a resonance or tuning effect. It is anomalous for two reasons: (1) The flutter speed rises to a sharp peak about 10 percent above basic value, and (2) this occurs when nacelle frequency is twice as great as the flutter frequency. It should be pointed out that, for this rigidity, the flutter frequency is equal to the nacelle frequency with wing attachment constrained in bending as well as pitch.

Effect of a Concentrated Mass

Many aircraft structures have engines, stores, or external fuel tanks attached to the wing in such a way that they act dynamically as concentrated masses. It has long been known that the location of such a mass has a significant effect on flutter. Unfortunately, other aerodynamic and some structural problems do not permit location of such a mass so that maximum flutter speed is obtained. On the other hand, within the restrictions imposed by other considerations, it is often possible to improve flutter characteristics significantly by proper choice of mass location.

This investigation has included a detailed examination of the effect of a concentrated mass on the flutter characteristics of several configurations of the four basic airplane wings. Preliminary study of this

effect showed such interesting and unusual effects that the scope of the investigation was expanded beyond that originally proposed. The resulting data are so voluminous that it is difficult to present them effectively. In particular, it is impractical to construct a table which gives all of the data obtained, and so graphical presentation is required. Two methods have been adopted in this report. For a given spanwise location of the mass, the flutter speed can be plotted as a function of the chordwise location. This has been done for all cases investigated. Since the concentrated mass is alined with the airstream, it is most convenient in cases with sweepback to move the mass parallel to the airstream rather than perpendicular to the elastic axis. Where sufficient data are available, these curves can be summarized in a single diagram in which lines of constant flutter speed are shown on a drawing of the wing plan form. For the concentrated mass located anywhere on such a contour line, the flutter speed will be the same. The result is essentially a topographic map of the flutter-speed surface, where each point on the plan form represents a possible location for the concentrated mass.

Several difficulties arise with both methods of presentation. The main source of difficulty lies in the fact that several important flutter roots exist for a wing with concentrated mass. For certain locations of the mass, one root will show lowest flutter speed, while for other locations another root will have the lowest flutter speed. Since the analog computer is essentially an electrical model, it is usually impossible to find one of these flutter speeds if another root has a flutter speed far below the first. It is possible, therefore, to find with certainty only those portions of a given flutter-root surface which lie beneath all other flutter-root surfaces. For one configuration studied, four such distinct surfaces were positively identified and it was not possible to establish that surfaces appearing at widely separated regions were or were not related. In most cases the roots were differentiated by obtaining essentially marginal stability for two distinct roots along the line where the two surfaces intersect. It can be readily appreciated that many points are required to establish the flutter-speed contours, particularly where several intersecting surfaces are involved. It was, in fact, impossible in the time available to obtain sufficient data to establish all interesting features about these contours. However, it is believed that all important features are shown correctly in the figures presented here.

The curves which show flutter speed as a function of chordwise position at a fixed span frequently show intersections between different flutter roots. In identifying these roots, it is useful to know the flutter frequency associated with each root. The simplest way to present these data is to show the value of frequency at a few selected points along each curve. Where roots intersect and both frequencies were measured, both values are shown. In some cases where actual frequencies were not measured, low, medium, or high frequency are shown.

For convenience, the concentrated mass was always placed at the center of a finite-difference cell except in three cases where additional information was obtained by placing it halfway between cells. It is convenient to identify these locations by the cell number as has been done in table XIV, which assigns a case number to each configuration. It must be remembered, however, that the cell divisions are slightly different for bomber and fighter airplanes, and therefore the spanwise station for a given cell number will be different. The location of these stations in terms of unit span is given in table XIII. In the figures, the spanwise position is correctly given as a fraction or per unit value of the wing semispan.

The size of the concentrated mass and its pitching and rolling inertia also affect the flutter speed. Since past experience has shown that rolling inertia has a small effect, a few cases were chosen for further investigation of the magnitude of this effect. For a concentrated mass located in the wing it is reasonable to assume a radius of gyration which is a small fraction of the average half chord. For a mass suspended below the wing, it is unlikely that the distance will exceed half of the average half chord. Two values for radius of gyration were chosen, equal to 0.1 and 0.5 times the average chord for the fighter planes. In all cases considered there was no significant difference in flutter characteristics when the rolling inertia was varied from zero to the maximum value. The variation was, in fact, so insignificant that none of the data is presented in this report. In what follows it may be assumed that the rolling inertia of the concentrated mass has any value between the above limits. Since the mass of the concentrated mass and its pitching inertia have a greater effect, it is necessary to consider variations in these quantities in several typical cases. The basic values for mass and pitching inertia (or radius of gyration k) have been discussed in the section entitled "Characteristics of Four Representative Aircraft" and are given in table XIII. The variations of these values are summarized in table XIV.

The most logical way to give the results is to present first the flutter characteristics for the basic mass on each particular airplane. Five airplanes were chosen:

(1) Fighter A, $\Lambda = 0^\circ$
(2) Fighter A, $\Lambda = 45^\circ$
(3) Bomber A, $\Lambda = 0^\circ$
(4) Bomber B, $\Lambda = 0^\circ$
(5) Bomber B, $\Lambda = 30^\circ$

Since it was difficult to choose a typical radius of gyration for a mass on a fighter plane, three values were used. These values are 6, 15, and 30 inches, as shown in table XIV. Figures 18(a) and 18(b) show the effect of chordwise location of the mass at five spanwise positions for

fighter A with $\Lambda = 0^\circ$. Results for all three radii of gyration in pitch are plotted on the same sheet using different symbols for each value. Circles are used for the smallest value, $k = 6$ inches; triangles are used for $k = 30$ inches; a solid line with no symbols is used for the intermediate value. Abscissas for all curves are chordwise distance from the elastic axis measured as per unit value of the wing semispan. Similar data for fighter A, $\Lambda = 45^\circ$, are shown in figures 18(c) and 18(d); six spanwise stations were used in this case. One surprising feature can be noted in all of these figures: The characteristics are relatively independent of the pitching inertia, even though this inertia is varied from a very large value ($k = 30$ inches) to nearly zero ($k = 6$ inches). This does not mean that at any particular point the flutter speeds are identical, but the overall shapes of the curves show remarkable similarity.

Although these figures (figs. 18(a) to 18(k)) give a good picture of the flutter characteristics, it is easier to interpret the results if all data are combined to construct flutter contours as discussed earlier. Such contours for the minimum and maximum values of k are shown in figures 19(a) to 19(h). These figures support the following conclusions:

(1) A chordwise position aft of the elastic axis is almost always undesirable.

(2) The 30- to 50-percent-span position and the tip location are generally undesirable.

(3) A position forward of the elastic axis and near the 70- to 80-percent-span position will, in general, greatly increase the flutter speed.

Since time did not permit a complete study of the characteristics for fighter B, data were obtained only for the cases of 0° and 45° sweepback with mass at the tip. Comparison of the results shown in figure 18(e) with the corresponding data for fighter A in figures 18(a), 18(b), 18(c), and 18(d) shows that for this location there does not seem to be any significant difference in characteristics. Whether it is safe to extrapolate this result to other mass locations cannot be said at this time.

Since the study of fighter A showed that the pitch radius of gyration had a small effect, and since the pitch radius of gyration of a bomber engine is relatively well defined, it was decided to use only one value in the study of bomber airplanes. However, the practice of using one engine or two engines on a single pylon, as well as the different sizes of engines, gives a possible variation in mass which might well exceed a factor of two. All bomber data were therefore obtained with both basic mass and half basic mass. For ease of comparison of the two sets of

data, they are plotted side by side in the figures. Data for bomber A, $\Lambda = 0^{\circ}$, are contained in figures 18(f) and 18(g). Results for bomber B, $\Lambda = 0^{\circ}$, are given in figures 18(h) and 18(i), and the case of bomber B, $\Lambda = 30^{\circ}$, is summarized in figures 18(j) and 18(k). Again it is possible to simplify interpretation of these figures by combining the results into flutter-speed contours. However, it can be seen that data for basic mass and half basic mass are very similar, and so such contours have been prepared only for the cases with basic mass. The flutter-speed contours are shown in figures 19(i) to 19(n). A study of these figures shows some deviations from the results for fighter airplanes. The following conclusions can be drawn:

(1) A position aft of the elastic axis is almost always undesirable.

(2) The tip region is generally undesirable as a location for the mass.

(3) With few exceptions, any position forward of the elastic axis and between the root and the 90-percent-span position will give flutter speed equal to or greater than the bare-wing flutter speed.

(4) However, there are, in most cases, no practical locations which give any significant improvement in flutter characteristics. Two cases will be noted in which the speed might be increased 40 percent. The others are restricted to a 10- or 20-percent improvement.

Since fighter planes showed remarkable variation in flutter characteristics with mass position, it was believed necessary to examine the effect of changes in the size (mass) of the concentrated mass. This was first studied at two spanwise positions for fighter A, $\Lambda = 0^{\circ}$. The positions are the tip and station 5 (0.79 span). Flutter characteristics as functions of chordwise position were measured for several values of mass. The three values of radius of gyration given in table XIII were used for all mass values, except that for very small values of mass only the 6-inch value was used. However, because of the similarity of results, data are presented only for the maximum value (k = 30 inches) and minimum value (k = 6 inches). Case numbers are listed in table XIV.

The results for tip location shown in figure 20(a) show a very interesting progression in characteristics as the mass is reduced to zero. Most striking is the fact that no significant change takes place when the mass is varied from twice basic value to half basic value. Even with mass reduced to 8 percent of basic value, the three flutter roots for antisymmetric motion and the two flutter roots for symmetric motion can still be identified, though their characteristics are by this time somewhat altered. Similar data for the mass at 0.79 span are presented in figure 20(b). Figure 20(a) concluded illustrates graphically the danger in extrapolating results. For a mass at the 0.10 chordwise

position and symmetric motion, a mass equal to 0.008 basic mass increases flutter speed to 1.07. Doubling the mass increases it to 1.16. Again doubling it will increase the speed to some unknown value greater than 1.40. However, if the mass is again increased by a factor of about 2.8, the flutter speed (of another root) will have dropped to 1.00 again.

Flutter characteristics were also measured for basic and half basic mass at the wing tip with sweepback angle of 45°. This case was chosen because the antisymmetric characteristic for a 30-inch radius of gyration (fig. 18(d)) showed a very unusual characteristic. Figure 21(a) shows that reduction of the mass by a factor of two eliminates the anomalous behavior, but in all other respects gives results which are essentially the same as the basic mass. Figure 21(b) gives similar data for the mass at the 0.79 span position with $\Lambda = 45^\circ$. Again the results for basic mass and half basic mass are not significantly different. It is perhaps unwise to attempt any general statement, but there is every indication that the essential features shown in the flutter-speed contours of figure 19 would not be profoundly altered if either mass or pitching inertia were increased or decreased by a factor as large as 2.0.

Accuracy and Probable Errors

A brief statement about the expected accuracy of these results has been purposely deferred until the end of this report. It is believed that this discussion will be more meaningful after the reader has observed the nature and scope of the data obtained. The analog computer is not composed of perfect electrical elements. For example, the inductors used in this study have loss characteristics corresponding to a damping factor of about $g = 0.01$. Transformers also have significant losses. The electrical analog of the airplanes studied in this report had an electrical damping corresponding to a structural damping between $g = 0.02$ and $g = 0.03$. This is not greatly different from the damping to be found in conventional aircraft construction, so no corrections were made for this internal damping.

No general statement can be made about the effect of random computer errors. Some give rise primarily to an error in the damping factor of the roots, in which the $(g - v)$ curve is shifted vertically. Other errors give rise basically to an error in velocity, in which the curve is primarily shifted horizontally. Since the slope of the curve of g against v is by no means constant, it becomes impossible to give a specific figure for accuracy of flutter speed. In unusual cases, where roots are of the type shown in figure 12, flutter may be predicted when in fact it will not occur for this root at all. This distinction, which must be made mathematically, is of no importance in practical cases. An airplane which shows a flutter damping of $g = 0.01$ and is therefore theoretically stable is not to be regarded as any more satisfactory or useful than one which

shows a damping $g = -0.01$ and would therefore theoretically fly apart. Manufacturing tolerances and the safety factors required in aircraft will not permit use of an aircraft unless it is moderately stable for a significant variation in all structural parameters. It is believed that, exclusive of errors introduced by the finite-difference structure and approximations in the aerodynamic theory, the results obtained in this study have a probable error in damping factor of about $g = \pm 0.02$ or a probable error in flutter speed of about 2 percent, whichever is applicable in the light of the above discussion. However, trends obtained by variation of structural parameters are considerably more accurate than this would imply, since any error would persist with roughly the same value in all cases involving such parameter variations.

For cases 1 to 181, it is possible to construct curves of g against v although they have not been made a part of this report. These curves serve to show the steepness with which the roots pass through flutter and give some indication of the accuracy of the flutter speed. This situation does not exist for cases 181 to 289. For concentrated-mass variations, computations were carried out in such a way that only flutter speeds and frequency were obtained. Consequently, it is not possible to delineate areas which are "safe" from the standpoint of flutter. It is known, for example, that where a long pendant lobe is observed, as for case 235 in figure 18(d), the system is barely unstable everywhere within this lobe. There are similar regions elsewhere, for example case 212, which is antisymmetric (fig. 20(b)), where the system is barely unstable within an elliptical-shaped boundary. Similarly, case 214 is barely stable in this region and yet no flutter root is even shown since the system does not become actually unstable at any point.

These remarks are not made to show the flutter curves to be valueless, but to caution the reader against making inferences not contained in the report and not legitimately supported by the data presented here.

SUMMARY OF RESULTS

Certain trends in flutter characteristics for typical modern aircraft seem to be indicated by this study of the incompressible flutter characteristics of aircraft wings. In some cases a few deviations are found. It is probable that if more extreme aircraft designs were considered, even more would be observed. Nevertheless, this summary may serve as a useful guide.

(1) In the following table are listed the average changes in flutter speed for a 1-percent change in each parameter, the change being made from the basic value except for center-of-mass and elastic-axis location, in which cases several locations are assumed.

Change in parameter	Average change in flutter speed, percent
Increase wing mass 1 percent	0
Increase wing pitching inertia 1 percent	-.1
Increase bending rigidity 1 percent	0
Increase torsional rigidity 1 percent	.5
Increase wing chord 1 percent	-.7
Center of mass forward 1 percent of chord from -	
40-percent location	3.0
50-percent location	1.7
60-percent location	.8
Elastic axis forward 1 percent of chord from -	
40-percent location	3.2
50-percent location	1.8

(2) Localized change in torsional rigidity is most effective in changing flutter speed of a bare-wing airplane if the change is made between midspan and root. For bombers with large concentrated mass on the wing, torsional rigidity either inboard or outboard of the mass will usually govern flutter speed, depending on the type of flutter existing. The effect of sweepback was not observed to have a systematic effect. Pitching flexibility of the concentrated-mass support has a definite influence on flutter speed. In many cases a tuning effect was observed, with a 10- to 40-percent decrease in flutter speed. This effect was not always observed; in some cases, the flutter speed was significantly increased.

(3) Perhaps the most interesting results will be found in the effects of a concentrated-mass location. For a wide range of mass and radius-of-gyration values the results were very systematic. For fighter-type planes it was found that:

(a) Aft chordwise positions are usually undesirable.

(b) The 30- to 50-percent-span and tip locations are generally undesirable.

(c) A forward location near the 70- to 80-percent-span position will, in general, greatly increase flutter speed.

For bomber-type planes these results are somewhat modified:

(a) Aft chordwise positions are usually undesirable.

(b) The tip location is generally undesirable.

(c) With few exceptions, any location forward of the elastic axis and between root and 0.90-span position is satisfactory, although flutter speed is rarely greater than bare-wing flutter speed by any significant amount.

There is perhaps no need to remark that these results can be altered by introduction of a flexibility in the concentrated-mass support.

California Institute of Technology,
Pasadena, Calif., June 6, 1955.

REFERENCES

1. MacNeal, R. H., McCann, G. D., and Wilts, C. H.: The Solution of Aeroelastic Problems by Means of Electrical Analogies. Jour. Aero. Sci., vol. 18, no. 12, Dec. 1951, pp. 777-789.

2. Benscoter, Stanley U., and MacNeal, Richard H.: Introduction to Electrical-Circuit Analogies for Beam Analysis. NACA TN 2785, 1952.

3. Sewall, John L.: Experimental and Analytical Investigation of Flutter of a Nonuniform Sweptback Cantilever Wing With Two Concentrated Weights. NACA RM L51H09a, 1951.

4. Nelson, Herbert C., and Tomassoni, John E.: Experimental Investigation of the Effects of Sweepback on the Flutter of a Uniform Cantilever Wing With a Variably Located Concentrated Mass. NACA RM L9F24, 1949.

5. Barmby, J. G., Cunningham, H. J., and Garrick, I. E.: Study of Effects of Sweep on the Flutter of Cantilever Wings. NACA TN 2121, 1950.

6. Scanlan, Robert H., and Rosenbaum, Robert: Introduction to the Study of Aircraft Vibration and Flutter. The Macmillan Co., 1951.

7. McCann, G. D., and Braham, H. S.: A Study of the Accuracy of Lumped Parameter and Analog Computer Representations of Cantilevered Beams Under Conditions of Static Stress and Dynamic Vibrations. Rep. No. 3, Contract AF 18(600)-669, Office of Sci. Res. and C.I.T., 1955.

8. Goland, Martin, and Luke, Y. L.: The Flutter of a Uniform Wing With Tip Weights. Jour. Appl. Mech., vol. 15, no. 1, Mar. 1948, pp. 13-20.

9. Runyan, Harry L., and Watkins, Charles E.: Flutter of a Uniform Wing With an Arbitrarily Placed Mass According to a Differential-Equation Analysis and a Comparison With Experiment. NACA Rep. 966, 1950. (Supersedes NACA TN 1848, 1949.)

10. Wilts, C. H.: Finite Difference Errors in the Flutter Speed of a Uniform Wing With an Arbitrarily Placed Mass. Analysis Lab. Rep., C.I.T., June 1954.

11. Runyan, Harry L., and Sewall, John L.: Experimental Investigation of the Effects of Concentrated Weights on Flutter Characteristics of a Straight Cantilever Wing. NACA TN 1594, 1948.

TABLE I.- PHYSICAL CHARACTERISTICS OF A PINNED-PINNED AIRFOIL

Length, in.	288
Half chord, b, in.	48
Mass per unit length, m, lb-sec^2/sq in.	0.01035
Inertia per unit length, I, lb-sec^2	5.176
Bending rigidity, EI, lb-in.^{2}	$1.412(10^9)$
Torsional rigidity, GJ, lb-in.^{2}	$6.87(10^8)$
x_1, in.	9.6
x_3, in.	-9.6
Air density, ρ, lb-sec^2/in.^{4}	$0.0845(10^{-6})$

TABLE II.- COMPUTED FLUTTER SPEED AND FREQUENCY OF FINITE-DIFFERENCE PINNED-PINNED AIRFOIL

Number of cells	v_f, mph	$\Delta v_f/v_\infty$	f_f, cps	$\Delta f_f/f_\infty$
∞	692	0	12.7	0
8	688	.006	12.6	.008
4	677	.022	12.3	.032
2	644	.069	11.0	.134

TABLE III.- PHYSICAL CHARACTERISTICS OF UNIFORM CANTILEVER WING

Half chord, b, in.	4
Span, l, in.	48
Mass per unit length, m, lb-sec^2/sq in.	$1.877(10^{-4})$
Pitching inertia per unit length, lb-sec^2	$8.00(10^{-4})$
Flexural rigidity, EI, (lb)(sq in.)	$1.407(10^{5})$
Torsional rigidity, GJ, (lb)(sq in.)	$0.692(10^{5})$
Elastic-axis position, x_o, in.	-0.504
Center of mass position, x_3, in.	0.156
Mass of concentrated mass, m_c, lb-sec^2/in.	$8.23(10^{-3})$
Pitch inertia of concentrated mass, lb-sec^2/in.	0.1636
Center of mass of concentrated mass, $(x_3)_c$, in.	-3.274
Air density, ρ, lb-sec^2/in.^{4}	$1.155(10^{-7})$

TABLE IV.- THEORETICAL AND EXPERIMENTAL FLUTTER CHARACTERISTICS OF CANTILEVER WING WITH CONCENTRATED MASS

[Data taken from references 9 and 11]

Mass location, per unit span	Calculated			Experimental		
	v_f, mph	v_f, per unit (a)	f_f, cps	v_f, mph	v_f, per unit (a)	f_f, cps
0	227	0.400	25.27	228	0.401	22.1
.167	---	-----	-----	221	.388	19.1
.229	226	.397	19.23	221	.388	17.4
.292	---	-----	-----	233	.410	16.3
.333	---	-----	-----	256	.451	15.5
.354	277	.488	28.04	260	.458	[b]16.3-26.8
.625	[c]359	.631	30.68	---	-----	(d)
.938	273	.481	25.67	261	.459	(d)
.959	251	.442	24.87	251	.442	21.8
.979	---	-----	-----	231	.407	21.6
1.000	205	.360	23.60	218	.384	21.4

[a]1.0 per unit velocity is 10^4 in./sec or 568 mph.

[b]This experimental record seems to show nearly simultaneous divergence and flutter at two frequencies.

[c]Calculated divergence speed is about 279 mph. However, a flutter speed can still be calculated mathematically.

[d]Divergence was observed experimentally.

TABLE V.- FLUTTER CHARACTERISTICS OF FINITE-DIFFERENCE ANALOG OF UNIFORM CANTILEVER WING

Mass position (a)	V_f, mph	V_f, per unit (b)	f_f, cps
4 cell			
0	224	0.394	25.9
.125	212	.373	——
.150	213	.374	——
.225	225	.396	18.9
.250	241	.424	18.1
.275	275	.484	——
.325	269	.473	27.7
.350	258	.454	27.2
.375	245	.431	26.3
.500	275	.480	27.6
.600	297	.522	28.2
.625	305	.535	28.4
.650	376	.661	31.4
.875	327	.576	26.7
.950	237	.417	24.0
1.000	197	.346	22.4
$5\frac{1}{2}$ cell			
0	225	0.392	25.8
.182	218	.385	20.3
.236	227	.399	18.6
.254	236	.415	17.8
.273	249	.439	17.3
.291	295	.520	28.5
.309	289	.508	28.0
.328	284	.500	28.3
.364	274	.482	27.9
.454	244	.430	27.2
.546	284	.500	28.3
.600	313	.550	29.7
.636	333	.586	30.7
.855	377	.664	29.4
.909	305	.537	27.0
.946	258	.454	25.5
1.000	212	.373	23.9
6 cell			
0	228	0.401	25.7
.083	225	.393	25.3
.167	219	.386	20.8
.217	226	.398	18.7
.250	259	.420	18.0
.267	255	.448	17.1
.284	286	.504	16.7
.317	296	.521	28.2
.367	270	.476	27.5
.417	252	.443	26.8
.450	258	.454	27.2
.500	266	.468	27.6
.550	277	.487	27.8
.583	282	.496	28.2
.600	306	.539	28.9
.616	334	.588	30.1
.667	≈477	≈.840	——
.868	349	.614	28.4
.883	319	.562	27.4
.917	276	.486	26.3
.950	242	.426	25.1
.965	226	.398	24.6
.984	213	.375	24.2
1.000	201	.353	23.6

[a]Mass position is per unit span measured from root.

[b]1.0 per unit velocity = 568 mph.

TABLE VI.- PHYSICAL CHARACTERISTICS OF SWEPTBACK WING WITH CONCENTRATED MASS

[Data taken from reference 3. Mass of wing is for portion outboard of root restraint. More detailed information will be found in reference 3. Data for concentrated masses are not given explicitly in reference 3 and must be regarded as only approximate.]

Wing characteristics:	
[a]Span, in.	48.3
[b]Root half chord, b_r, in.	5.2
[b]Tip half chord, b_x, in.	2.36
Wing total mass, m_w, lb-sec^2/in.	0.00784
Tunnel fluid density, ρ, lb-sec^2/in.^{4}	$3.40(10^{-7})$
Sweepback angle, Λ, deg	34.5

Concentrated-mass characteristics:	Inboard	Outboard
Mass, m_c, lb-sec^2/in.	0.00806	0.00452
Pitch inertia about elastic axis, lb-sec^2/in.	0.0712	0.0192
Per unit spanwise position (from root)	0.30	0.78
Center of mass position, $(x_3)_c$, in.	-1.74	0.50

(a) Measured along elastic axis.
(b) Measured perpendicular to elastic axis.

TABLE VII.- EXPERIMENTAL AND COMPUTED FLUTTER CHARACTERISTICS OF SWEPTBACK WING WITH CONCENTRATED MASS

Type of frequency	Normal mode frequencies, cps, at -		
	Mode 1	Mode 2	Mode 3
Experimental model frequency	6.97	30.9	37.9
Measured analog frequency	6.91	32.6	39.1

Type of result	Flutter characteristics		
	v_f, mph	$\Delta v_f/v_{f_e}$	f_f, cps
Wind-tunnel results, v_{f_e}	193	0	20.1
Analog results, normal-component method	170	-.12	24.2
Analog results, airstream method[a]	157	-.19	24.0
Analog results, airstream method[b]	173	-.11	24.0

[a]Lift coefficient $C_{L_\alpha} = 2\pi$.

[b]Lift coefficient $C_{L_\alpha} = 2\pi \cos \Lambda$.

TABLE VIII.- CHARACTERISTICS OF BASIC FIGHTER A

(a) Physical Characteristics

Sweepback angle, Λ, deg	0
Semispan of wing,[a] l, in.	238
Cell size for finite-difference structure, Δy, in.	34
Root chord,[b] b_r, in.	106
Tip chord,[b] b_x, in.	53
Taper ratio	2.00
Aspect ratio	6
Wing elastic axis, percent chord	40
Wing center of mass, percent chord	40
Total wing mass external of fuselage, m_{wf}, lb-sec^2/in.	10.7
Fuselage mass, m_f, lb-sec^2/in.	21
Fuselage radius of gyration, pitch,[c] in.	100
Fuselage radius of gyration, roll, in.	25
Fuselage center of mass aft of elastic axis, in.	0
Tail center of pressure aft of elastic axis, in.	230
Tail area, sq in.	3,000
Air density, ρ, lb-sec^2/in.^{4}	1.146(10^{-7})

(b) Inertia and stiffness values lumped for finite-difference structure

Station	1	2	3	4	5	6
Per unit span,[a]	0.214	0.357	0.500	0.643	0.786	0.928
Half chord,[b] b, in.	47.3	43.5	39.8	36.0	32.2	28.4
Lumped mass, $\bar{m}$, lb-sec^2/in.	1.73	1.34	0.98	0.66	0.40	0.23
Lumped pitch inertia	695	568	405	253	126	53

$d_{10}\int^{10}$ (dy/EI)	19.8	61.3	112	205	415	773	----
$d_{10}\int^{10}$ (dy/GJ)	56.3	145	219	365	667	1,260	850

[a]Measured along elastic axis.

[b]Measured perpendicular to elastic axis.

[c]About elastic axis.

[d]Stiffness values are lumped between mass stations.

TABLE IX.- CHARACTERISTICS OF BASIC FIGHTER B

(a) Physical characteristics

Sweepback angle, Λ, deg	30
Semispan of wing,[a] l, in.	238
Cell size for finite-difference structure, Δy, in.	34
Root chord,[b] b_r, in.	106
Tip chord,[b] b_x, in.	53
Taper ratio	2.00
Wing elastic axis, percent chord	40
Wing center of mass, percent chord	40
Total wing mass external of fuselage, m_{wf}, lb-sec^2/in.	14.06
Fuselage mass, m_f, lb-sec^2/in.	21
Fuselage radius of gyration, pitch,[c] in.	100
Fuselage radius of gyration, roll, in.	25
Fuselage center of mass aft of elastic axis, in.	0
Tail center of pressure aft of elastic axis, in.	230
Tail area, sq in.	3,000
Air density, ρ, lb-sec^2/in.^{4}	$1.146(10^{-7})$

(b) Inertia and stiffness values lumped for finite-difference structure

Station	1	2	3	4	5	6
Per unit span,[a]	0.214	0.357	0.500	0.643	0.786	0.928
Half chord,[b] b_x, in.	47.3	43.5	39.8	36.0	32.2	28.4
Lumped mass, $\bar{m}$, lb-sec^2/in.	1.52	1.43	1.32	1.16	0.94	0.66
Lumped pitch inertia	628	577	503	411	310	204

$d_{10}\int_{10}$ (dy/EI)	33.0	100	156	221	321	447	---
$d_{10}\int_{10}$ (dy/GJ)	71.4	193	283	551	400	436	224

[a]Measured along elastic axis.

[b]Measured perpendicular to elastic axis.

[c]About elastic axis.

[d]Stiffness values are lumped between mass stations.

TABLE X.- CHARACTERISTICS OF BASIC BOMBER A

(a) Physical characteristics

Sweepback angle, Λ, deg	0
Semispan of wing,[a] l, in.	845
Cell size for finite-difference structure, Δy, in.	130
Root chord,[b] b_r, in.	200
Tip chord,[b] b_x, in.	80
Taper ratio	2.50
Aspect ratio	12
Wing elastic axis, percent chord	40
Wing center of mass, percent chord	40
Total wing mass external of fuselage, m_{wf}, lb-sec^2/in.	39.7
Fuselage mass, m_f, lb-sec^2/in.	120
Fuselage radius of gyration - pitch,[c] in.	240
Fuselage radius of gyration - roll, in.	50
Fuselage center of mass aft of elastic axis, in.	0
Tail center of pressure aft of elastic axis, in.	700
Tail area, sq in.	20,000
Air density, ρ, lb-sec^2/in.^{4}	$1.146(10^{-7})$

(b) Inertia and stiffness values lumped for finite-difference structure

Station	1	2	3	4	5	6
Per unit span,[a]	0.154	0.308	0.461	0.615	0.769	0.923
Half chord,[b] b, in.	90.8	81.5	72.3	63.1	53.9	44.6
Lumped mass, $\bar{m}$, lb-sec^2/in.	6.28	5.46	4.16	2.47	0.98	0.50
Lumped pitch inertia	13,300	10,600	7,150	3,640	1,170	360

$d_{10}{}^{10}\int$ (dy/EI)	3.3	8.4	14.3	30.5	101	650	---
$d_{10}{}^{10}\int$ (dy/GJ)	10.0	23.1	30.9	47.5	143	618	618

[a]Measured along elastic axis.

[b]Measured perpendicular to elastic axis.

[c]About elastic axis.

[d]Stiffness values are lumped between mass stations.

TABLE XI.- CHARACTERISTICS OF BASIC BOMBER B

(a) Physical characteristics

Sweepback angle, Λ, deg	30
Semispan of wing,[a] l, in.	845
Cell size for finite-difference structure, Δy, in.	130
Root chord,[b] b_r, in.	170
Tip chord,[b] b_x, in.	70
Taper ratio	2.43
Wing elastic axis, percent chord	40
Wing center of mass, percent chord	40
Total wing mass external of fuselage, m_{wf}, lb-sec^2/in.	48.7
Fuselage mass, m_f, lb-sec^2/in.	120
Fuselage radius of gyration, pitch,[c] in.	240
Fuselage radius of gyration, roll, in.	50
Fuselage center of mass aft of elastic axis, in.	150
Tail center of pressure aft of elastic axis, in.	700
Tail area, sq in.	20,000
Air density, ρ, lb-sec^2/in.^{4}	$1.146(10^{-7})$

(b) Inertia and stiffness values lumped for finite difference structure

Station	1	2	3	4	5	6	
Per unit span,[a]	0.154	0.308	0.461	0.615	0.769	0.923	
Half chord,[b] b, in.	77.3	69.6	61.9	54.2	46.5	38.8	
Lumped mass, $\bar{m}$, lb-sec^2/in.	6.28	5.23	4.26	3.35	2.74	2.47	
Lumped pitch inertia	3,940	3,080	2,200	1,560	910	390	
$d_{10}\int^{10}$ (dy/EI)[d]	7.12	18.8	31.0	54.9	91.6	141.0	--
$d_{10}\int^{10}$ (dy/GJ)[d]	6.31	15.5	22.6	42.2	77.8	110.0	60

[a]Measured along elastic axis.

[b]Measured perpendicular to elastic axis.

[c]About elastic axis.

[d]Stiffness values are lumped between mass stations.

TABLE XII.- ASSIGNMENT OF CASE NUMBERS

Variable factor	Value or type	Case Number of -													
		Fighter A; $\Lambda = 0°$	Fighter A; $\Lambda = 45°$	Fighter B; $\Lambda = 0°$	Fighter B; $\Lambda = 45°$	Bomber A; $\Lambda = 0°$; ^{a}M	Bomber A; $\Lambda = 30°$; ^{a}M	Bomber A; $\Lambda = 0°$; ^{a}B	Bomber B; $\Lambda = 30°$; ^{a}M	Bomber B; $\Lambda = 0°$; ^{a}M	Bomber B; $\Lambda = 45°$; ^{a}M	Bomber B; $\Lambda = 30°$; ^{a}B	Bomber B; $\Lambda = 0°$; ^{a}B	Bomber B; $\Lambda = 45°$; ^{a}B
Basic		1	—	25	49	73	74	97	98	121	122	145	146	169
Mass factor	2 0.5	3 4	—	27 28	51 52	75 76	76 77	99 100	100 101	123 124	124 125	147 148	148 149	171 172
Pitch inertia factor	2 0.5	5 6	—	29 30	53 54	77 78	78 79	101 102	102 103	125 126	126 127	149 150	150 151	173 174
Bending rigidity factor	3/5 5/5	7 8	—	31 32	55 56	79 80	80 81	103 104	104 105	127 128	128 129	151 152	152 153	175 176
Torsional rigidity factor	3/5 5/5	9 10	—	33 34	57 58	81 82	82 83	105 106	106 107	129 130	130 131	153 154	154 155	177 178
Local stiffness variation		11	—	35	59	83	84	107	108	131	132	155	156	179
^{b}Center of mass, percent	25 30 35 40 45	12 13 14 15 16	— — — — —	36 37 38 39 40	60 61 62 63 64	85 86 87 88 89	86 87 88 89 90	109 110 111 112 113	110 111 112 113 114	133 134 135 136 137	134 135 136 137 138	157 158 159 160 161	158 159 160 161 162	181 182 183 184 185
^{b}Elastic axis, percent	35 40 45	17 18 19	— — —	41 42 43	65 66 67	90 91 92	91 92 93	114 115 116	115 116 117	138 139 140	139 140 141	162 163 164	163 164 165	186 187 188
Chord factor	3/5 5/5	20 21	— —	44 45	68 69	93 94	94 95	117 118	118 119	141 142	142 143	165 166	166 167	189 190
Sweepback angle, deg	0 15 25	22 23 24	— — —	46 47 48	70 71 72	95 96 97	96 97 98	119 120 121	120 121 122	143 144 145	144 145 146	167 168 169	168 169 170	191 192 193
Bendix pitch flexibility	Mass at station 3 Mass at tip	—	—	—	—	98	99	122	123	146	147	170	171	194

^{a}M; concentrated mass on wing 3, bare wing.
^{b}Center of mass and elastic axis measured in percent chord from leading edge.

TABLE XIII.- CONCENTRATED-MASS CHARACTERISTICS AND LOCATIONS

(a) Characteristics

	Fighter	Bomber
Basic mass, lb-sec^2/in.	2.68	15.0
Pitch radius of gyration,[a] in. . . .	30 15 6	35 17.5 7
Roll radius of gyration, in. . . .	15 0	---- ----
Basic spanwise position,[b] in. . . .	----	390
Basic chordwise position,[c] in. . . .	----	60

[a]About elastic axis; airstream coordinates.

[b]Outboard from center line measured along elastic axis.

[c]Forward of elastic axis, parallel to airstream.

(b) Location

Airplane	Locations of concentrated mass, per unit span,[a] at station -								
	1	2	3	4	4.5	5	5.5	6	Tip
Fighter	0.214	0.358	0.500	0.643	------	0.786	------	0.929	1.00
Bomber	.154	.308	.461	.615	0.692	.769	0.846	.923	1.00

[a]Distances are measured in per unit span along elastic axis.

TABLE XIV.- CASE NUMBERS FOR CONCENTRATED-MASS VARIATIONS

m/m_{basic}	Station	Fighter A, A = 0°, with radius of gyration, in., of -			Fighter A, A = 45°, with radius of gyration, in., of -			Bomber A, A = 0°, with radius of gyration, in., of -	Bomber B, A = 0° with radius of gyration, in., of -	Bomber B, A = 0°, with radius of gyration, in., of -
		6	15	30	6	15	30	35	35	35
1	Root	---	---	---	---	---	---	248	---	---
	1	---	---	---	---	---	---	---	---	276
	2	---	182	183	218	219	220	249	264	277
	3	---	184	185	221	222	223	250	265	278
	4	---	---	---	224	225	226	251	266	279
	4.5	---	---	---	---	---	---	252	---	---
	5	186	187	188	227	228	229	253	267	280
	5.5	---	---	---	---	---	---	254	---	---
	6	189	190	191	230	231	232	255	268	281
	Tip	192	193	194	233	234	235	256	269	282
0.50	1	---	---	---	---	---	---	---	---	283
	2	---	---	---	---	---	---	257	270	284
	3	---	---	---	---	---	---	258	271	285
	4	---	---	---	---	---	---	259	272	286
	5	---	---	---	---	---	---	260	273	287
	5.5	---	---	---	---	---	---	261	---	---
	6	---	---	---	---	---	---	262	274	288
	Tip	---	---	---	---	---	---	263	275	289
2	Tip	195	196	197	---	---	---	---	---	---
1		192	193	194	233	234	235	---	---	---
.50		198	199	200	236	237	238	---	---	---
.16		201	202	203	---	---	---	---	---	---
.08		204	205	206	---	---	---	---	---	---
.037		207	208	209	---	---	---	---	---	---
.015		210	---	---	---	---	---	---	---	---
.008		211	---	---	---	---	---	---	---	---
1	5	186	187	188	227	228	229	---	---	---
.50		---	---	---	239	240	241	---	---	---
.16		212	213	214	---	---	---	---	---	---
.037		215	216	217	---	---	---	---	---	---
1	Tip	[a]242	[a]243	[a]244	[a]245	[a]246	[a]247	← Fighter B - all six cases		

[a]Case number for fighter B.

TABLE XV.- FLUTTER SPEED AND FREQUENCY

Case	Airplane	Symmetric			Antisymmetric		
		V_f, mph	V_f, per unit	f_f, cps	V_f, mph	V_f, per unit	f_f, cps
1	Fighter A	989	1.74	14.2	1,091	1.92	8.7
2		1,080	1.90	10.4	1,102	1.94	6.13
3		892	1.57	16.8	1,068	1.88	11.3
4		835	1.47	12.4	1,011	1.78	8.1
5		1,102	1.94	15.0	1,142	2.01	8.7
6		972	1.71	14.8	1,085	1.91	9.1
7		1,000	1.76	13.7	1,119	1.97	8.3
8		1,222	2.15	16.8	1,369	2.41	10.2
9		795	1.40	12.0	886	1.56	7.4
11		813	1.43	14.0	989	1.74	8.6
12		710	1.25	13.9	636 892	1.12 1.57	16.6 8.5
13		619	1.09	12.9	545 778	.96 1.37	16.0 7.9
14		773	1.36	14.1	858	1.51	8.2
15		795	1.4	12.0	790	1.39	7.1
16		1,295	2.28	15.7	———	———	———
17		938	1.65	14.4	733	1.29	17.2
18		949	1.67	15.0	750	1.32	17.7
19		1,028	1.81	15.7	881	1.55	17.5
20		1,415	2.49	14.5	1,267	2.23	16.1
21		847	1.49	14.9	784	1.38	17.0
22		790	1.39	14.6	795	1.40	15.9
23	Fighter B	1,074	1.89	7.4	1,017	1.79	6.9
24		1,006	1.77	5.3	1,057	1.86	4.8
25		875	1.54	10.8	938	1.65	9.2
26		989	1.74	6.6	926	1.63	6.1
27		1,131	1.99	8.0	1,074	1.89	7.4
28		1,023	1.80	8.2	1,017	1.79	7.2
29		1,040	1.83	6.8	1,017	1.79	6.8
30		1,273	2.24	8.4	1,244	2.19	8.3
31		835	1.47	6.7	830	1.46	5.9
33		881	1.55	8.0	898	1.58	6.5
34		767	1.35	8.1	824	1.45	6.1
35		653	1.15	7.3	710	1.25	———
36		1,244	2.19	7.8	1,227	2.16	7.3
37		852	1.50	7.4	813	1.43	6.5
38		784	1.38	7.1	727	1.28	5.5
39		1.358	2.39	8.5	1,392	2.45	8.3
40		943	1.66	8.1	750	1.32	11.2
41		932	1.64	9.0	801	1.41	11.4
42		983	1.73	9.2	1,023	1.80	11.5
43		1,051	1.85	6.7	1,131	1.99	9.2
44		847	1.49	11.8	847	1.49	13.9
45		864	1.52	8.0	1,080	1.90	10.0
46		1,074	1.89	9.8	1,159	2.04	12.6
47		983	1.73	10.2	983	1.73	12.9
48		960	1.69	8.7	1,074	1.89	11.2
49		1,176	2.07	11.7	1,313	2.31	13.8
50		801	1.41	8.3	801	1.41	10.6
51		2,171	3.82	11.5	2,057	3.62	13.8
52		1,188	2.09	8.8	1,142	2.01	12.0
53		898	1.58	9.3	1,017	1.79	11.2
54		835	1.47	8.9	1,307	2.30	7.9
55		756	1.33	8.4	989	1.74	6.4
56		1,347	2.37	10.2	1,250	2.20	12.4
57		784	1.38	8.0	949	1.67	11.4

TABLE XV.- FLUTTER SPEED AND FREQUENCY - Continued

Case	Airplane	Symmetric			Antisymmetric		
		V_f, mph	V_f, per unit	f_f, cps	V_f, mph	V_f, per unit	f_f, cps
58	Bomber A	710	1.25	9.4	869	1.53	8.8
59		625	1.10	7.5	648	1.14	7.0
60		943	1.66	12.2	972	1.71	16.8
61		602	1.06	8.2	682	1.20	7.5
62		784	1.38	10.2	1,040	1.83	9.9
63		688	1.21	9.7	761	1.34	8.6
64		733	1.29	9.3	1,000	1.76	12.6
65		898	1.58	11.4	1,227	2.16	----
66		563	.99	7.9	619	1.09	7.0
68		625	1.10	8.8	676	1.19	8.0
69		585	1.03	8.4	563	.99	7.4
70		540	.95	7.8	455	.80	6.7
71		534	.94	8.6	528	.93	7.7
72		1,085	1.91	17.9	699 855	1.23 1.47	9.6 (a)
73		1,193	2.10	17.7	886 1,011	1.56 1.78	10.6 18.9
74		.784	1.38	8.6	653	1.15	7.5
75		1.165	2.05	20.9	903	1.59	20.1
76		966	1.70	14.5	597 705	1.05 1.24	8.2 15.4
77		1,017	1.79	21.8	778	1.37	9.9
78		1,034	1.82	17.4	744	1.31	9.7
79		886	1.56	19.3	710	1.25	9.0
80		1,085	1.91	23.7	869	1.53	11.0
81		847	1.49	14.2	608	1.07	7.9
82		750	1.32	18.3	642 676	1.13 1.19	8.7 (a)
83		580	1.02	17.5	563 608	.99 1.07	17.4 8.0
84		818	1.44	9.4	886	1.56	9.9
85		864	1.52	7.8	767	1.35	8.7
86		761	1.34	11.4	983	1.73	9.6
87		676	1.19	8.0	864	1.52	7.1
88		909	1.60	10.8	852	1.50	12.0
89		790	1.39	9.6	989	1.74	8.1
90		830	1.46	9.6	773	1.36	10.1
91		1,017	1.79	11.8	949	1.67	12.5
92		648	1.14	7.8	807	1.42	6.6
94		705	1.24	9.5	648	1.14	9.8
95		636	1.12	8.9	563	.99	10.5
96		540	.95	8.1	466	.82	10.5
97		614	1.08	9.8	563	.99	10.7
98	Bomber B	1,295	2.28	10.7	1,261	2.22	9.8
99		1,290	2.27	7.3	1,250	2.20	7.0
100		1,278	2.25	14.1	1,341	2.36	14.3
101		1,216	2.14	9.9	1.176	2.07	9.5
102		1,341	2.36	11.1	1,318	2.32	10.3
103		1,307	2.30	10.9	1,244	2.19	10.2
104		1,273	2.24	10.5	1,278	2.25	10.6
105		1,563	2.75	12.9	1,568	2.76	13.0
106		1,068	1.88	8.9	1,017	1.79	8.3
107		1,148	2.02	10.1	1,108	1.95	9.4
108		1,040	1.83	9.2	1,011	1.78	8.9
109		898	1.58	8.1	875	1.54	8.0
110		1,023	1.80	9.3	1,000	1.76	9.1
111		966	1.70	8.8	909	1.60	8.2
112		1,699	2.99	12.5	1,750	3.08	12.6
113		1,295	2.28	10.2	1,332	2.38	8.8
114		1,489	2.62	11.7	1.432	2.52	11.3
115		1,284	2.26	7.1	1,261	2.22	6.6

[a]High frequency.

TABLE XV.- FLUTTER SPEED AND FREQUENCY - Concluded

Case	Airplane	Symmetric			Antisymmetric		
		V_f, mph	V_f, per unit	f_f, cps	V_f, mph	V_f, per unit	f_f, cps
116	Bomber B	1,284	2.26	13.7	1,347	2.37	15.3
117		1,227	2.16	9.4	1,239	2.18	8.4
118		1,341	2.36	10.8	1,477	2.60	{9.6 {11.4
119		1,284	2.26	10.2	1,284	2.26	9.3
120		1,250	2.20	10.6	1,347	2.37	11.3
121		1,534	2.70	13.0	1,653	2.91	13.8
122		1,051	1.85	8.3	1,051	1.85	7.6
123		1,108	1.95	9.2	1,074	1.89	8.3
124		985	1.73	8.6	955	1.68	7.8
125		813	1.43	7.4	775	1.36	7.0
126		1,525	2.68	8.8	1,477	2.60	7.8
127		1,472	2.59	15.5	1,409	2.48	14.8
128		1,392	2.45	10.4	1,335	2.35	10.5
129		1,557	2.74	12.2	1,500	2.64	12.0
130		1,528	2.69	11.5	1,477	2.60	11.0
131		1,420	2.50	11.3	1,386	2.44	10.7
132		1,738	3.06	12.6	1,699	2.99	13.1
133		1,250	2.20	9.4	1,205	2.12	9.0
134		1,364	2.40	11.0	1,284	2.26	11.0
135		1,261	2.22	10.2	1,188	2.09	10.6
136		1,119	1.97	8.7	1,080	1.90	10.2
137		1,165	2.05	7.1	1,244	2.19	10.3
138		1,023	1.80	4.5	1,239	2.18	7.0
139		1,261	2.22	13.7	1,205	2.12	14.2
140		1,108	1.95	7.0	1,170	2.06	9.8
141		1,182	2.08	7.3	1,284	2.26	10.4
142		1,205	2.12	8.1	1,267	2.23	10.7
143		1,108	1.95	6.1	1,239	2.18	9.6
144		1,358	2.39	7.5	1,517	2.67	11.8
145		985	1.73	6.6	1,054	1.82	8.7
146		1,074	1.89	7.3	1,131	1.99	10.2
147		1,023	1.80	7.7	1,054	1.82	9.6
148		898	1.58	8.3	898	1.58	8.6
149		972	1.71	6.7	1,023	1.80	9.7
150		881	1.55	7.2	909	1.60	8.5
151		1,485	2.61	7.3	1,665	2.93	10.8
152		1,216	2.14	10.1	1,216	2.14	10.4
153		1,114	1.96	6.6	1,421	2.50	10.4
154		1,193	2.10	6.5	1,216	2.14	6.7
155		1,159	2.04	13.8	1,170	2.06	13.9
156		1,136	2.00	9.4	1,142	2.01	9.2
157		1,261	2.22	10.5	1,261	2.22	10.4
158		1,199	2.11	10.0	1,193	2.10	9.9
159		1,199	2.11	9.9	1,182	2.08	10.1
160		1,466	2.58	12.1	1,449	2.55	12.4
161		977	1.72	8.1	977	1.72	8.1
162		1,057	1.86	9.9	1,057	1.86	9.8
163		949	1.67	9.4	960	1.69	9.6
164		818	1.44	8.7	818	1.44	8.6
165		1,040	1.83	4.3	1,438	2.53	7.16
166		1,244	2.19	10.2	1,375	2.42	14.0
167		1,080	1.90	6.4	1,347	2.37	10.0
168		1,125	1.98	6.6	1,460	2.57	10.5
169		1,205	2.12	7.4	1,455	2.56	11.2
170		1,000	1.76	5.5	1,386	2.44	9.7
171		1,227	2.16	6.7	1,699	2.99	11.9
172		985	1.73	6.0	1,188	2.09	9.1
173		1,040	1.83	6.5	1,313	2.31	10.9
174		1,000	1.76	6.5	1,216	2.14	11.0
175		920	1.62	6.5	1,085	1.91	10.5

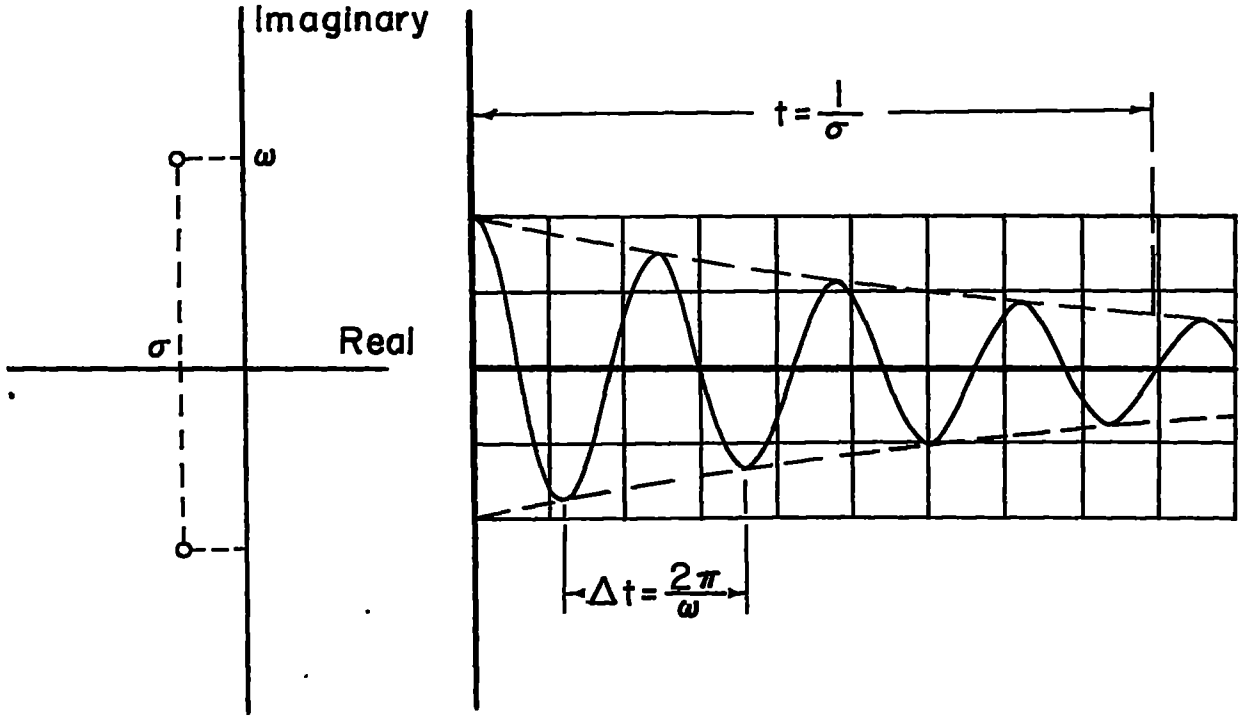

Figure 1.- Transient response corresponding to roots of characteristic equation.

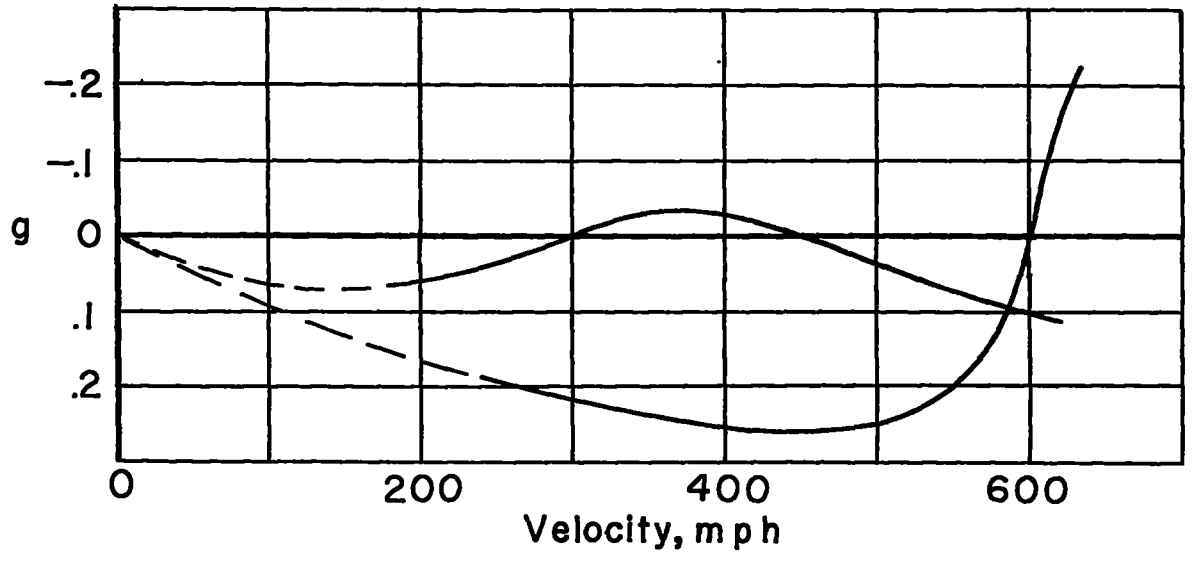

Figure 2.- Variation of g with velocity for typical flutter roots.

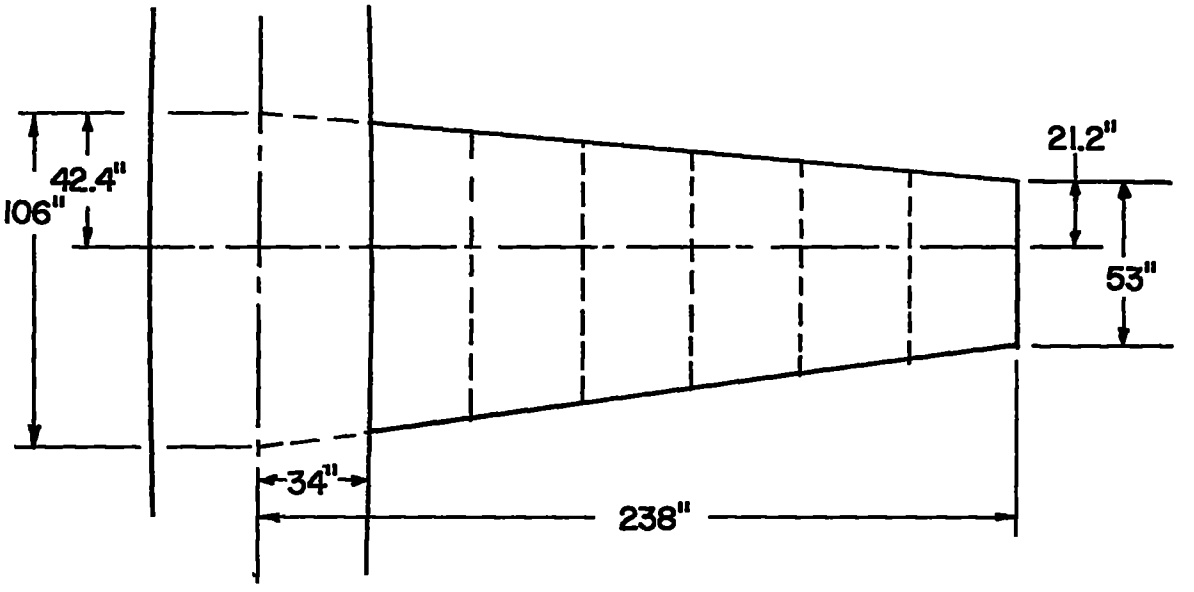

(a) Fighter A.

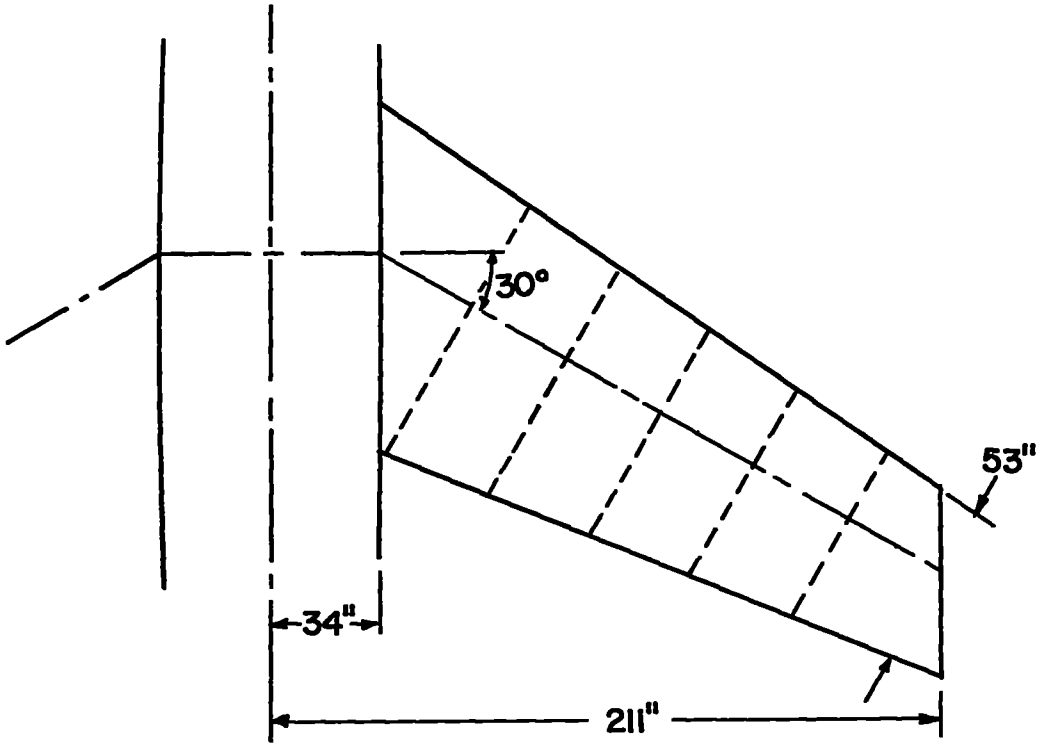

(b) Fighter B.

Figure 3.- Plan forms and cell divisions of basic airplane

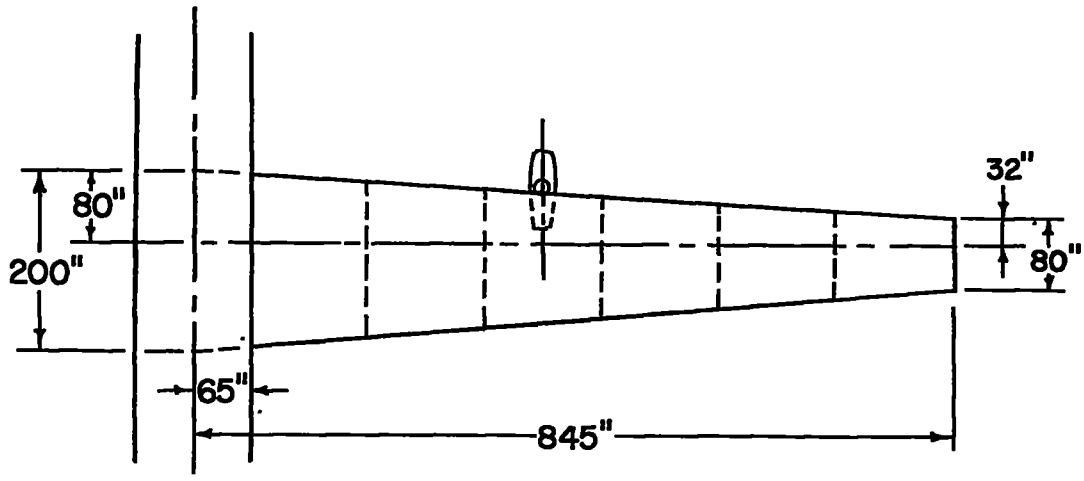

(c) Bomber A.

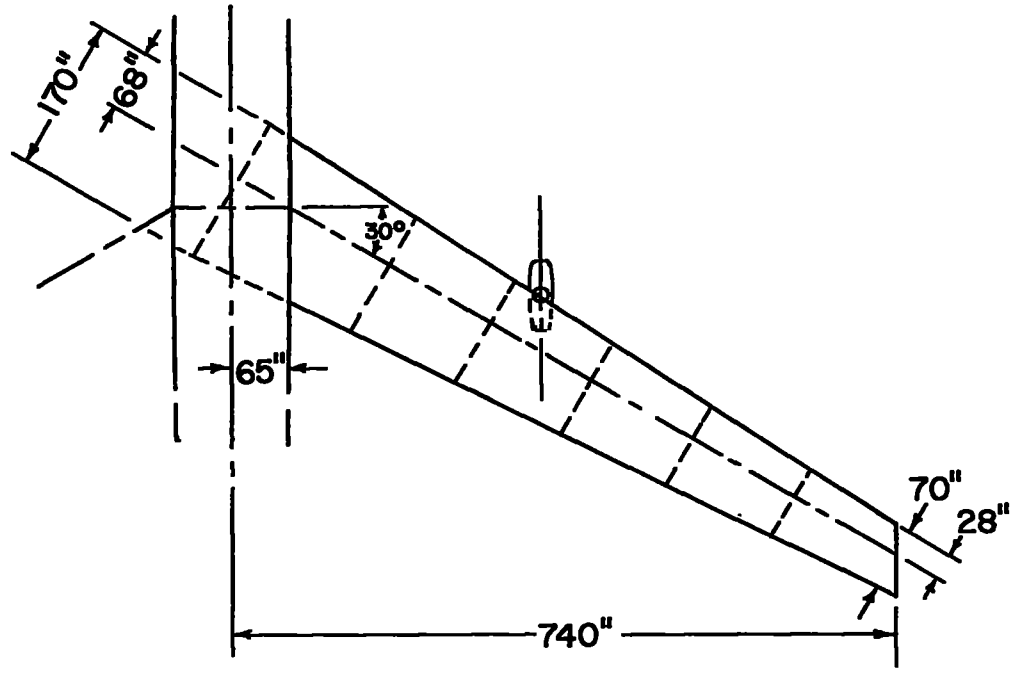

(d) Bomber B.

Figure 3.- Concluded.

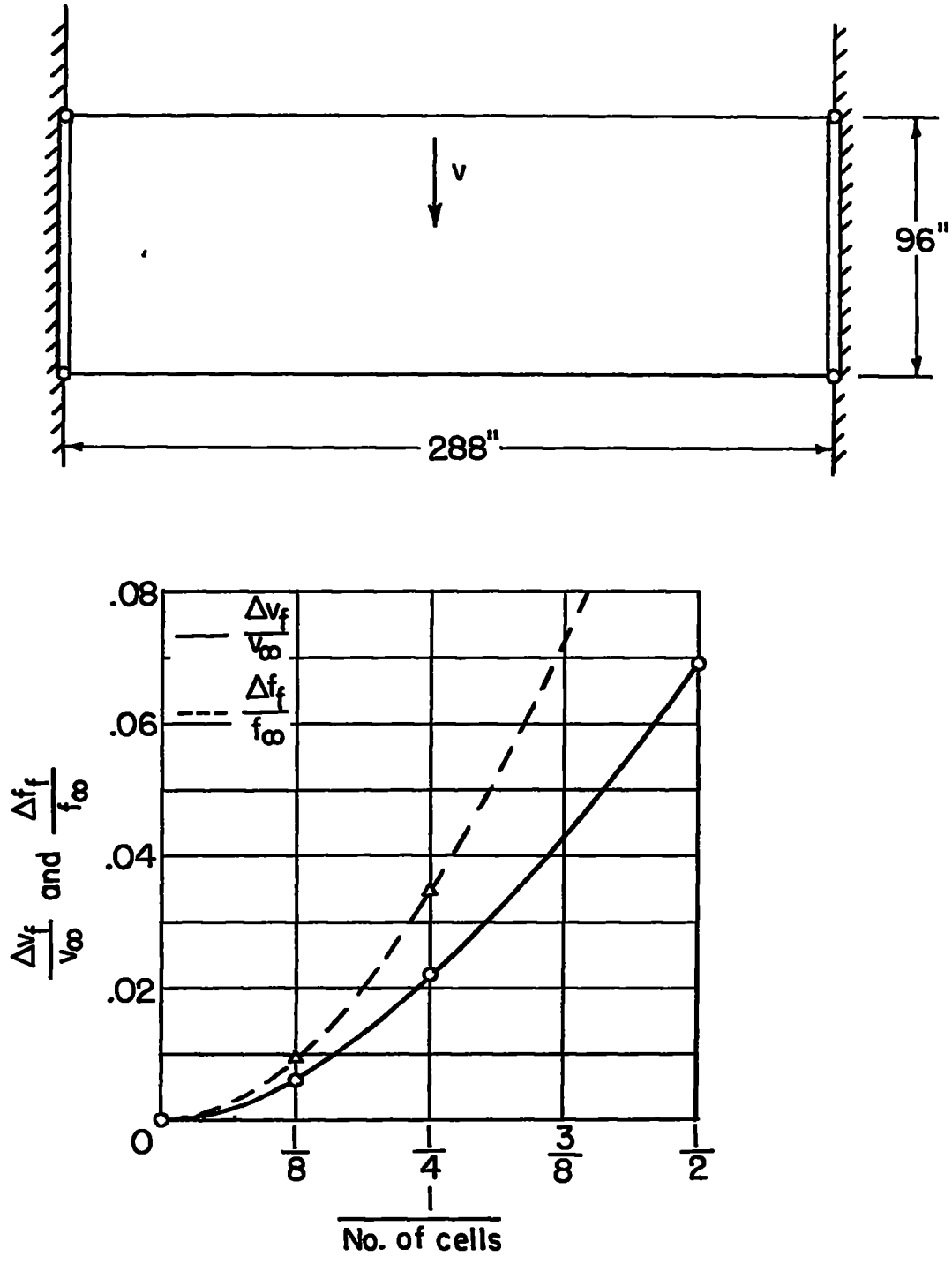

Figure 4.- Finite-difference flutter-speed errors of pinned-pinned beam.

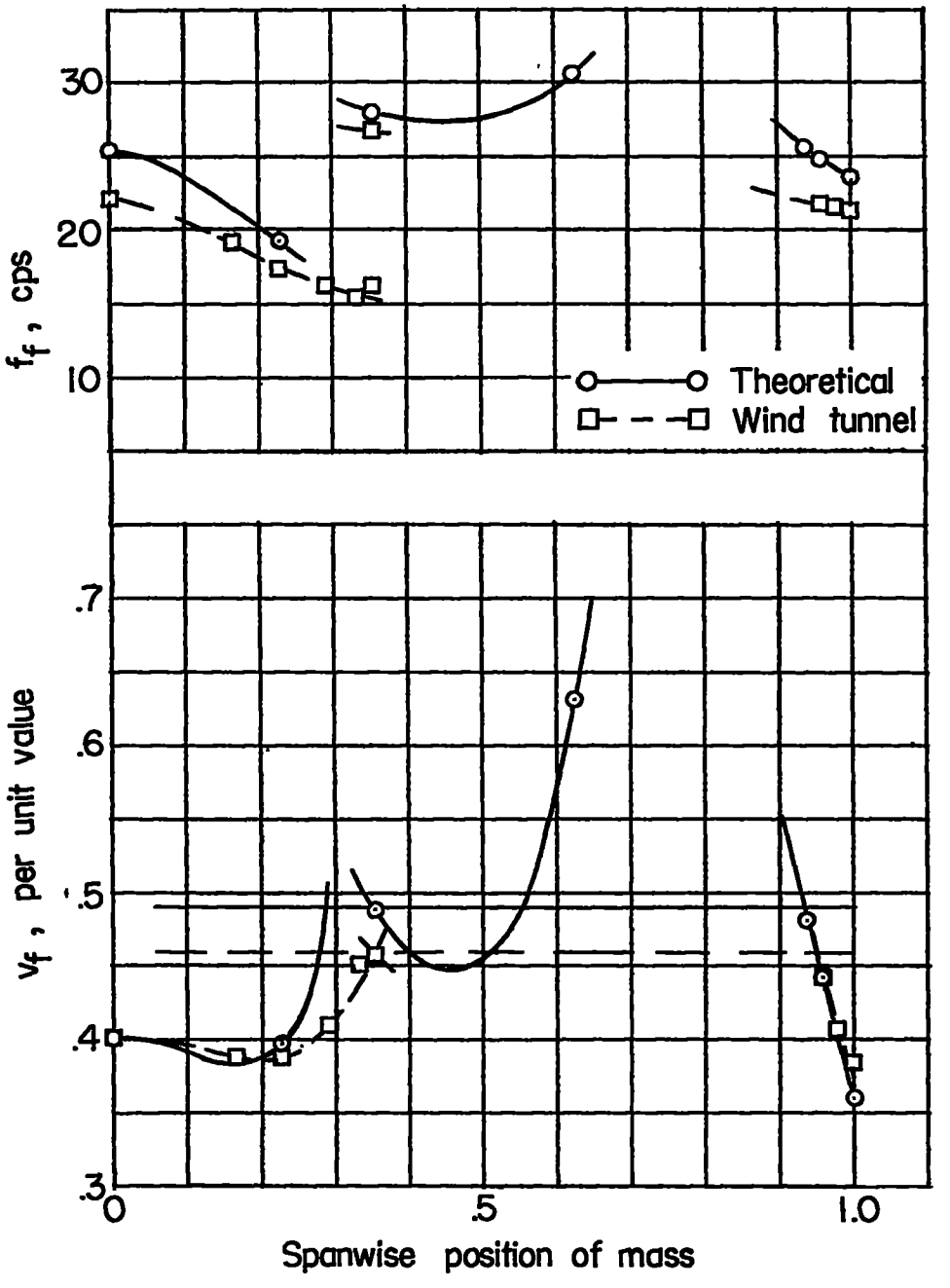

(a) Theoretical and wind-tunnel flutter characteristics.

Figure 5.- Flutter characteristics of uniform cantilever wing with concentrated mass.

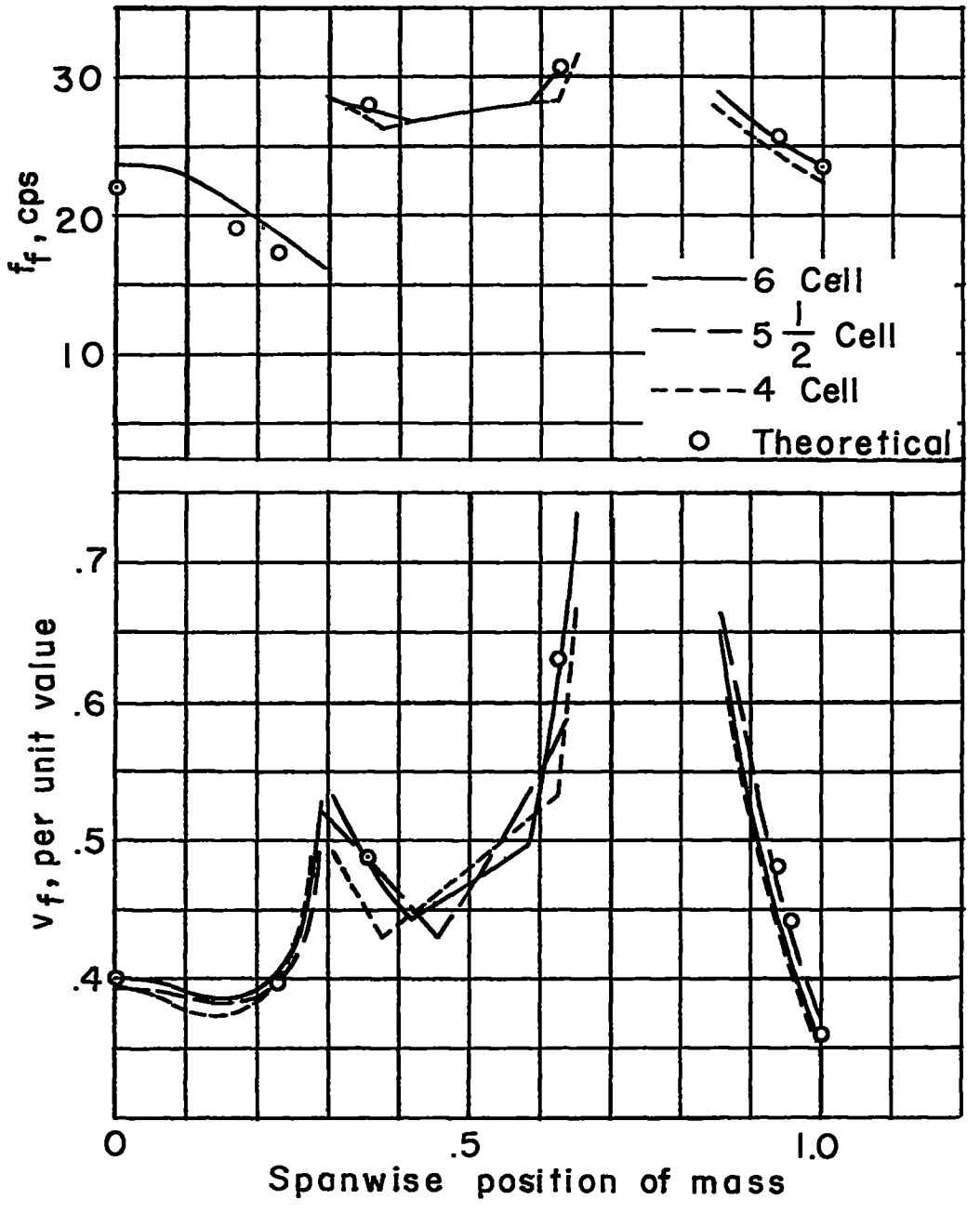

(b) Flutter characteristics of finite-difference analog.

Figure 5.- Concluded.

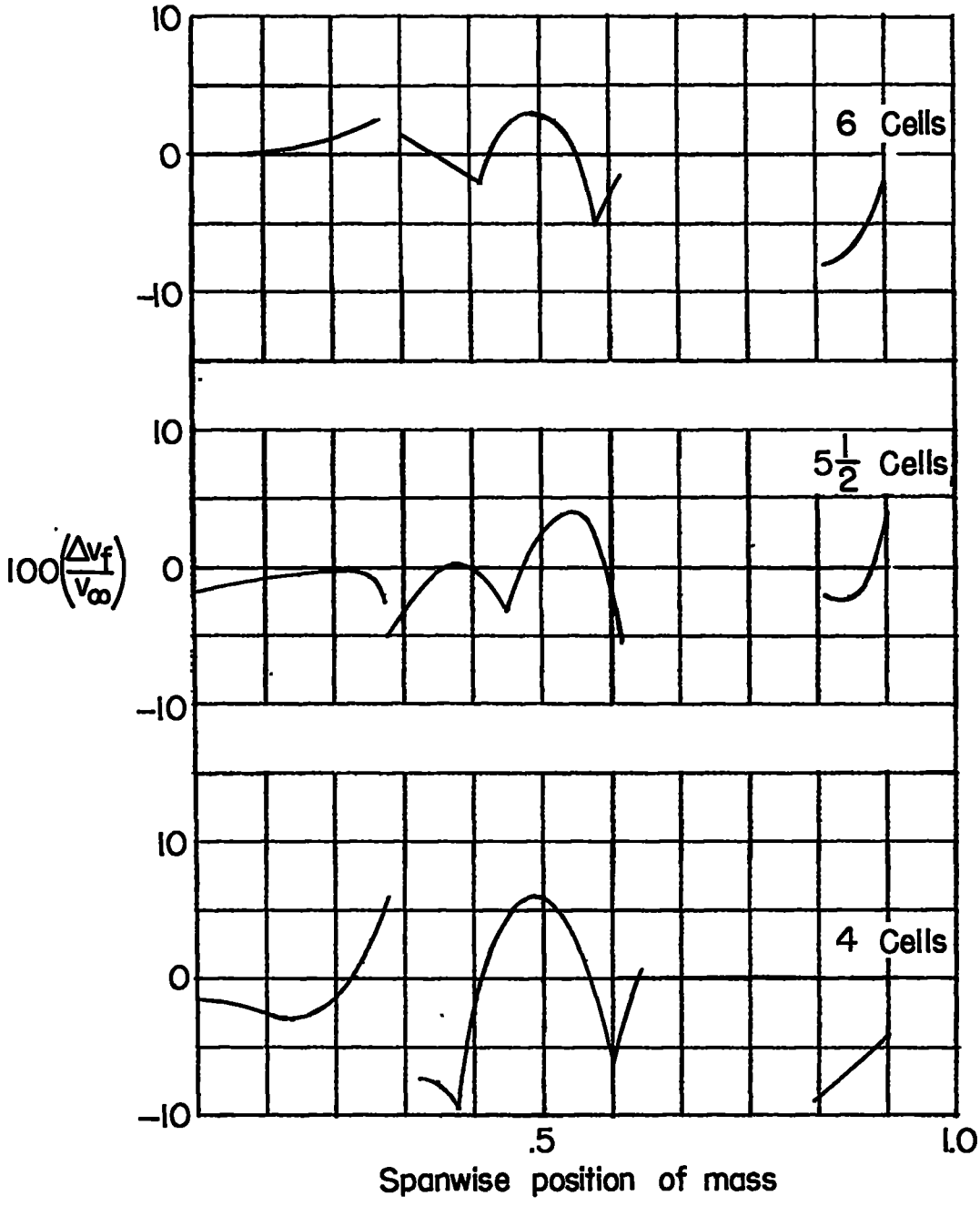

Figure 6.- Flutter-speed errors of finite-difference analog of uniform cantilever wing with concentrated mass.

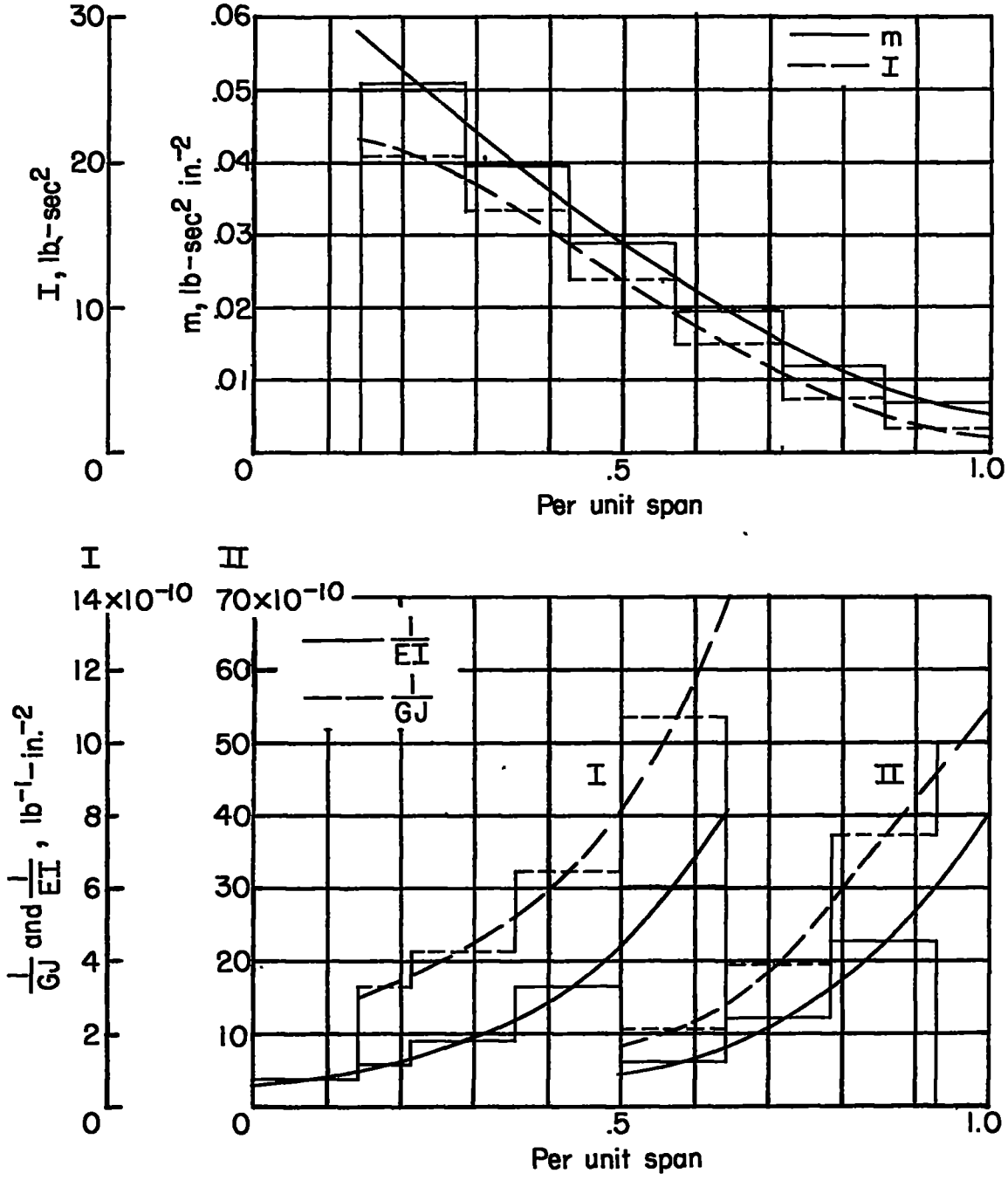

(a) Basic fighter A.

Figure 7.- Inertia and stiffness properties of wing.

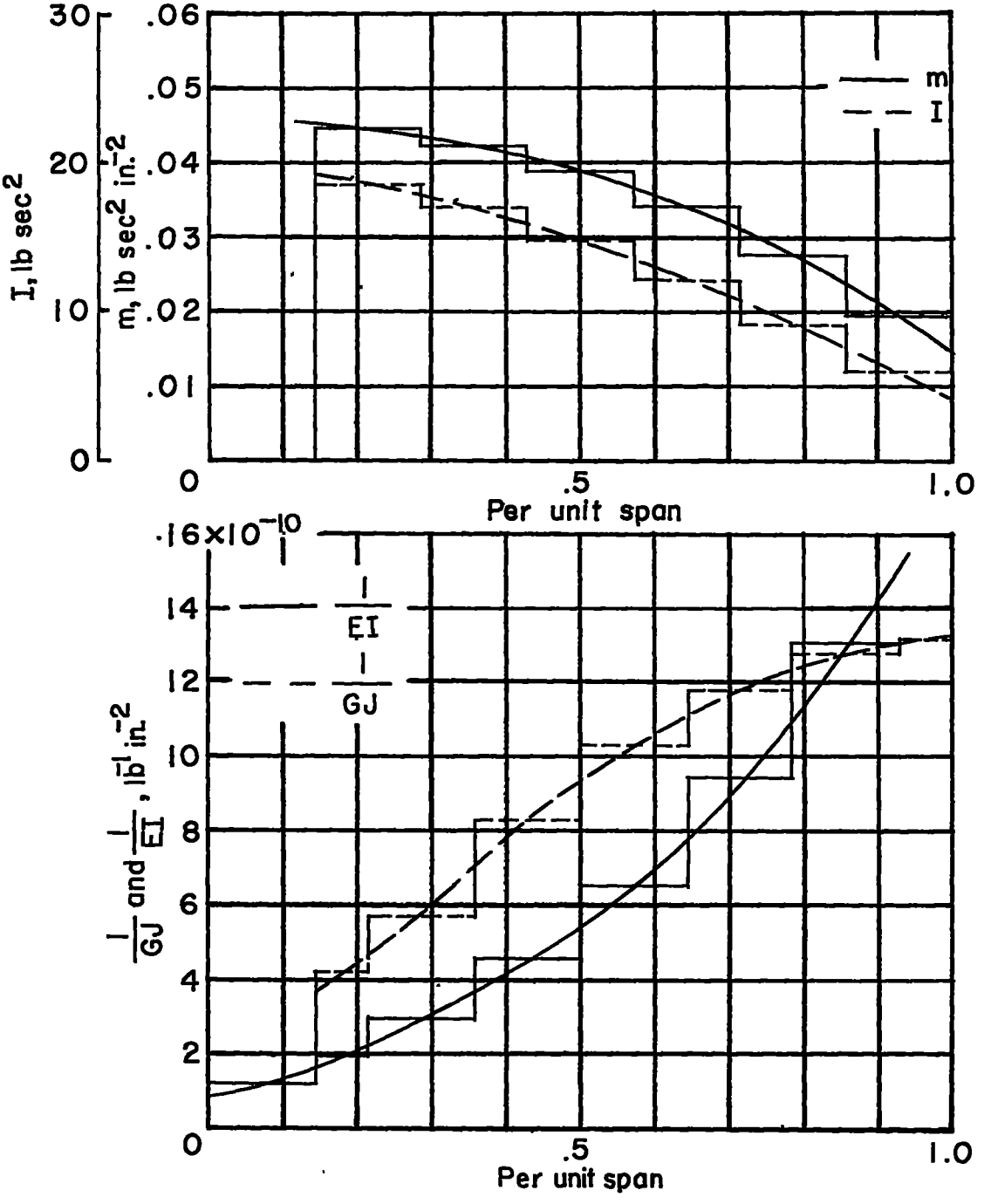

(b) Basic fighter B.

Figure 7.- Continued.

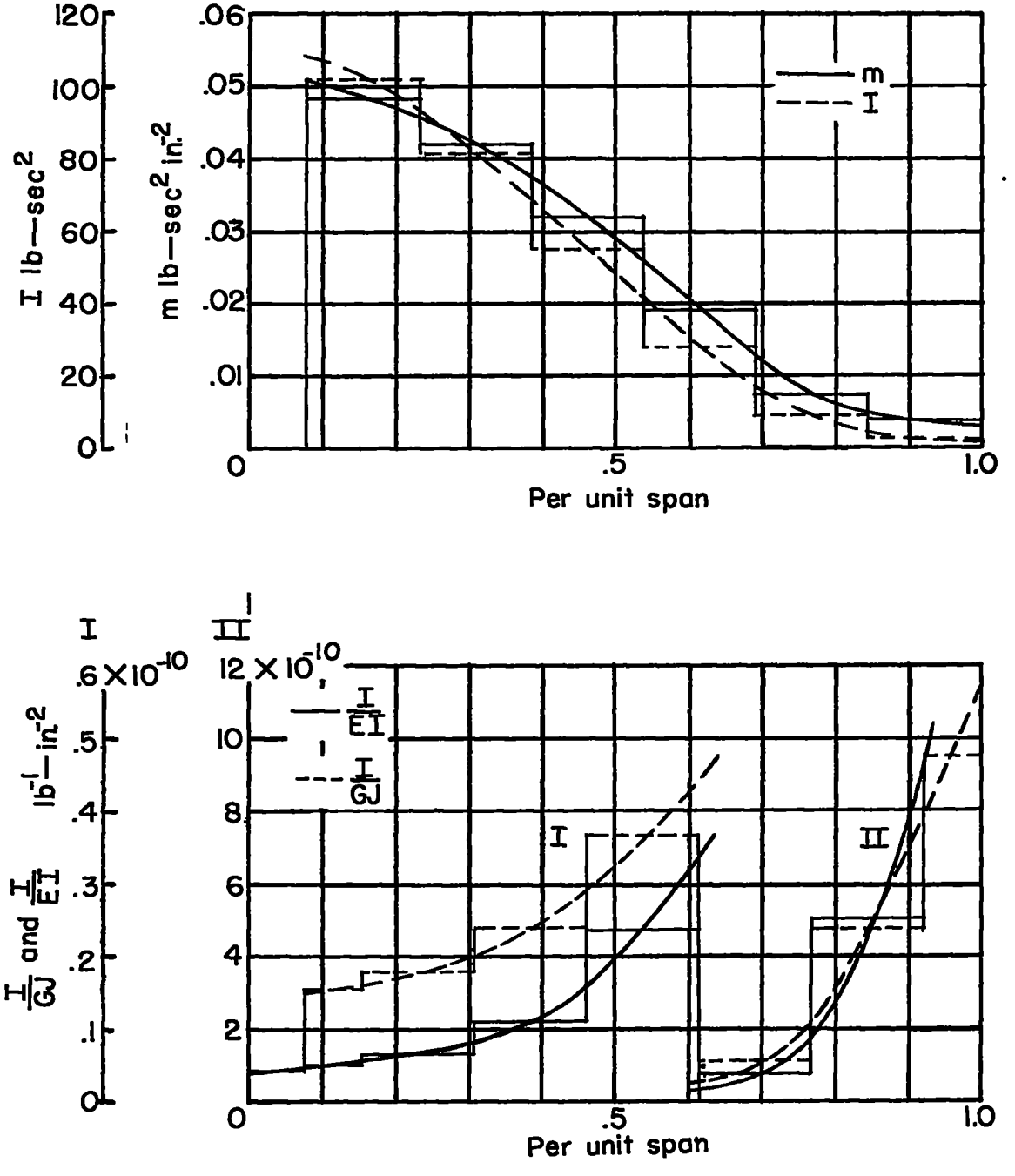

(c) Basic bomber A.

Figure 7.- Continued.

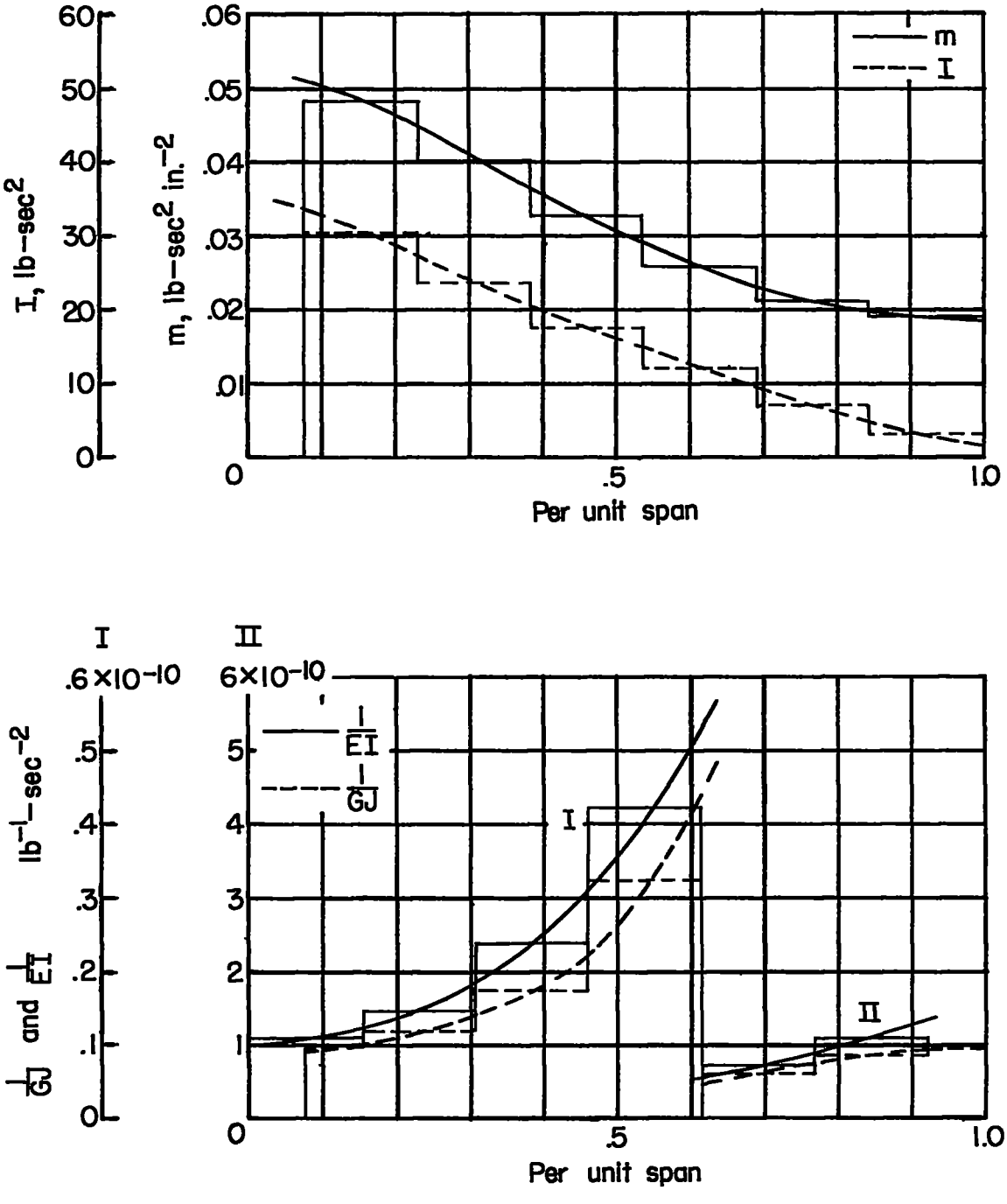

(d) Basic bomber B.

Figure 7.- Concluded.

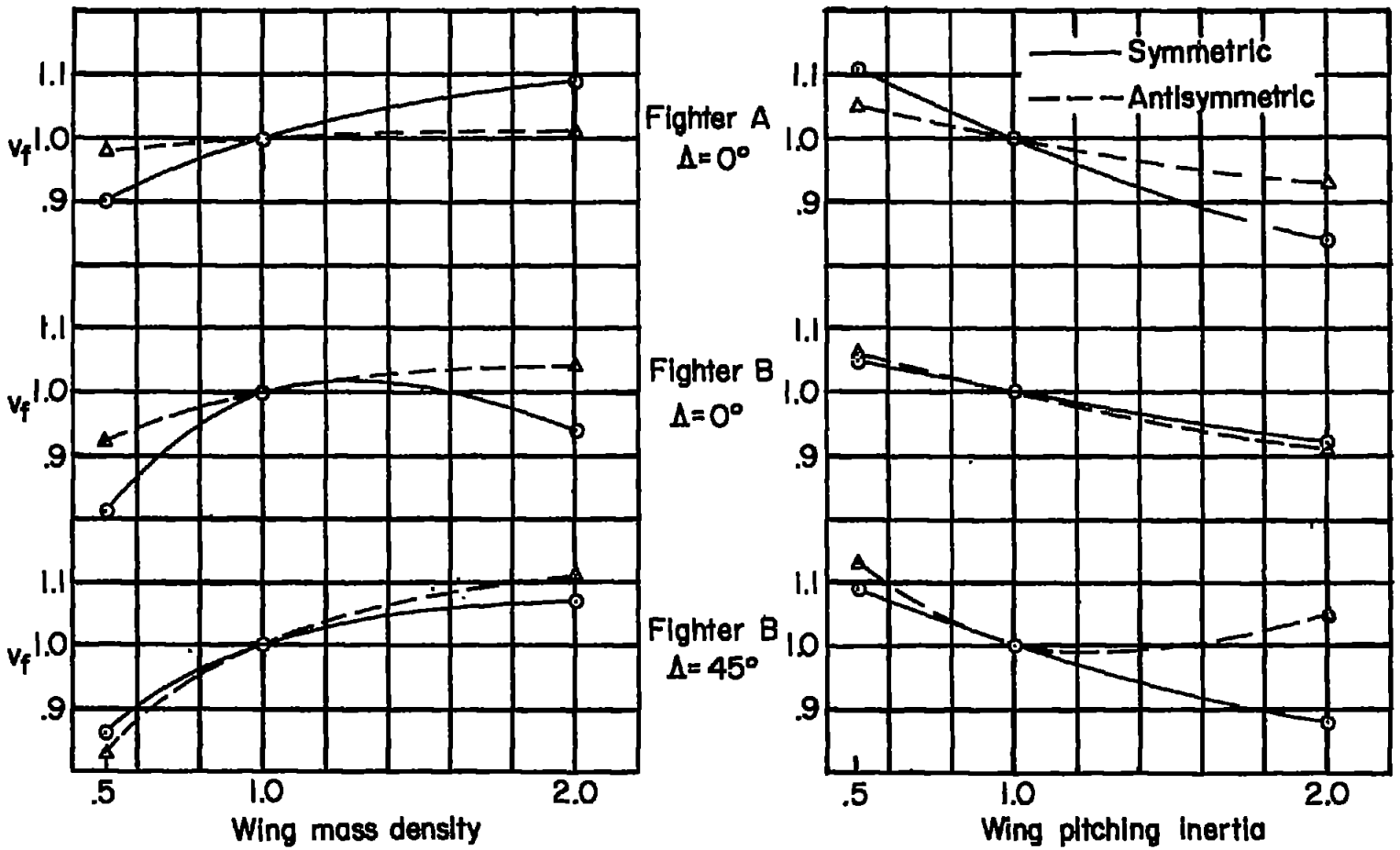

(a) Fighters A and B.

Figure 8.- Effect of wing mass and inertia variations.

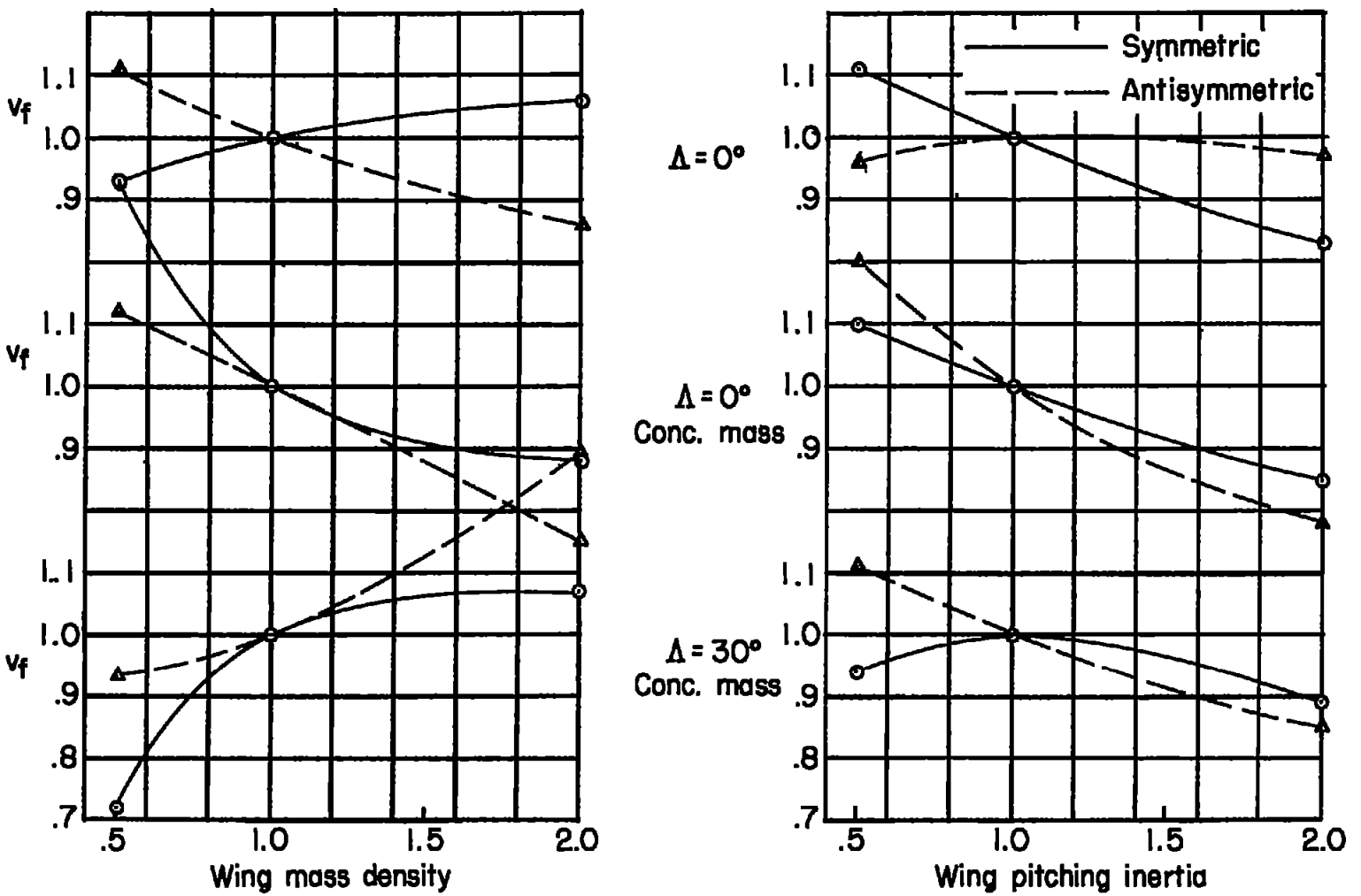

(b) Bomber A.

Figure 8.- Continued.

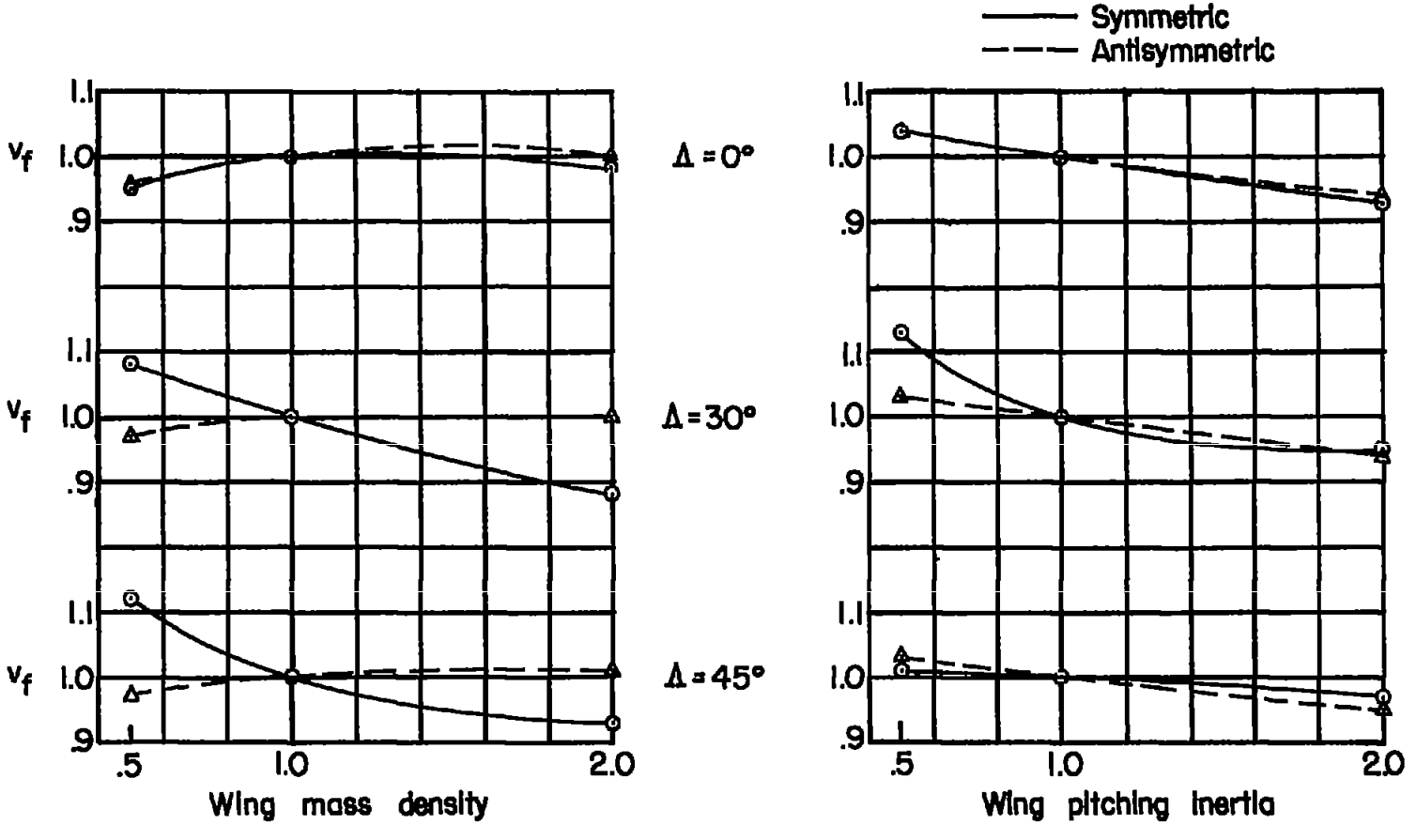

(c) Bomber B.

Figure 8.- Continued.

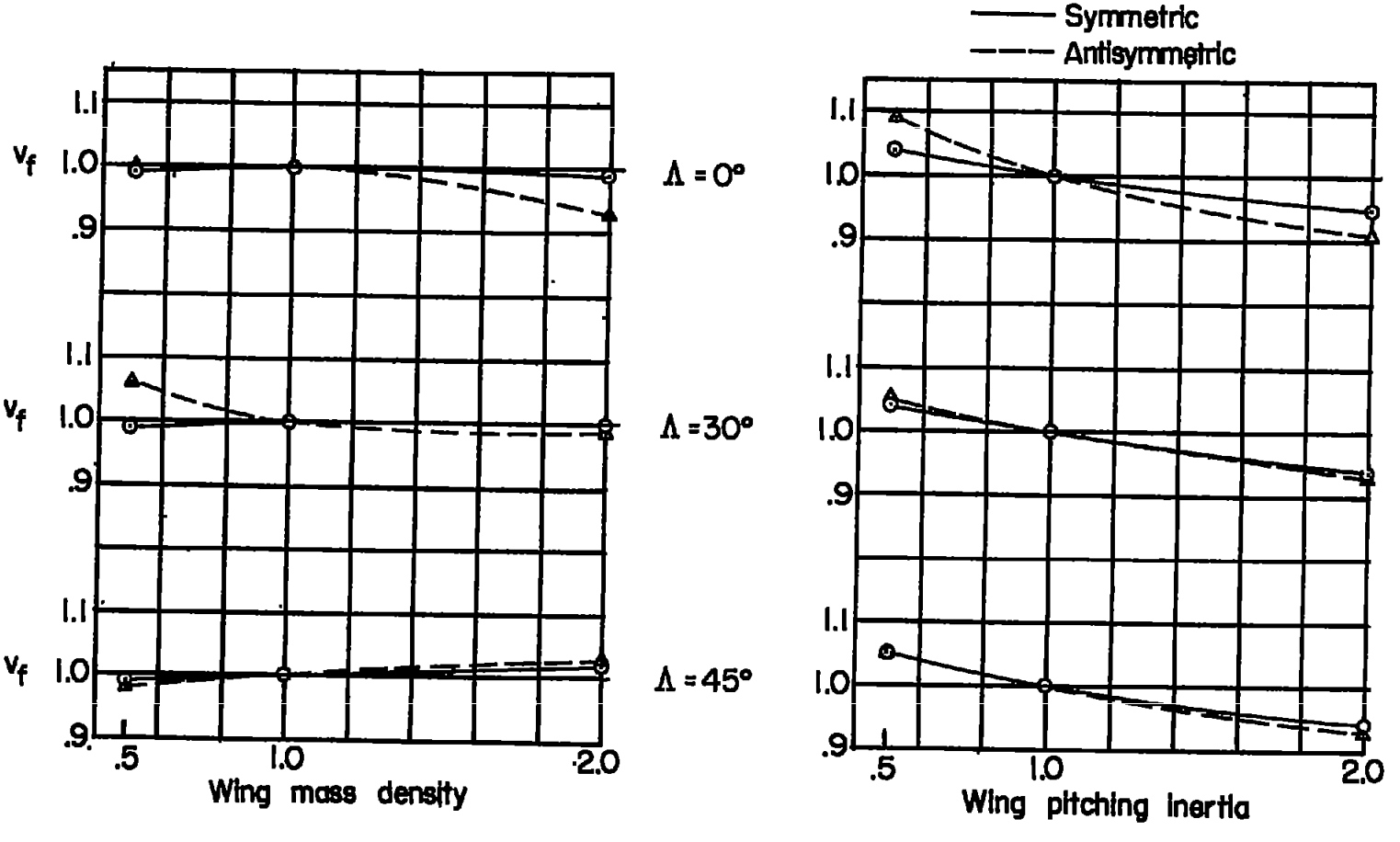

(d) Bomber B with concentrated mass.

Figure 8.- Concluded.

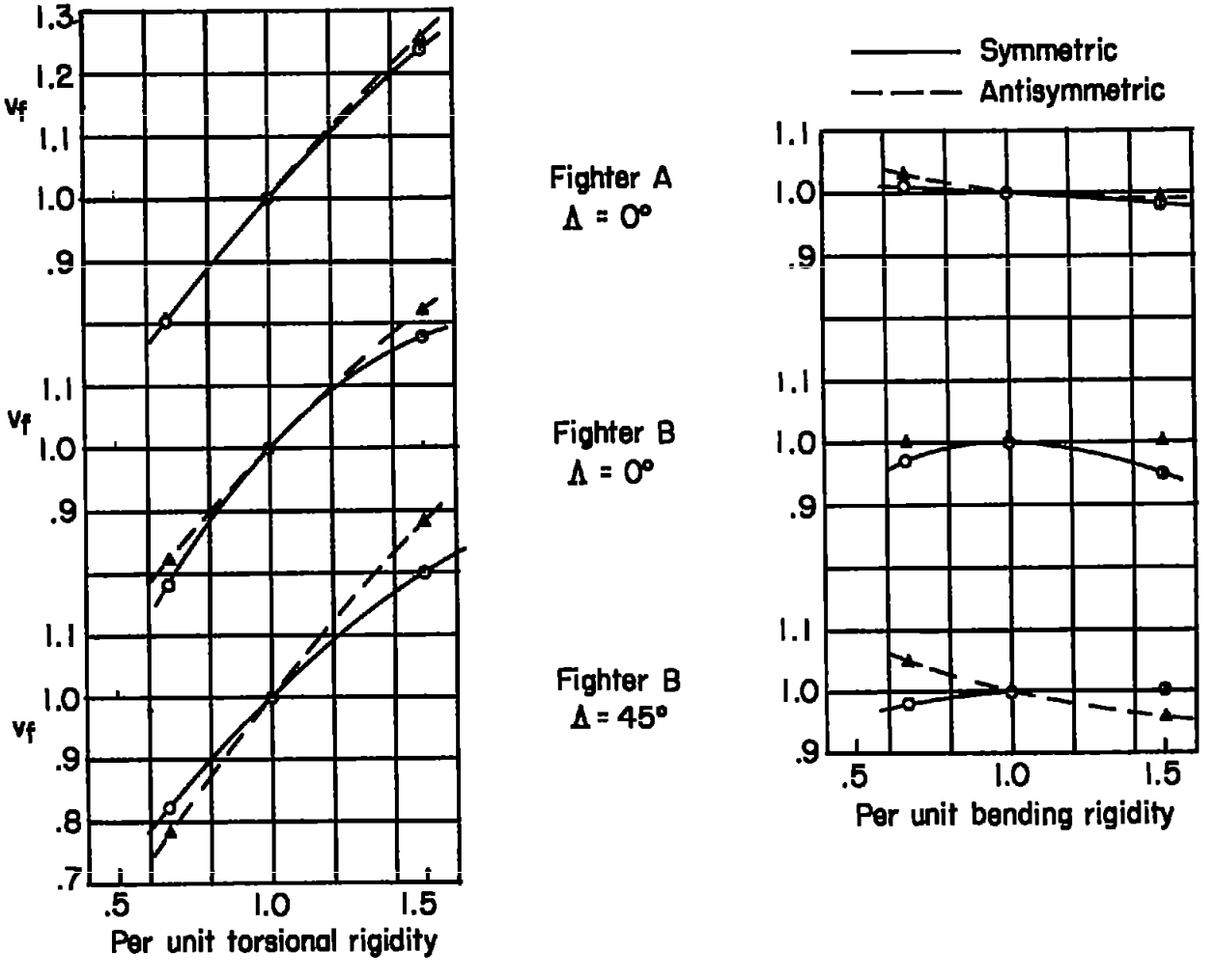

(a) Fighters A and B.

Figure 9.- Flutter speed as a function of wing rigidity.

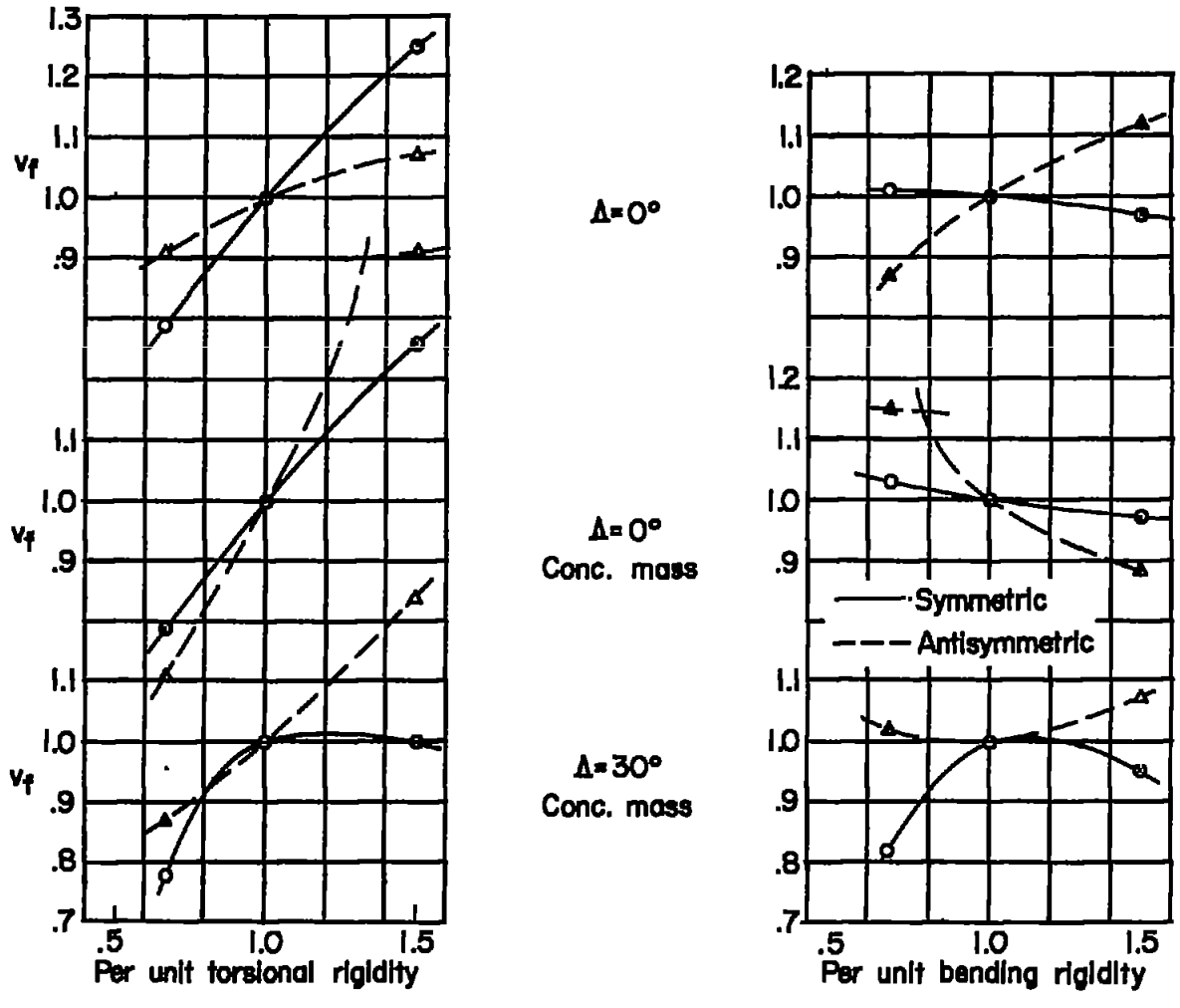

(b) Bomber A; bare wing and concentrated mass on wing.

Figure 9.- Continued.

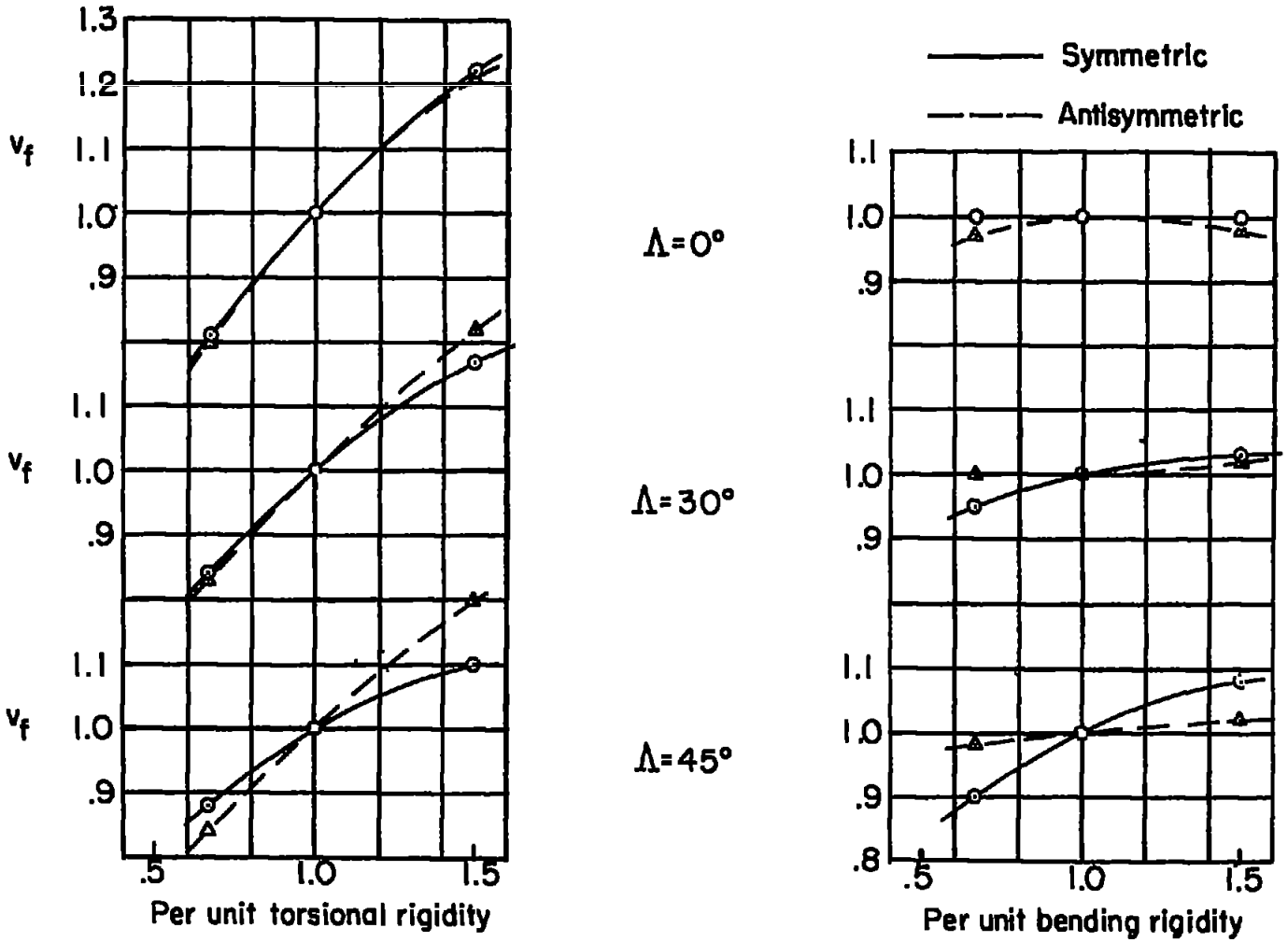

(c) Bomber B; bare wing.

Figure 9.- Continued.

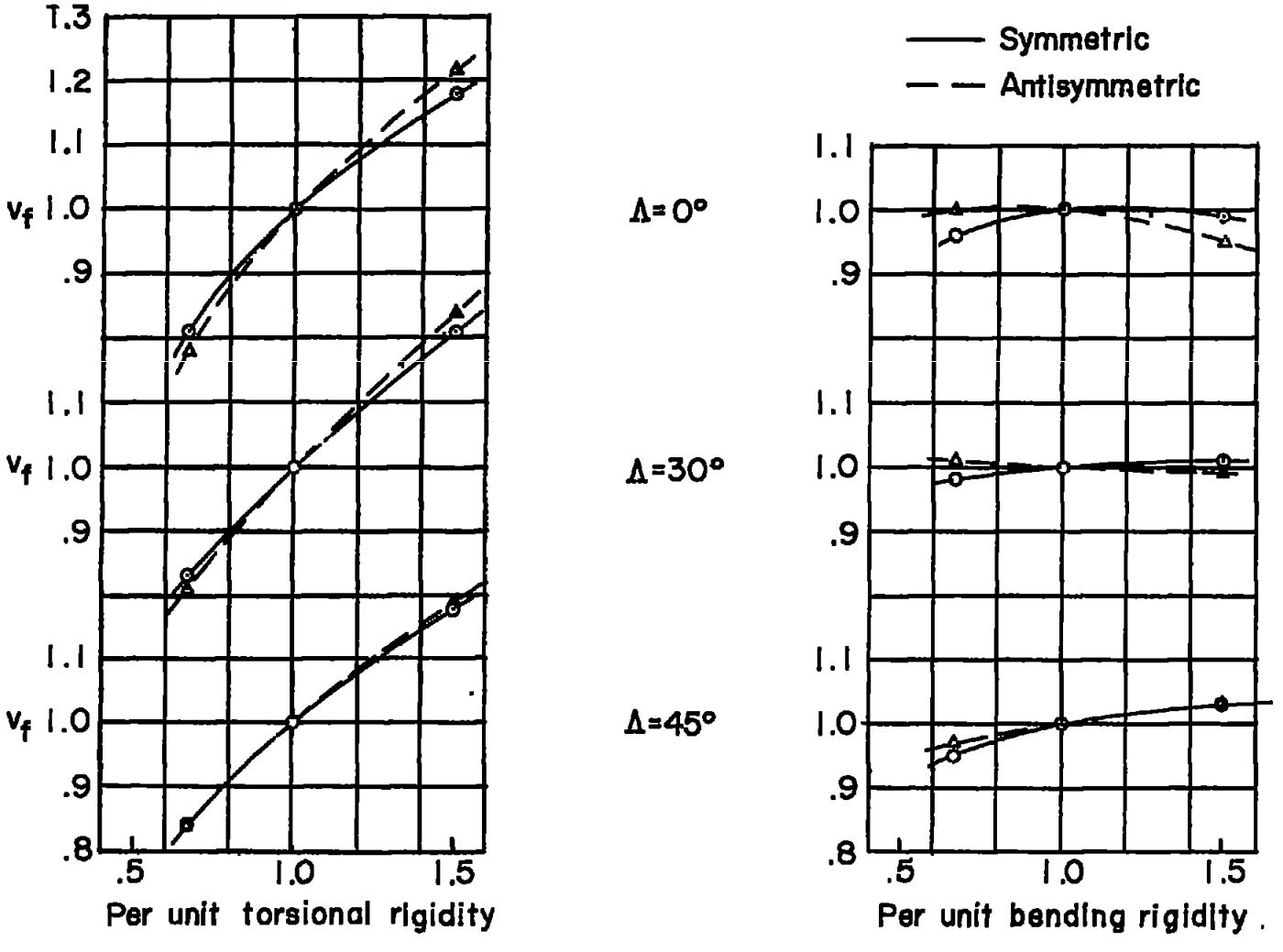

(d) Bomber B; concentrated mass on wing.

Figure 9.- Concluded.

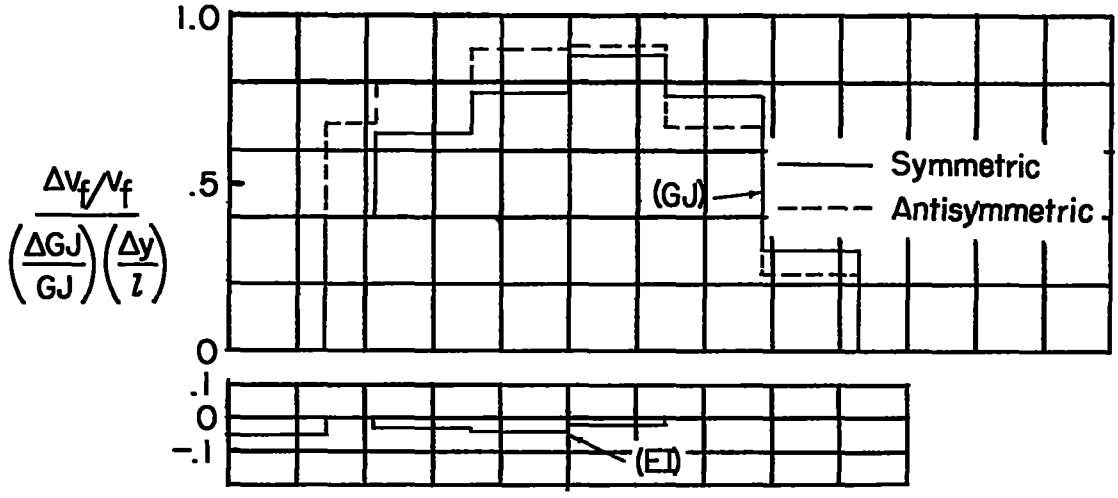

(a) Fighter A.

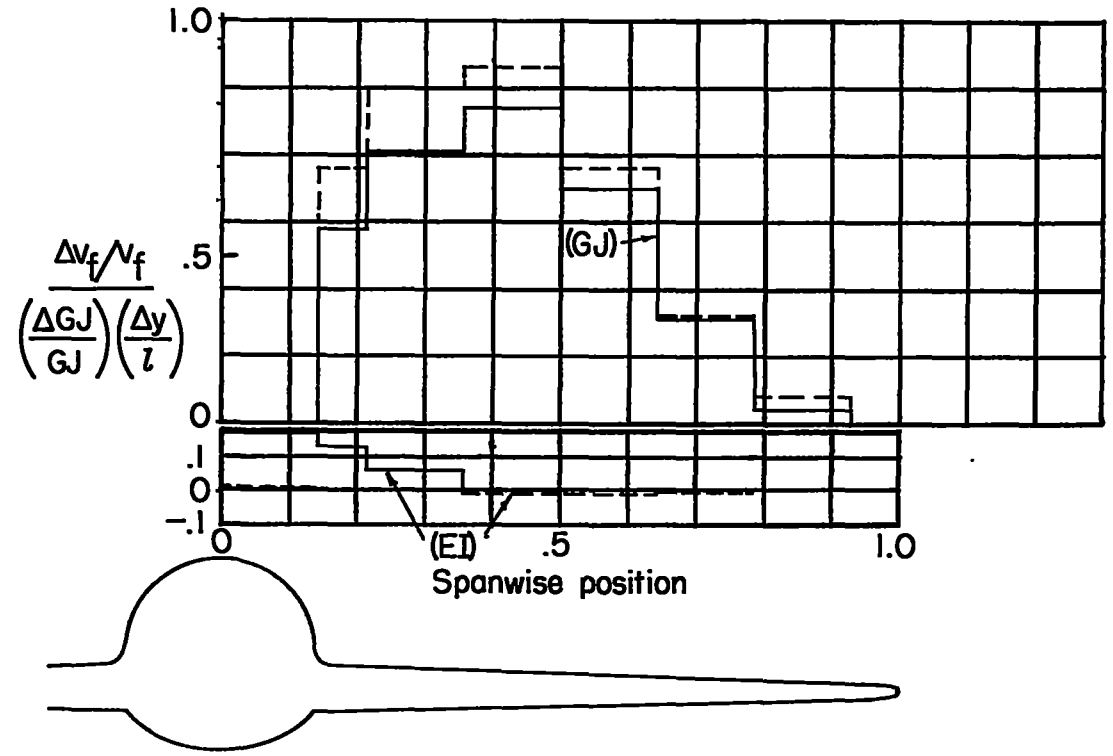

(b) Fighter B.

Figure 10.- Effect of local stiffness variation on flutter speed.

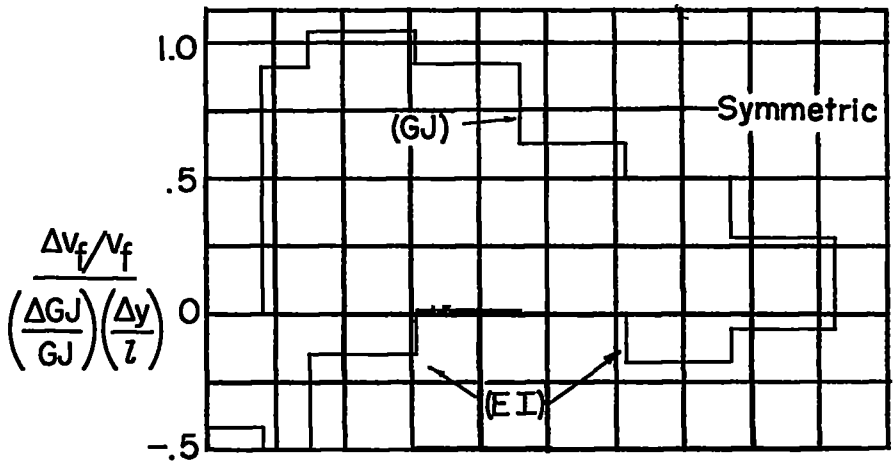

(c) Bomber A; bare wing.

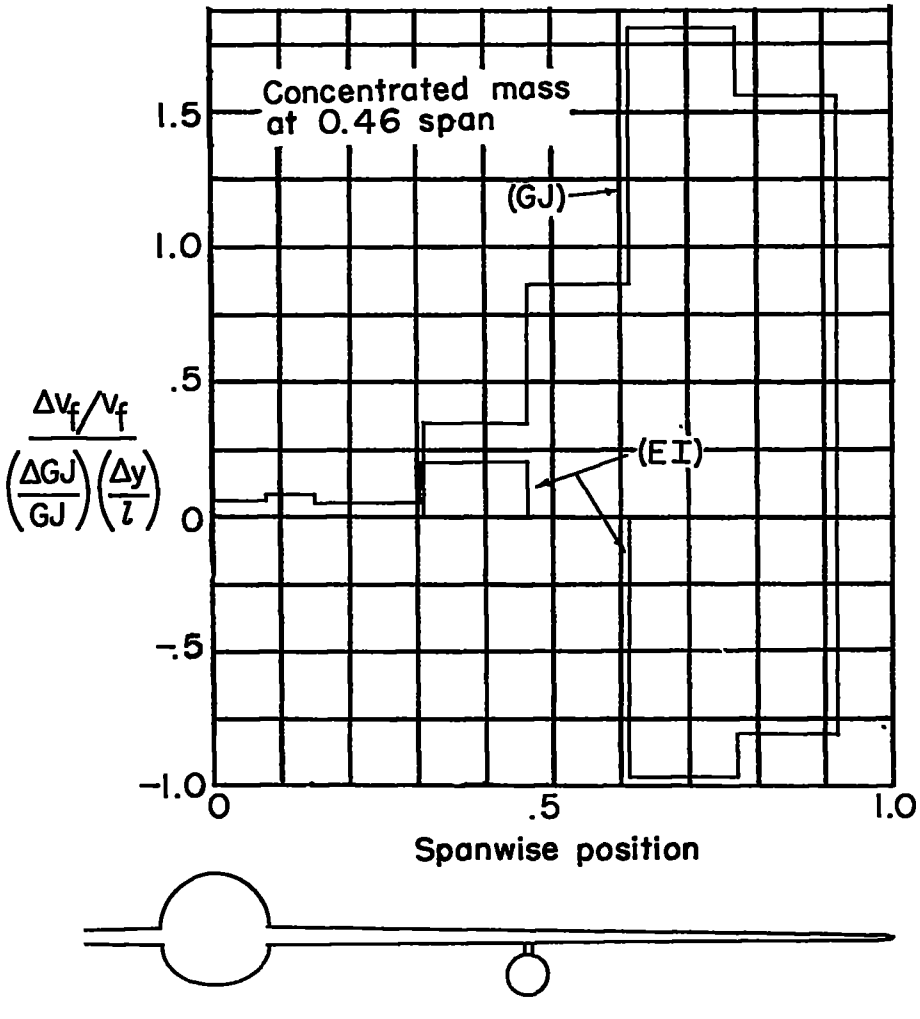

(d) Bomber A; concentrated mass at 0.46 span.

Figure 10.- Concluded.

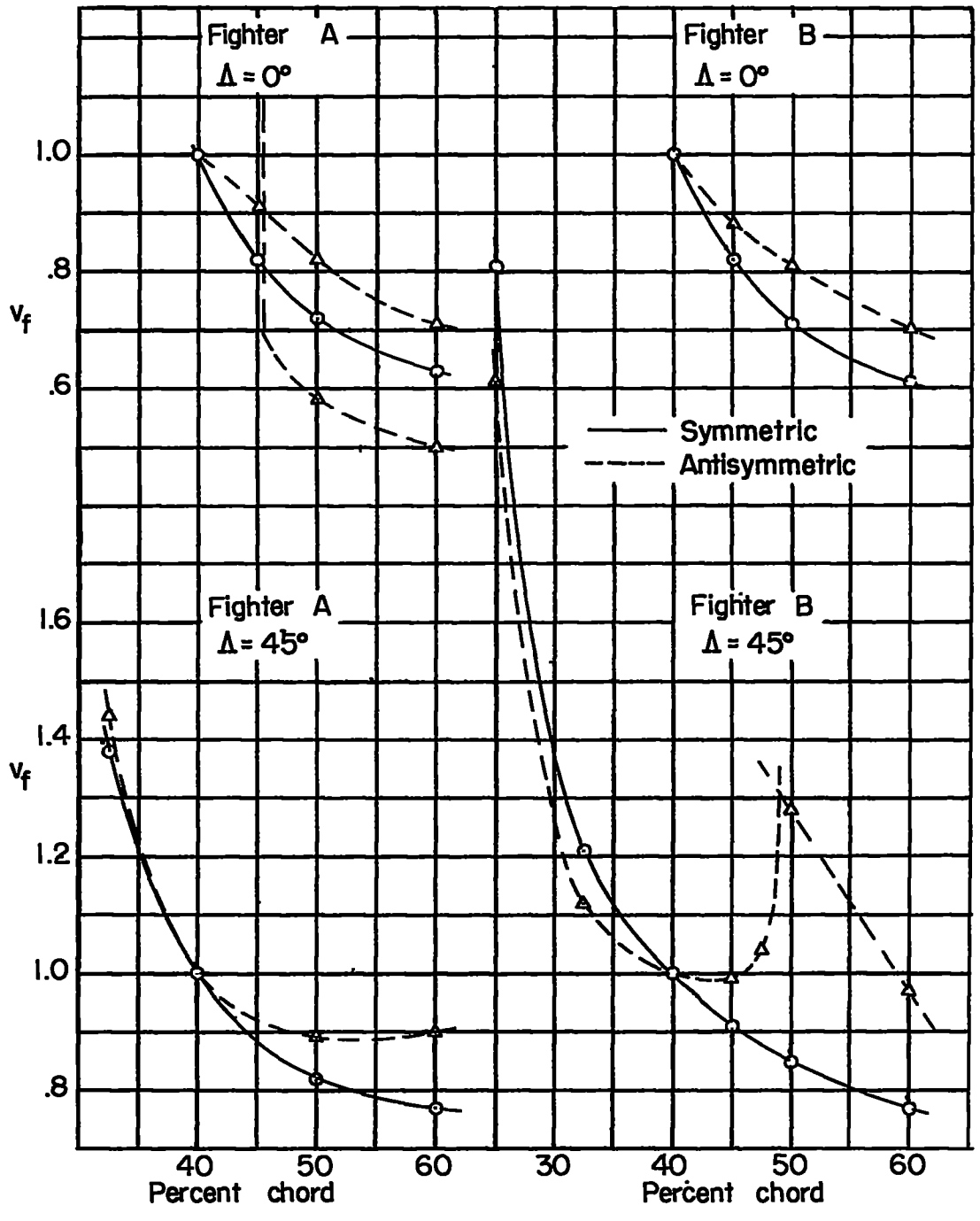

(a) Fighters A and B.

Figure 11.- Flutter speed as function of center-of-mass position in percent chord.

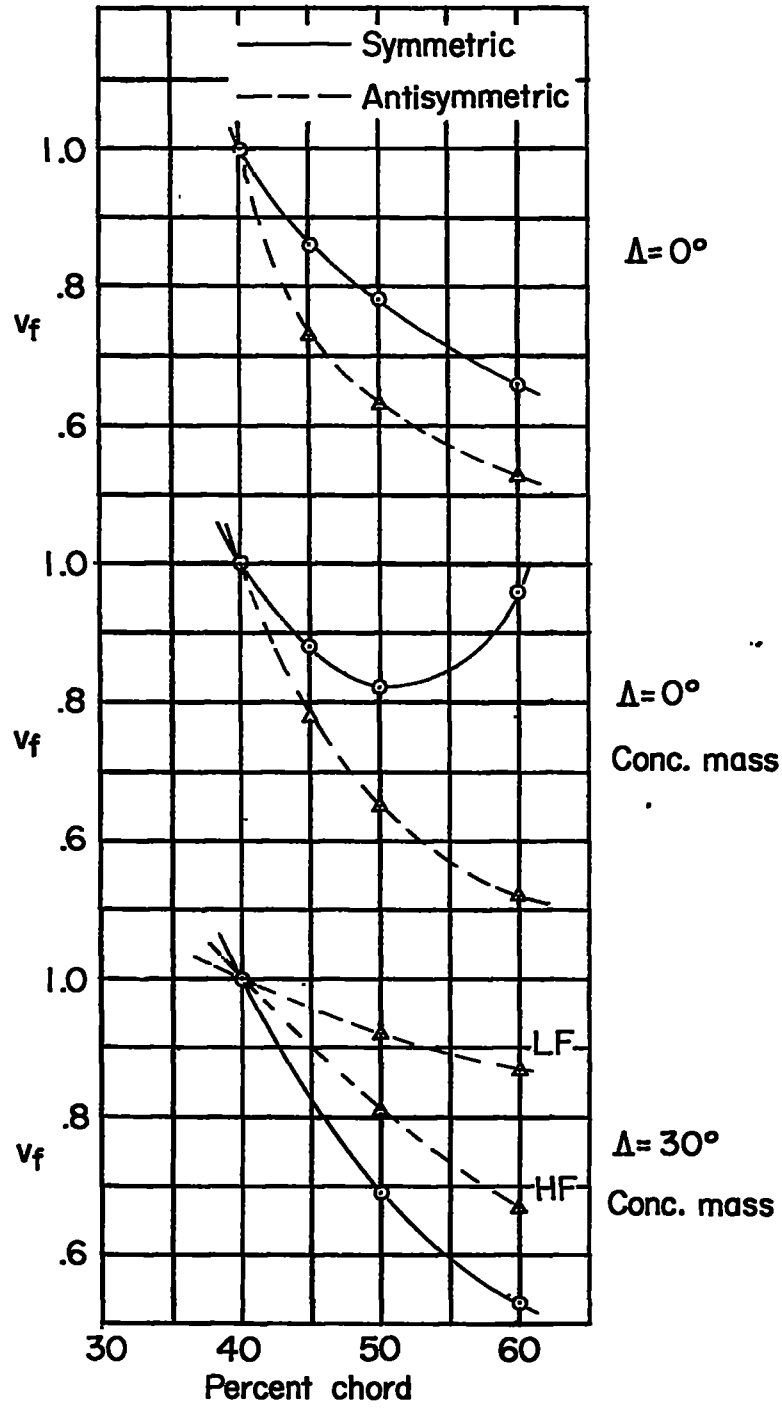

(b) Bomber A.

Figure 11.- Continued.

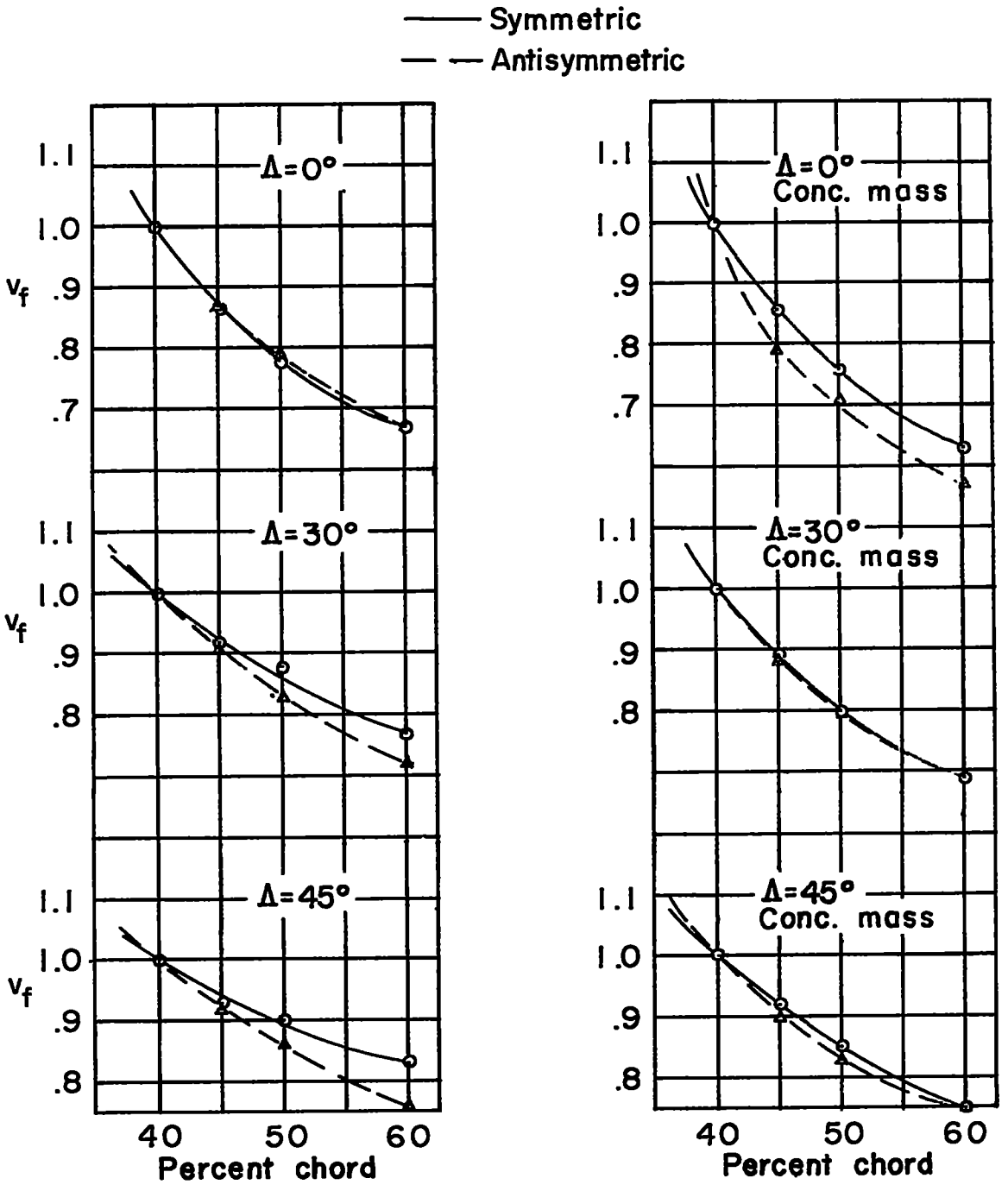

(c) Bomber B.

Figure 11.- Concluded.

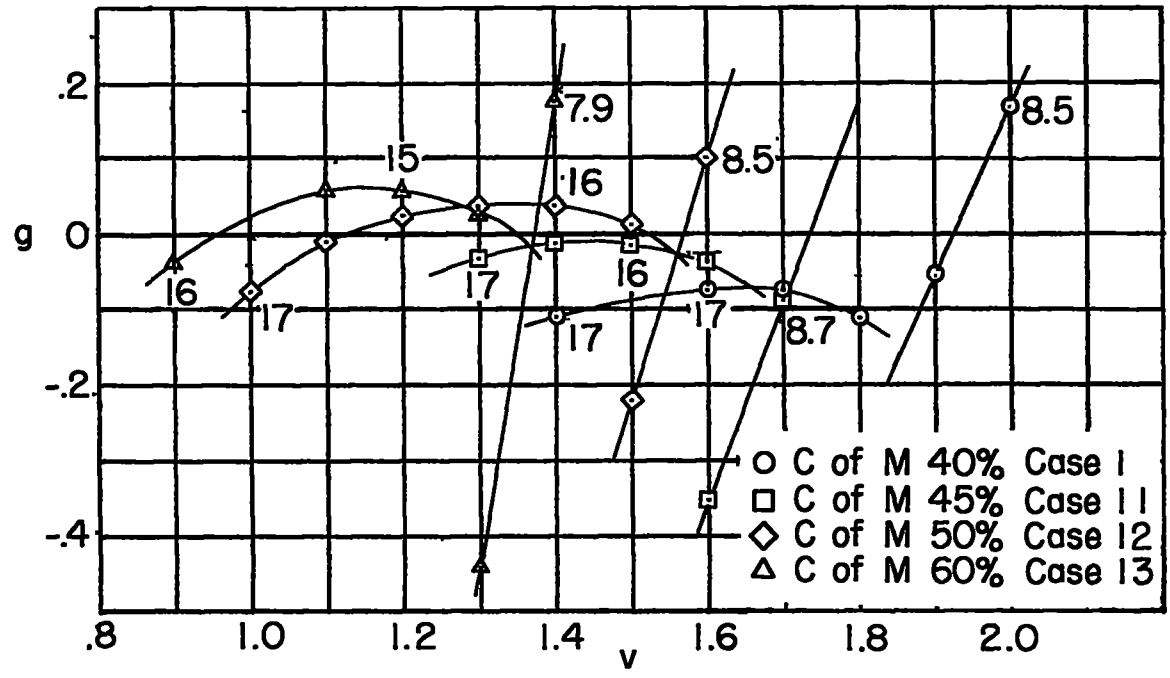

(a) Fighter A; $\Lambda = 0^{\circ}$; antisymmetric.

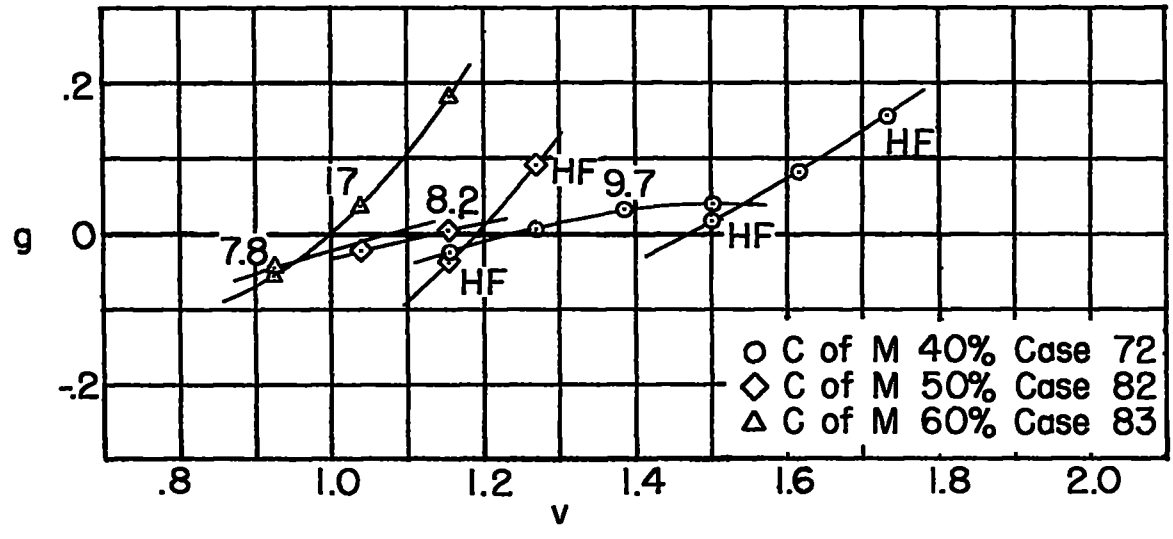

(b) Bomber A; $\Lambda = 30^{\circ}$; concentrated mass on wing; antisymmetric.

Figure 12.- Plot of damping factor g against velocity for some unusual flutter roots.

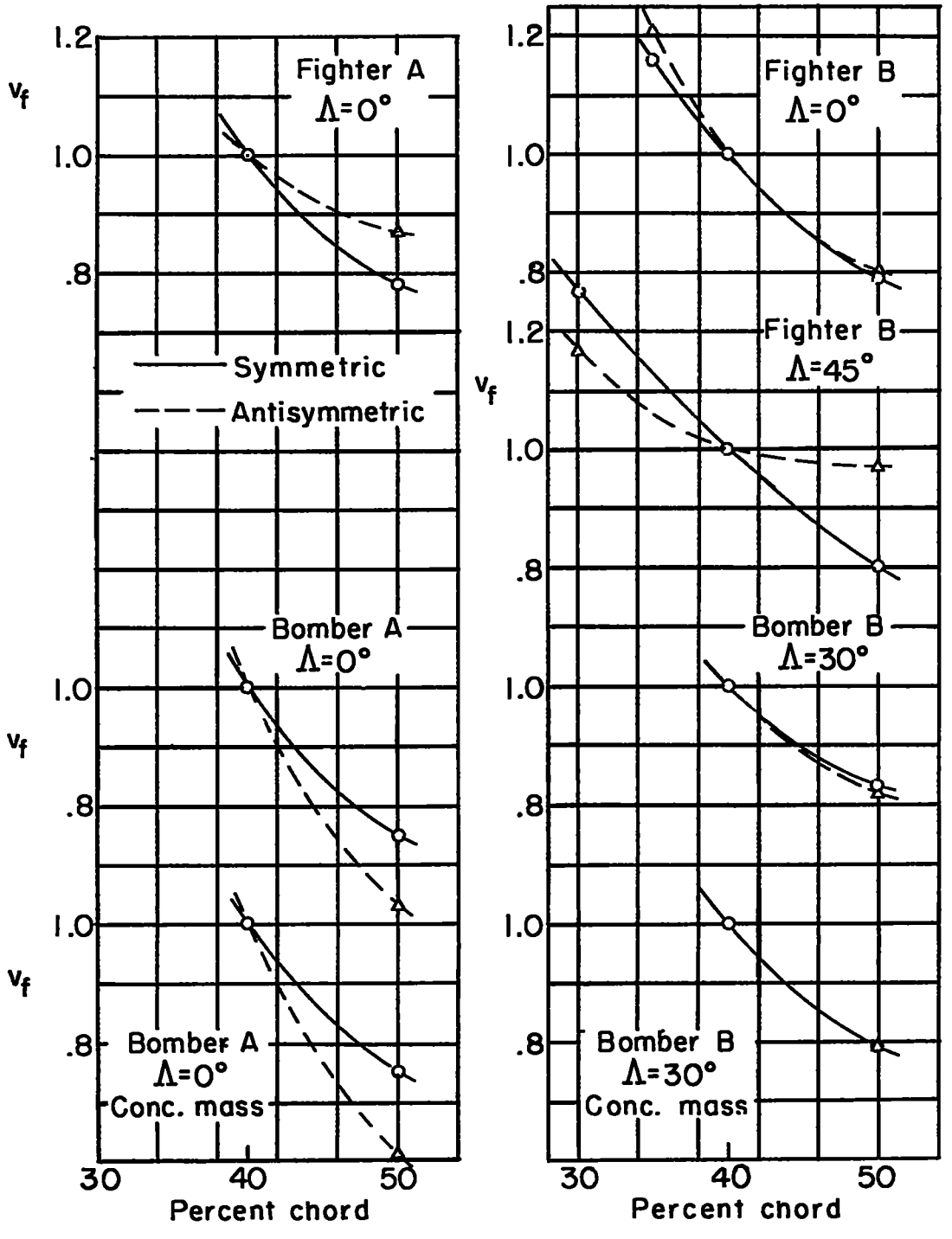

Figure 13.- Flutter speed as a function of elastic-axis position in percent chord.

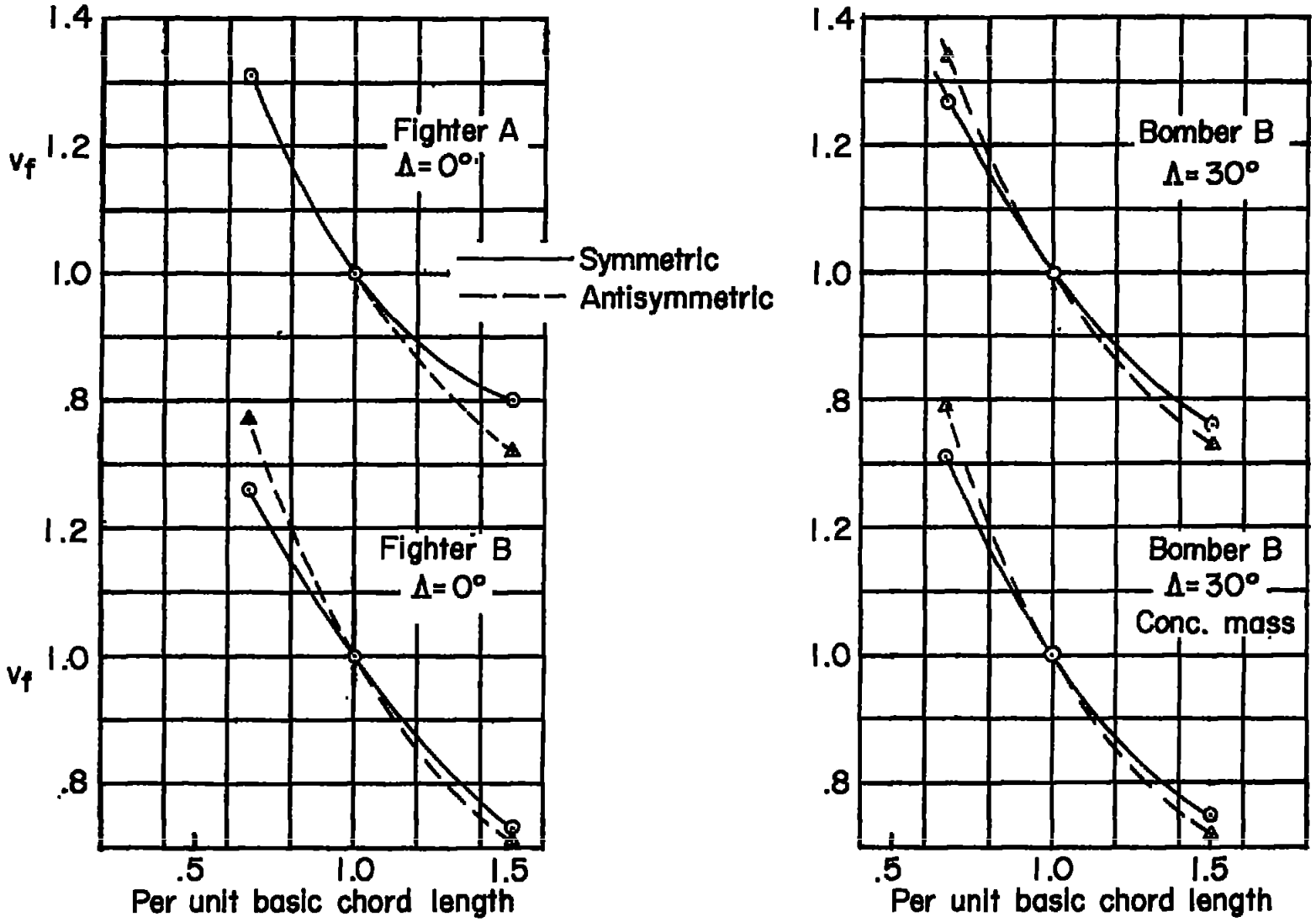

Figure 14.- Flutter speed as function of chord length.

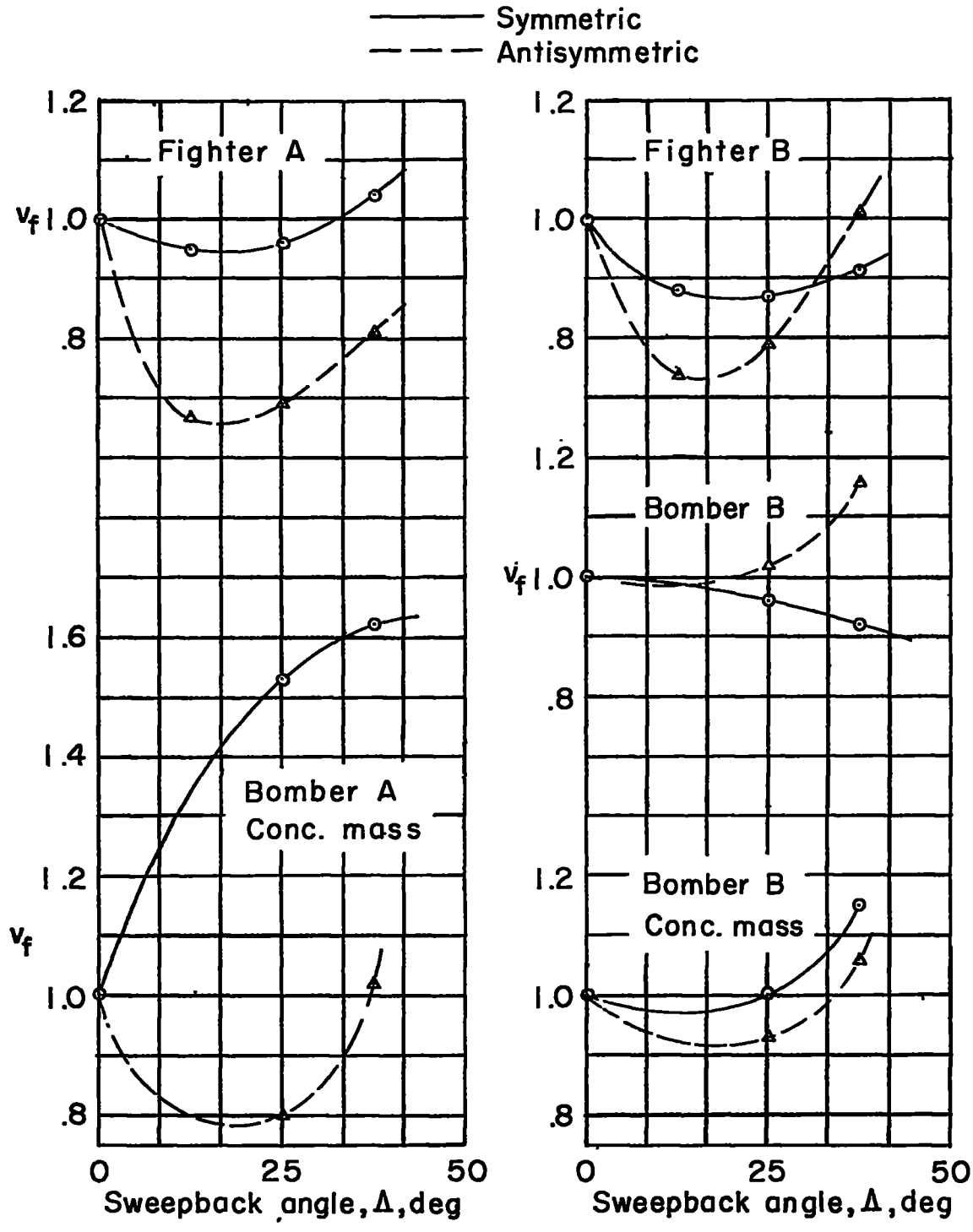

Figure 15.- Flutter speed as function of sweepback angle.

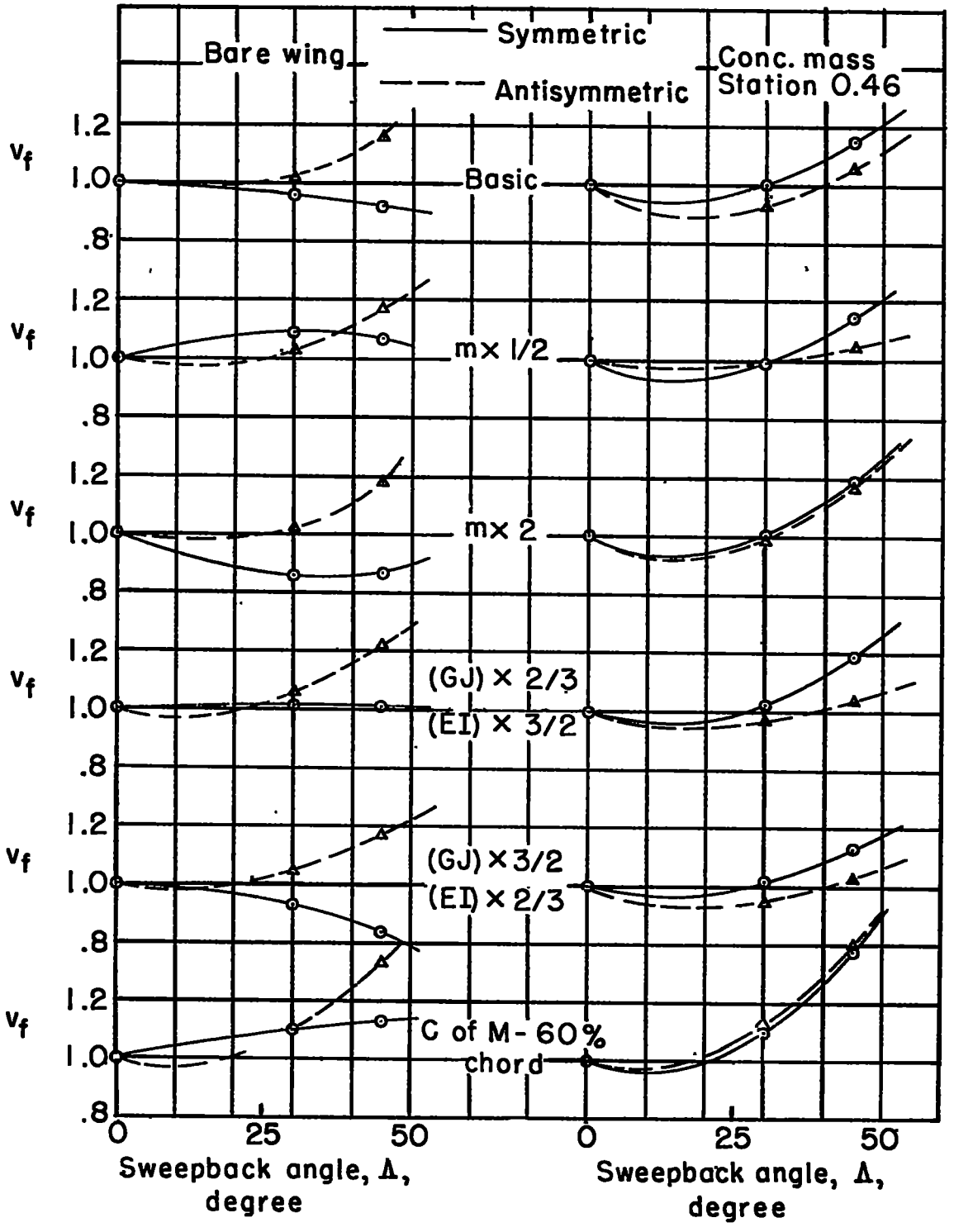

Figure 16.- Effect of sweepback on various modifications of bomber B.

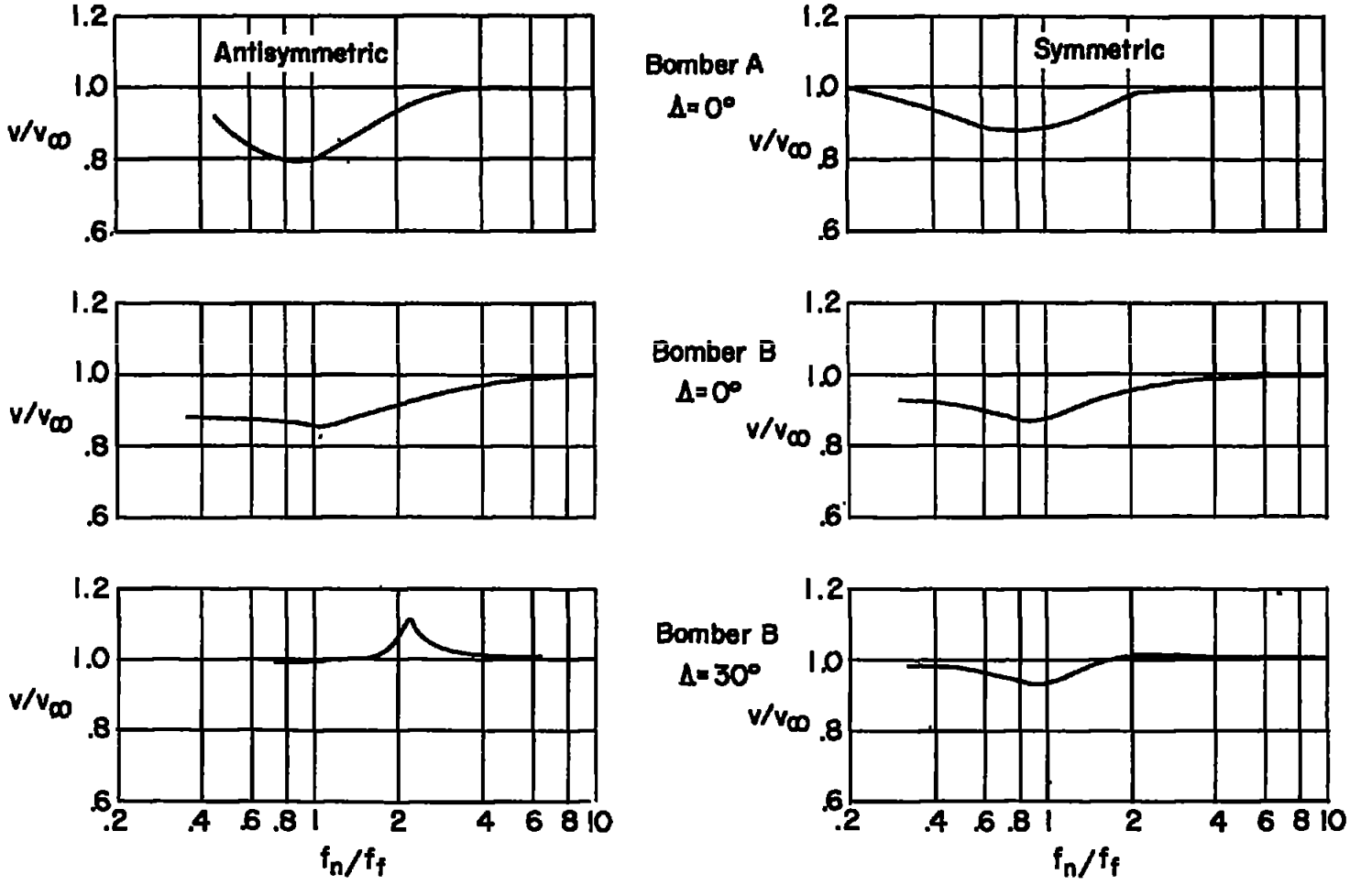

(a) Mass at 0.46 span.

Figure 17.- Flutter speed as a function of concentrated-mass pitching frequency.

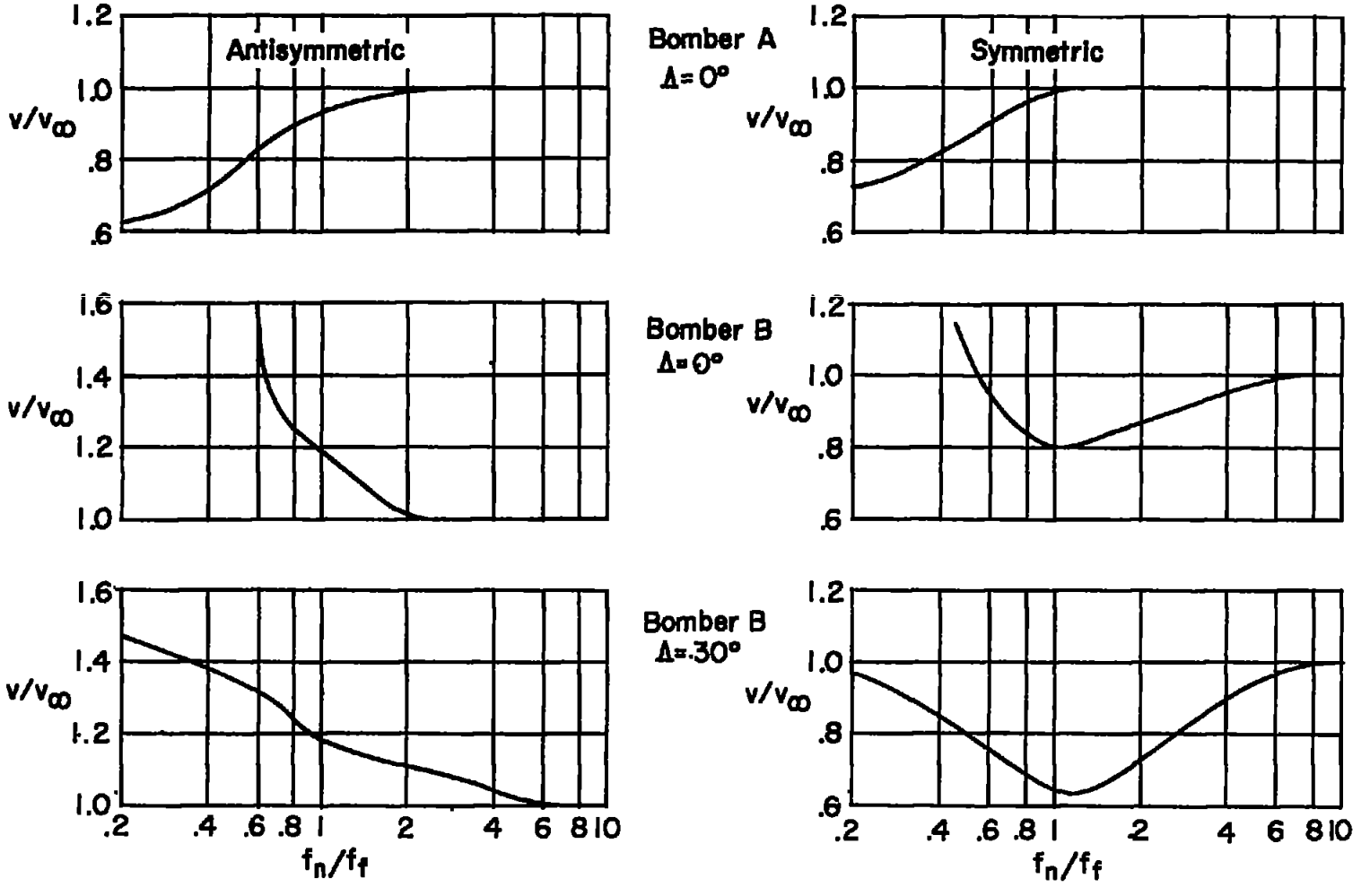

(b) Mass at tip.

Figure 17.- Concluded.

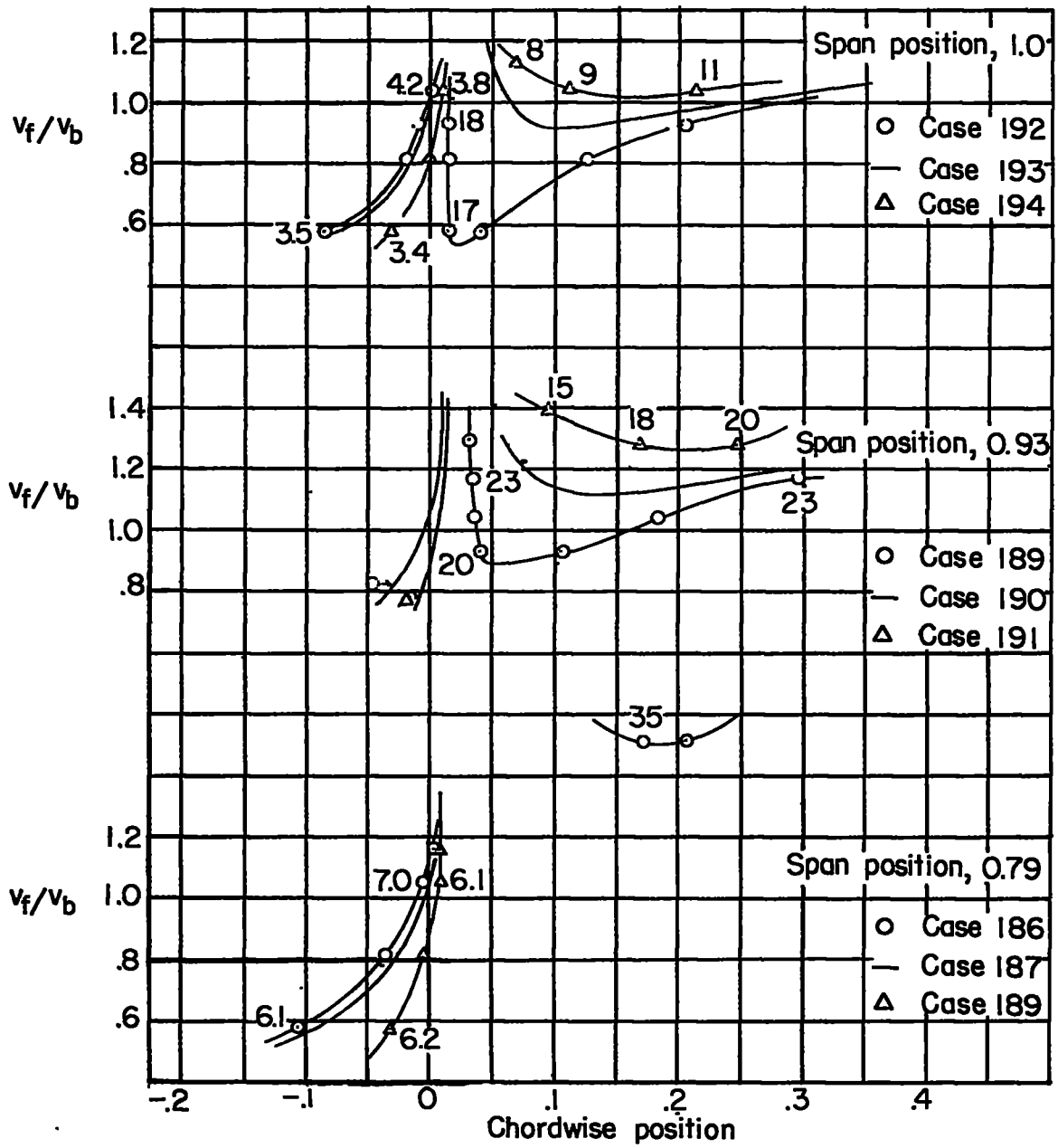

(a) Fighter A; $\Lambda = 0^\circ$; symmetric.

Figure 18.- Flutter characteristics against chordwise position of concentrated mass.

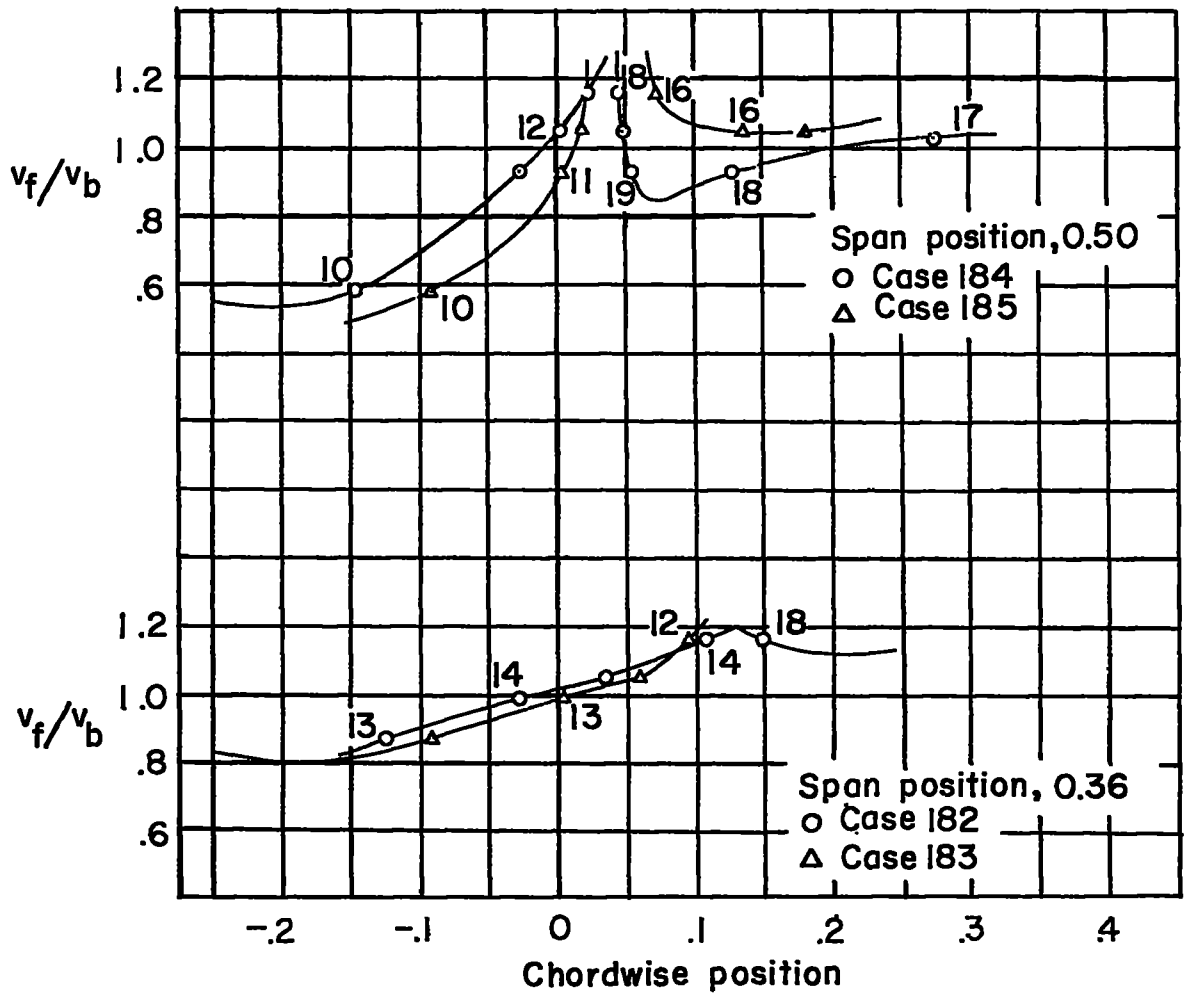

(a) Concluded.

Figure 18.- Continued.

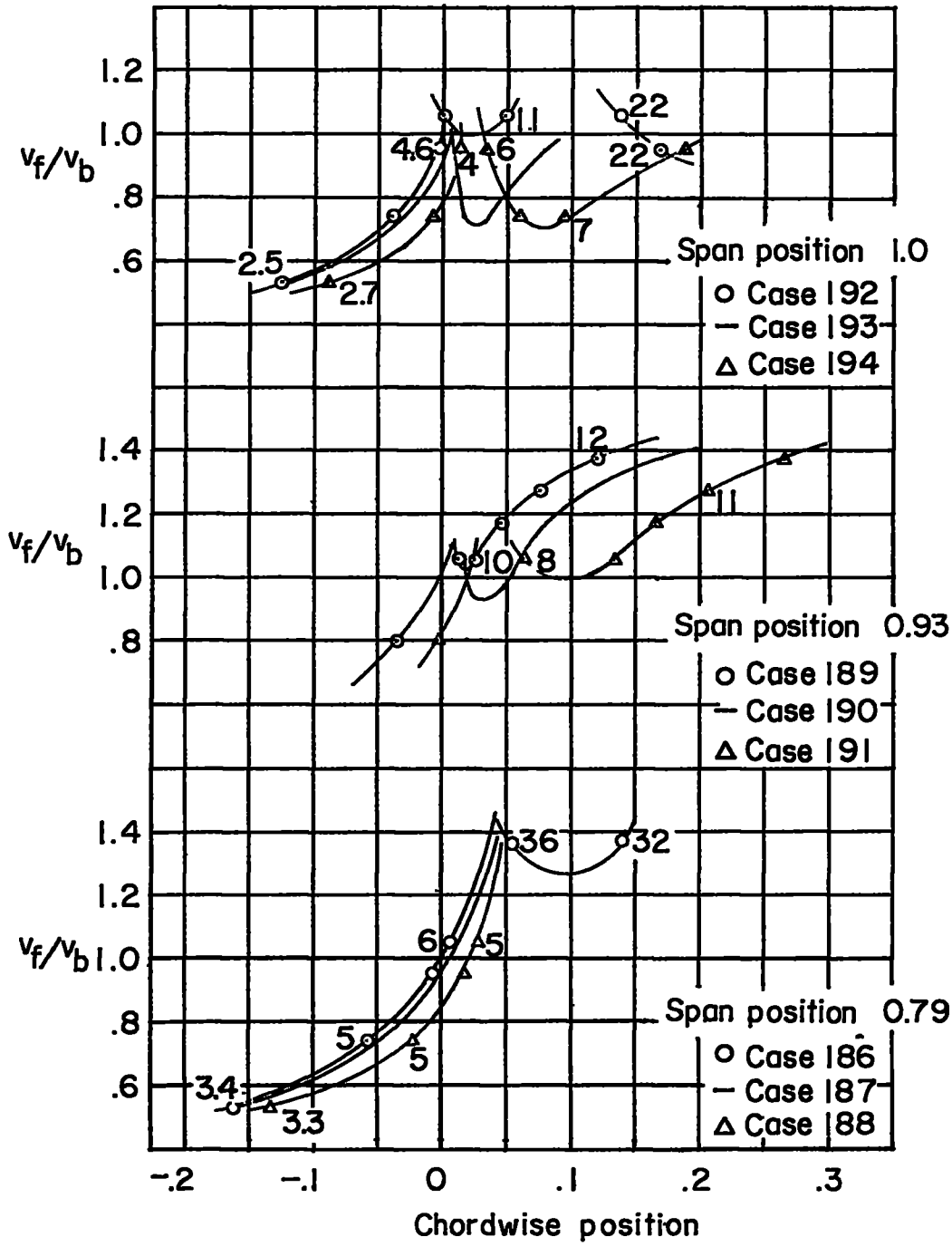

(b) Fighter A; $\Lambda = 0^\circ$; antisymmetric.

Figure 18.- Continued.

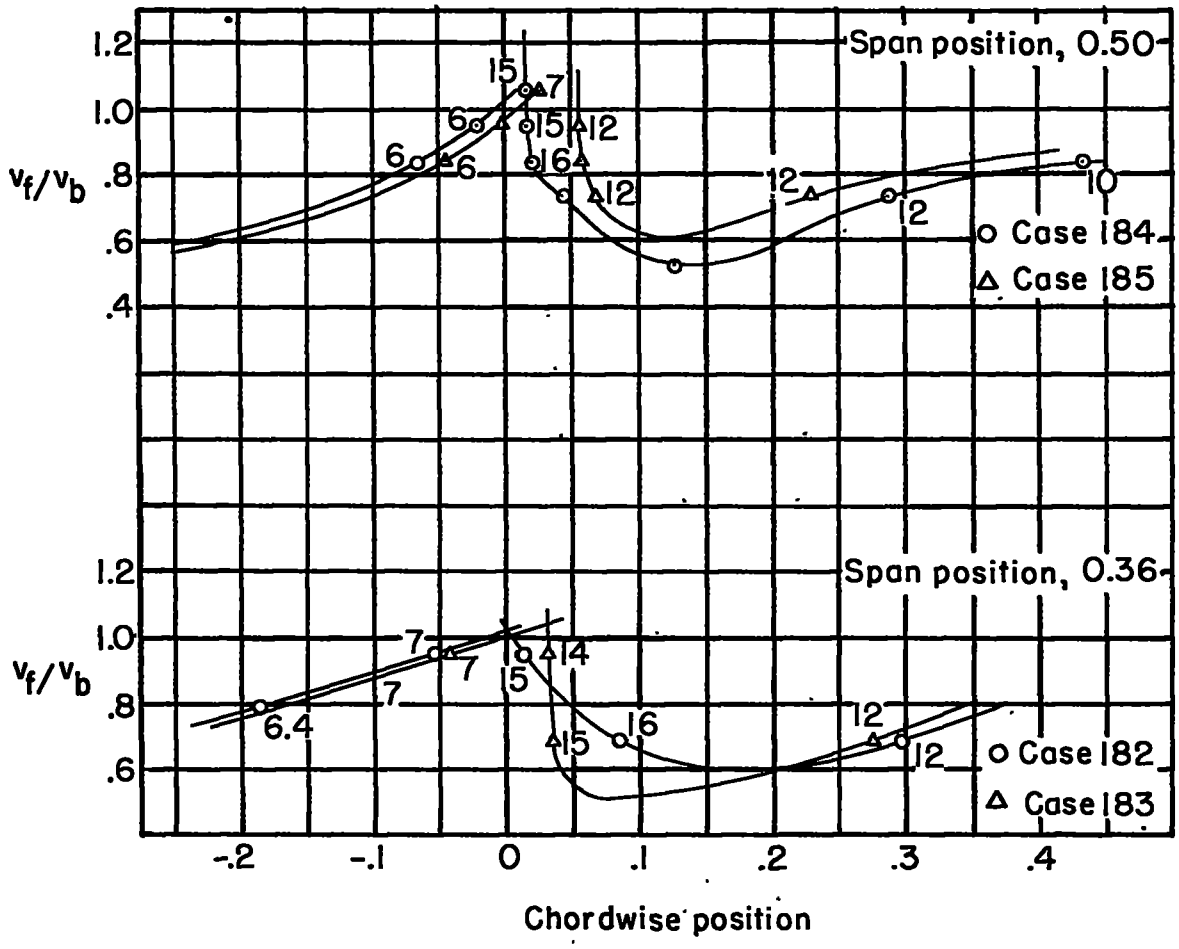

(b) Concluded.

Figure 18.- Continued.

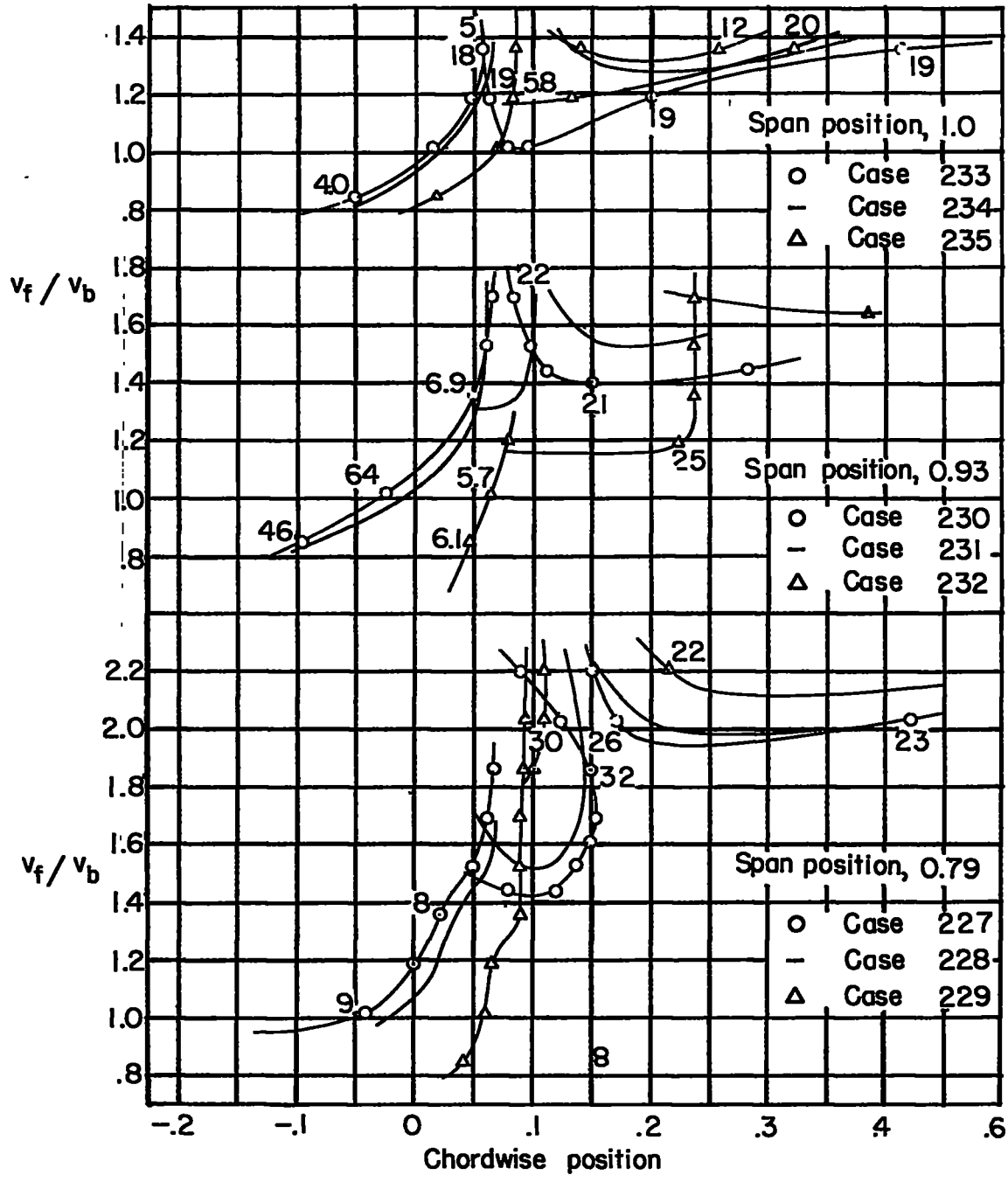

(c) Fighter A; $\Lambda = 45°$; symmetric. MF, medium frequency HF, high frequency.

Figure 18.- Continued.

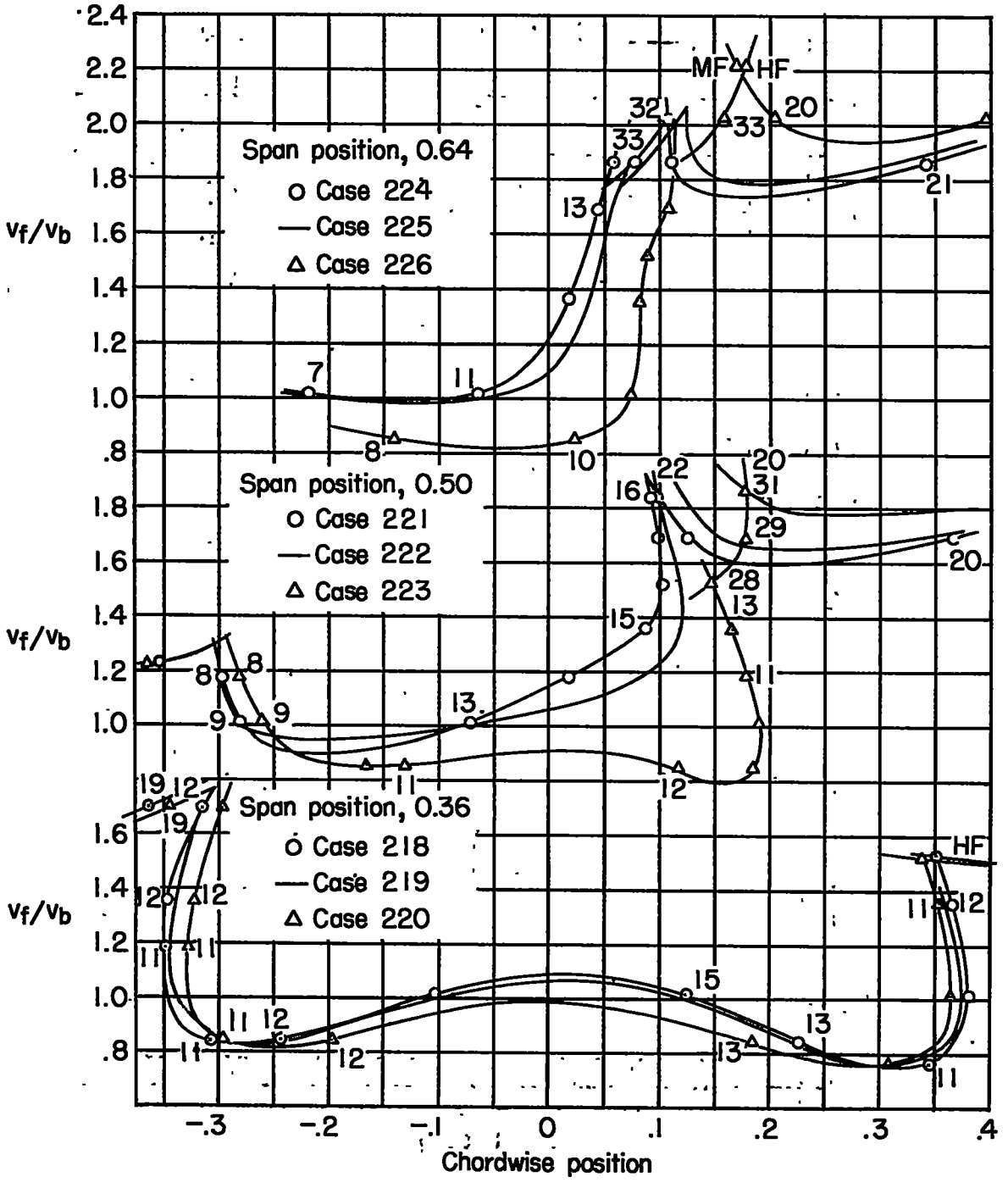

(c) Concluded.

Figure 18.- Continued.

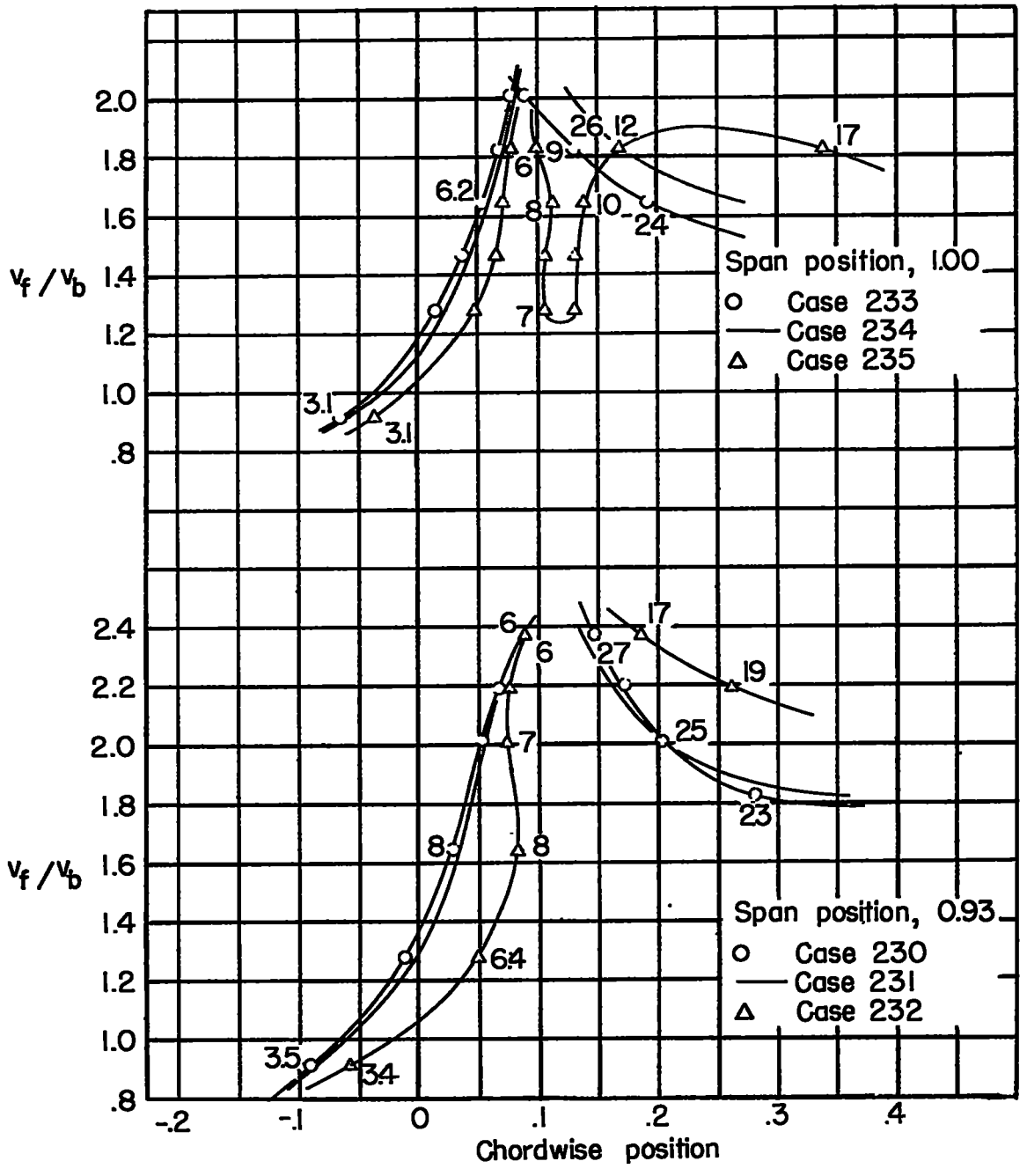

(d) Fighter A; $\Lambda = 45^{\circ}$; antisymmetric.

Figure 18.- Continued.

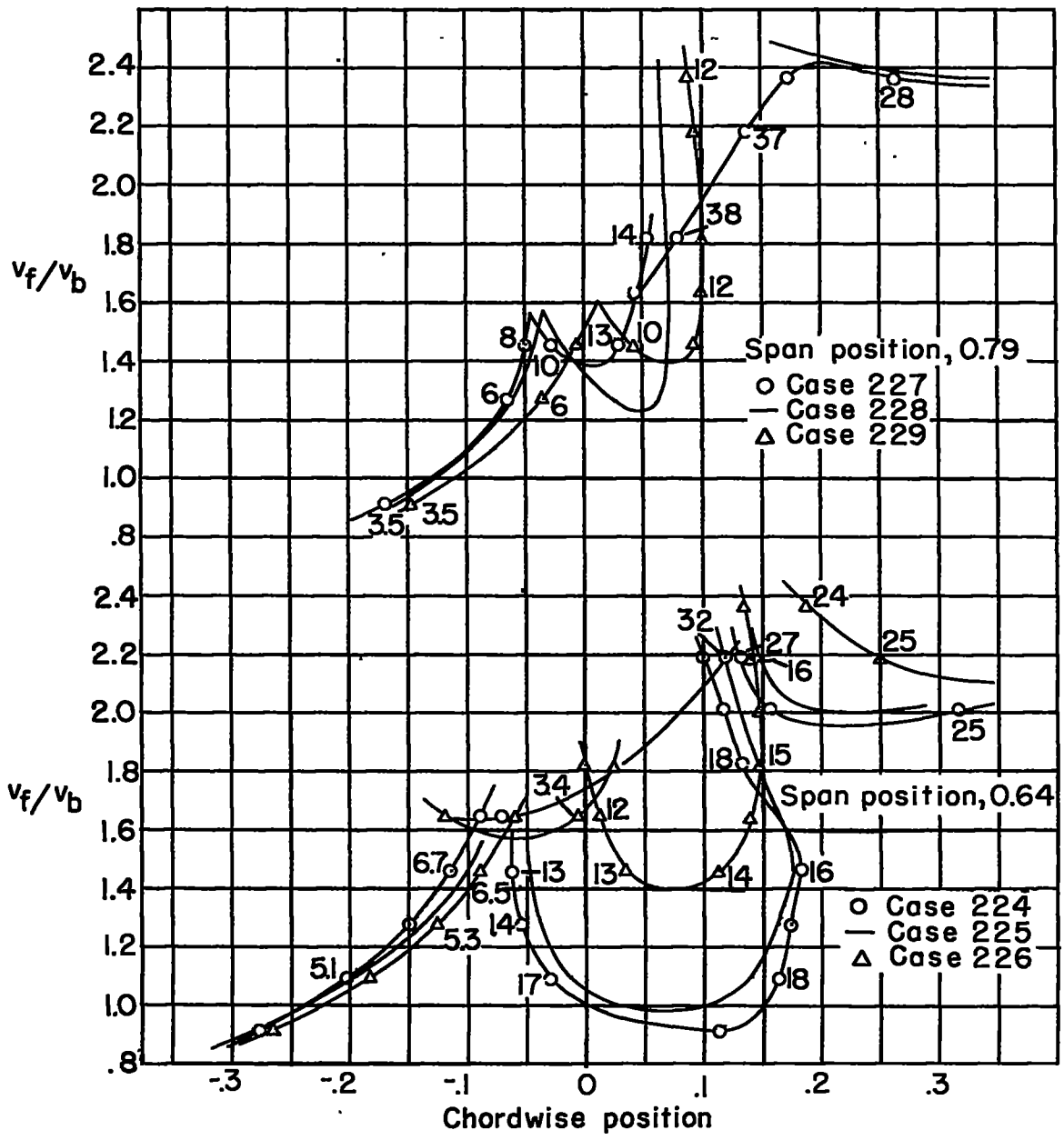

(d) Continued.

Figure 18.- Continued.

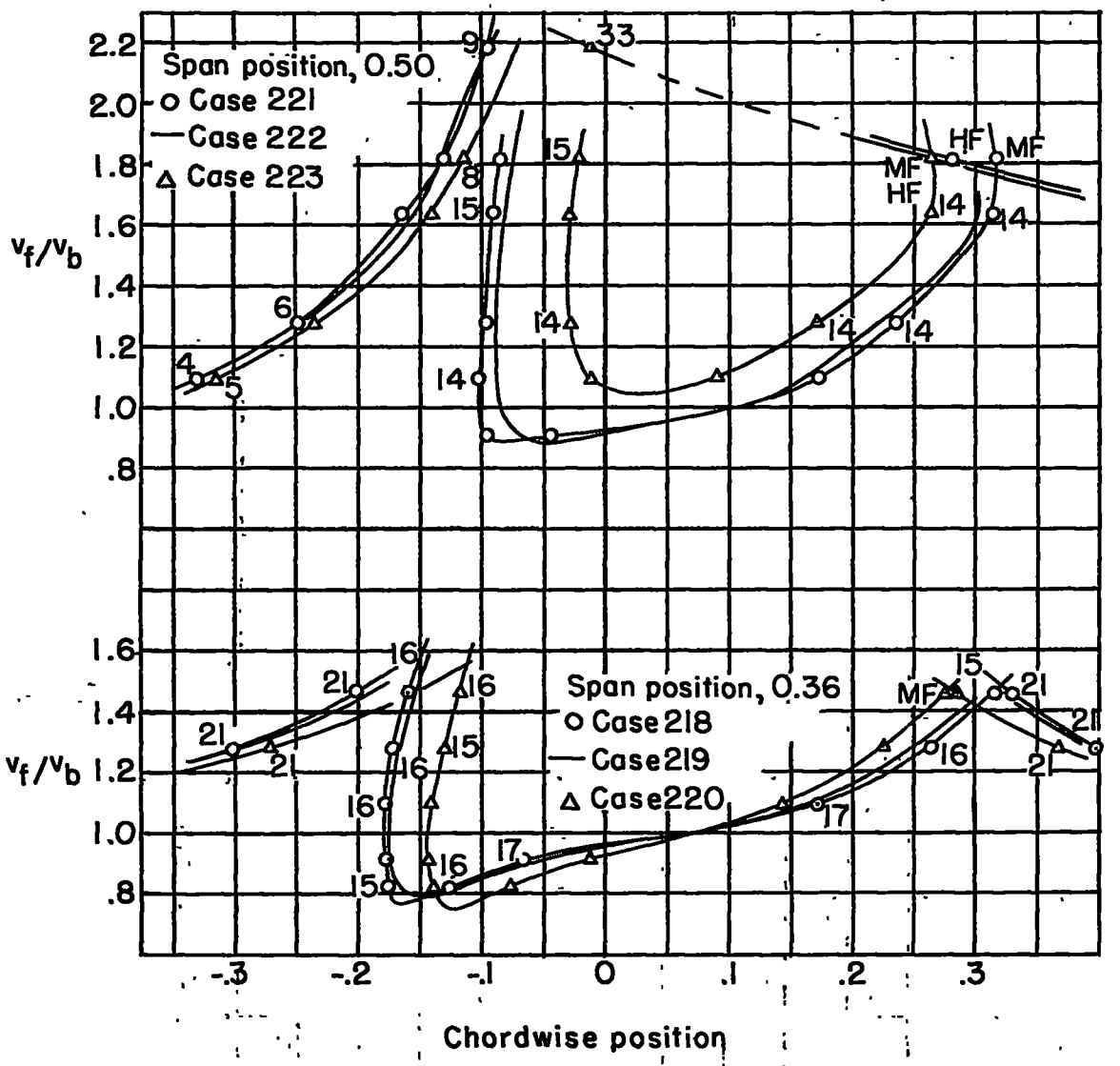

(d) Concluded.

Figure 18.- Continued.

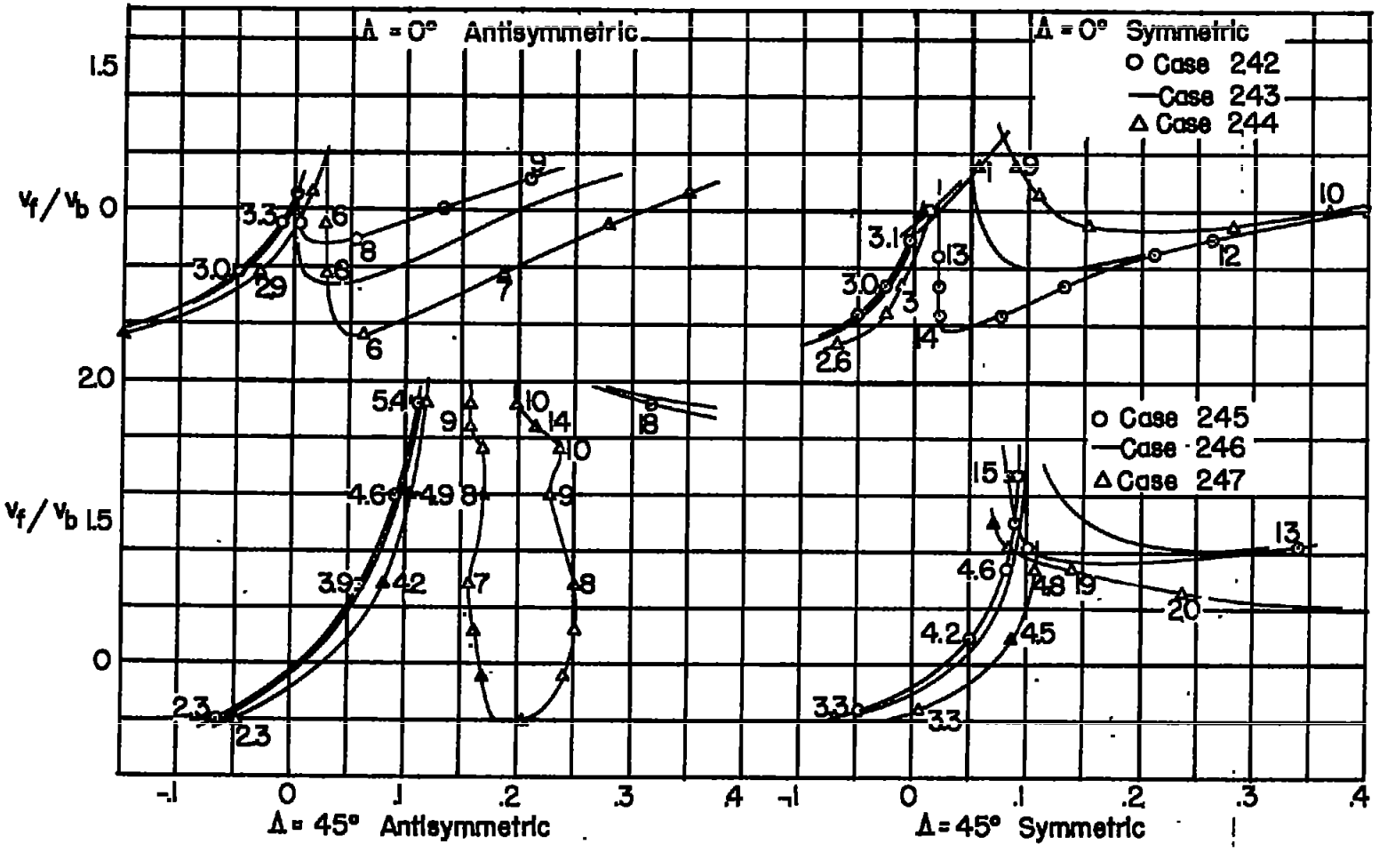

(e) Fighter B; data taken at tip.

Figure 18.- Continued.

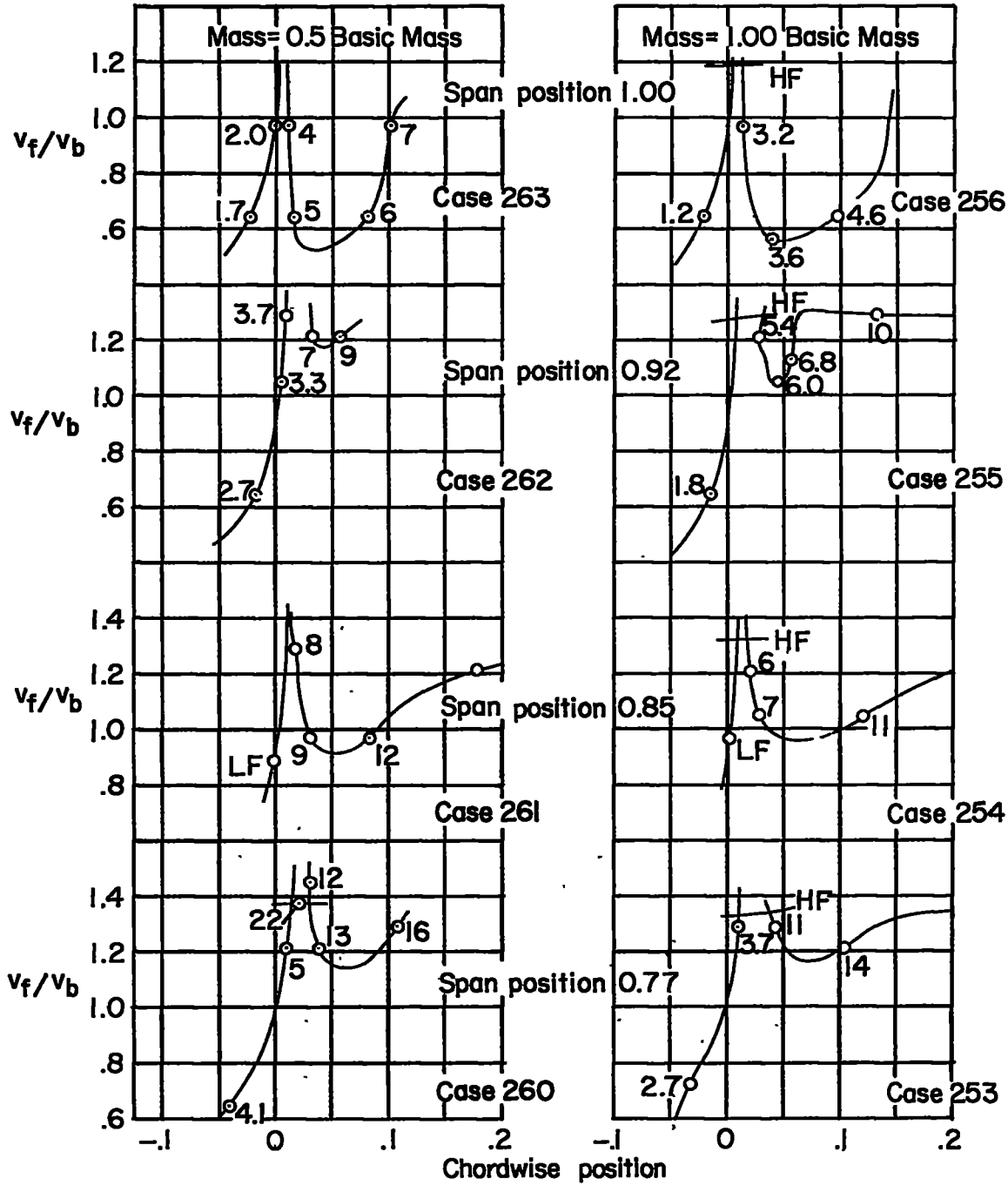

(f) Bomber A; $\Lambda = 0^o$; symmetric. HF, high frequency.

Figure 18.- Continued.

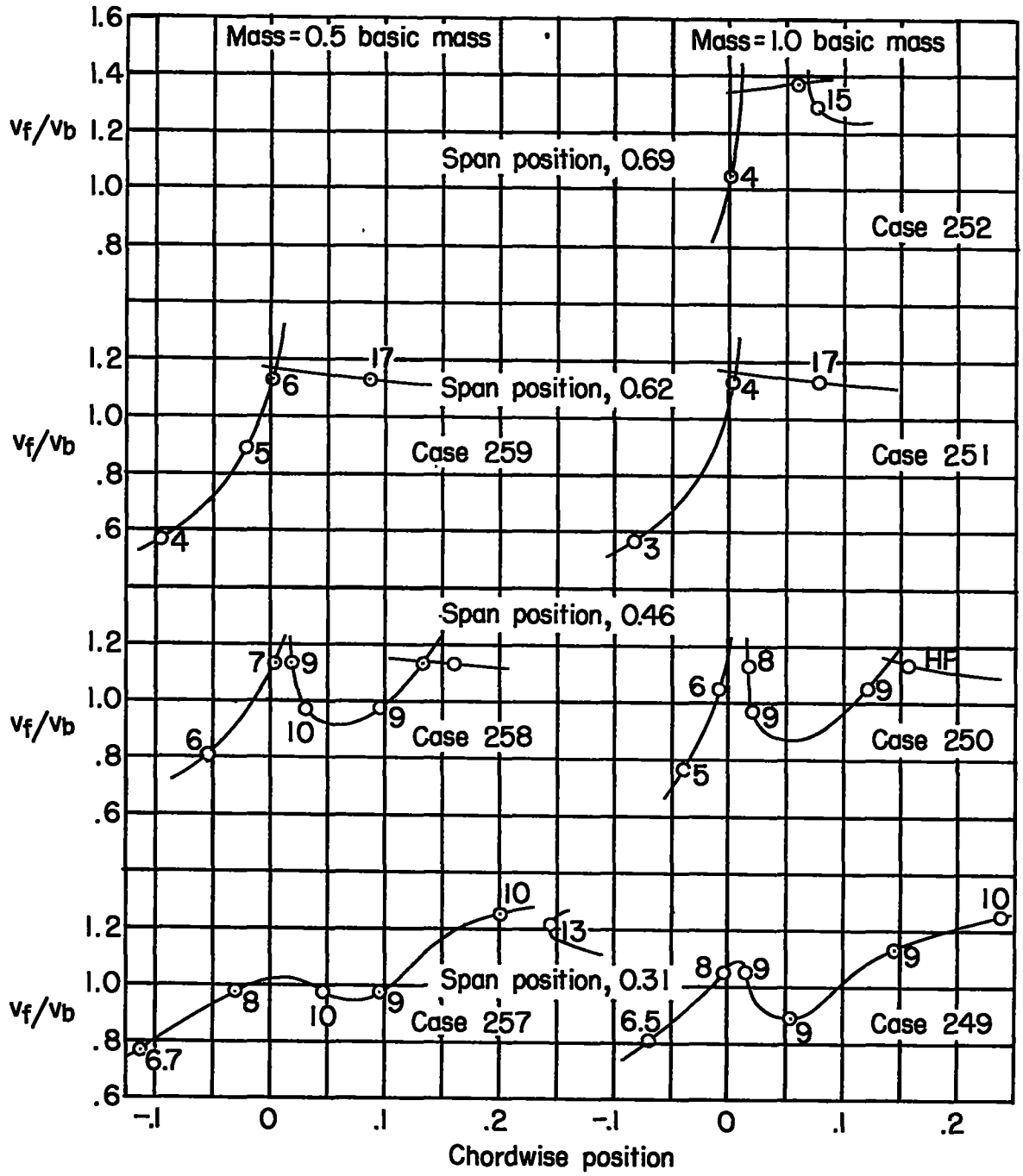

(f) Concluded.

Figure 18.- Continued.

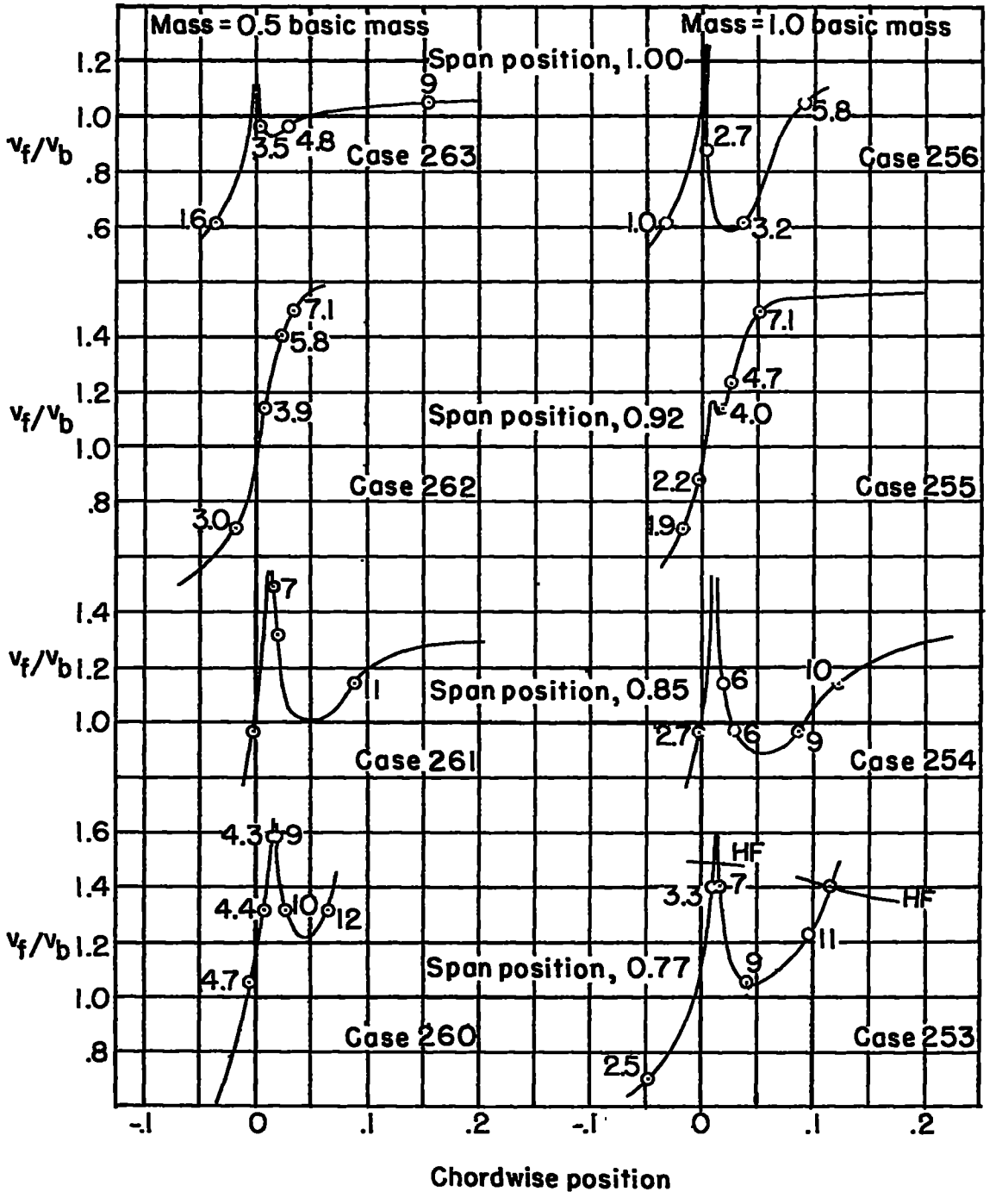

(g) Bomber A; $\Lambda = 0^{\circ}$; antisymmetric. HF, high frequency.

Figure 18.- Continued.

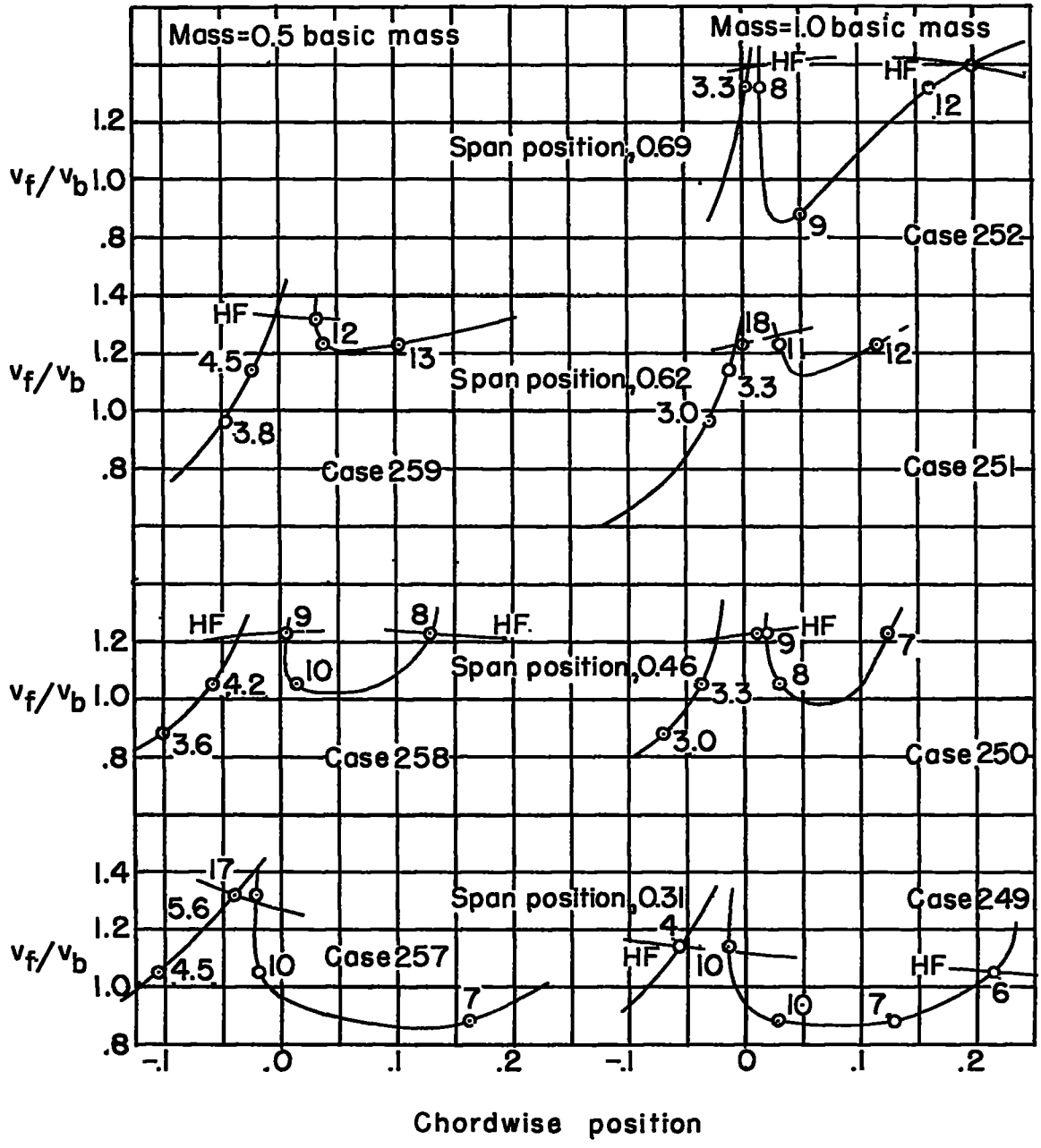

(g) Concluded.

Figure 18.- Continued.

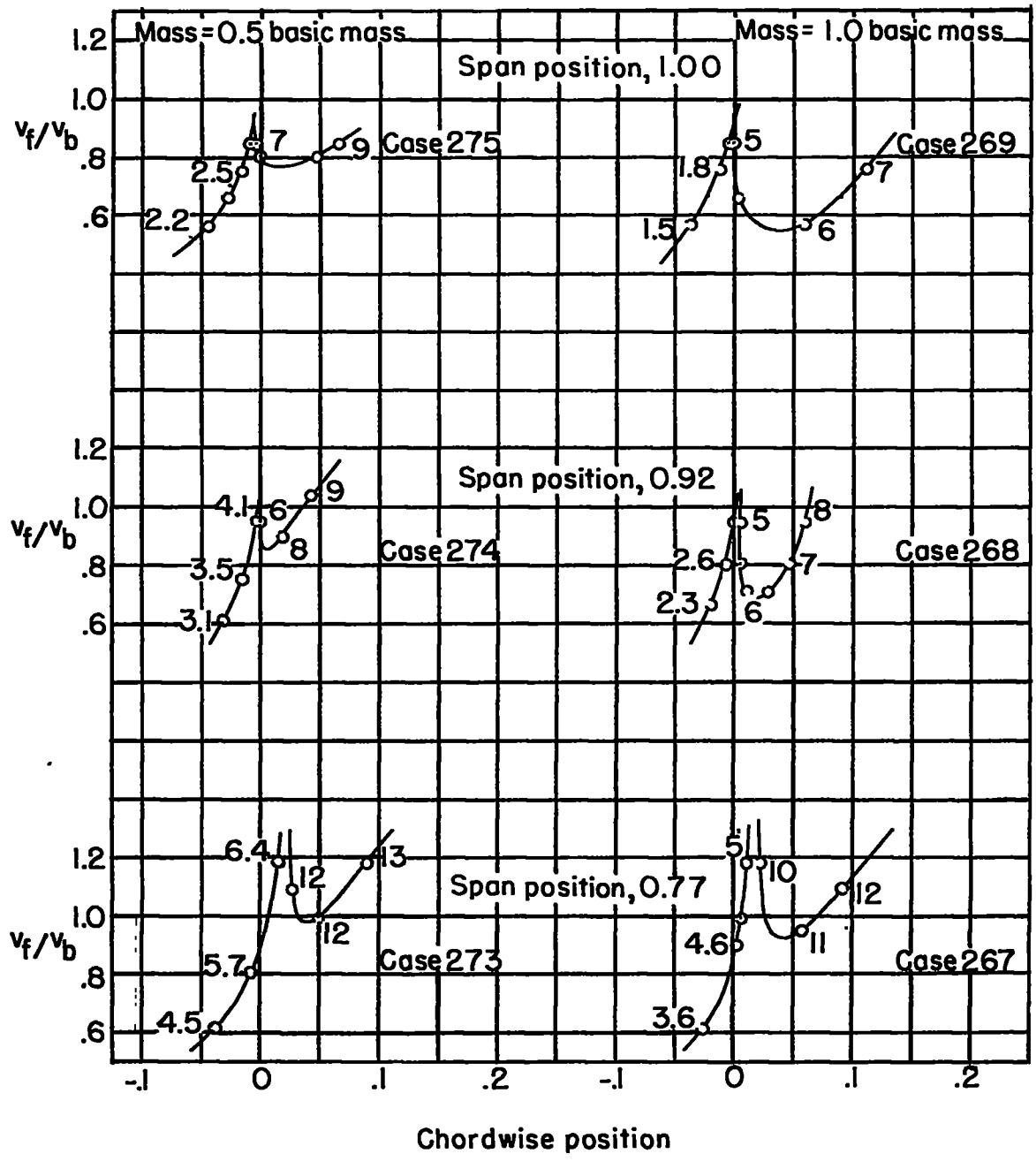

(h) Bomber B; $\Lambda = 0^{\circ}$; symmetric.

Figure 18.- Continued.

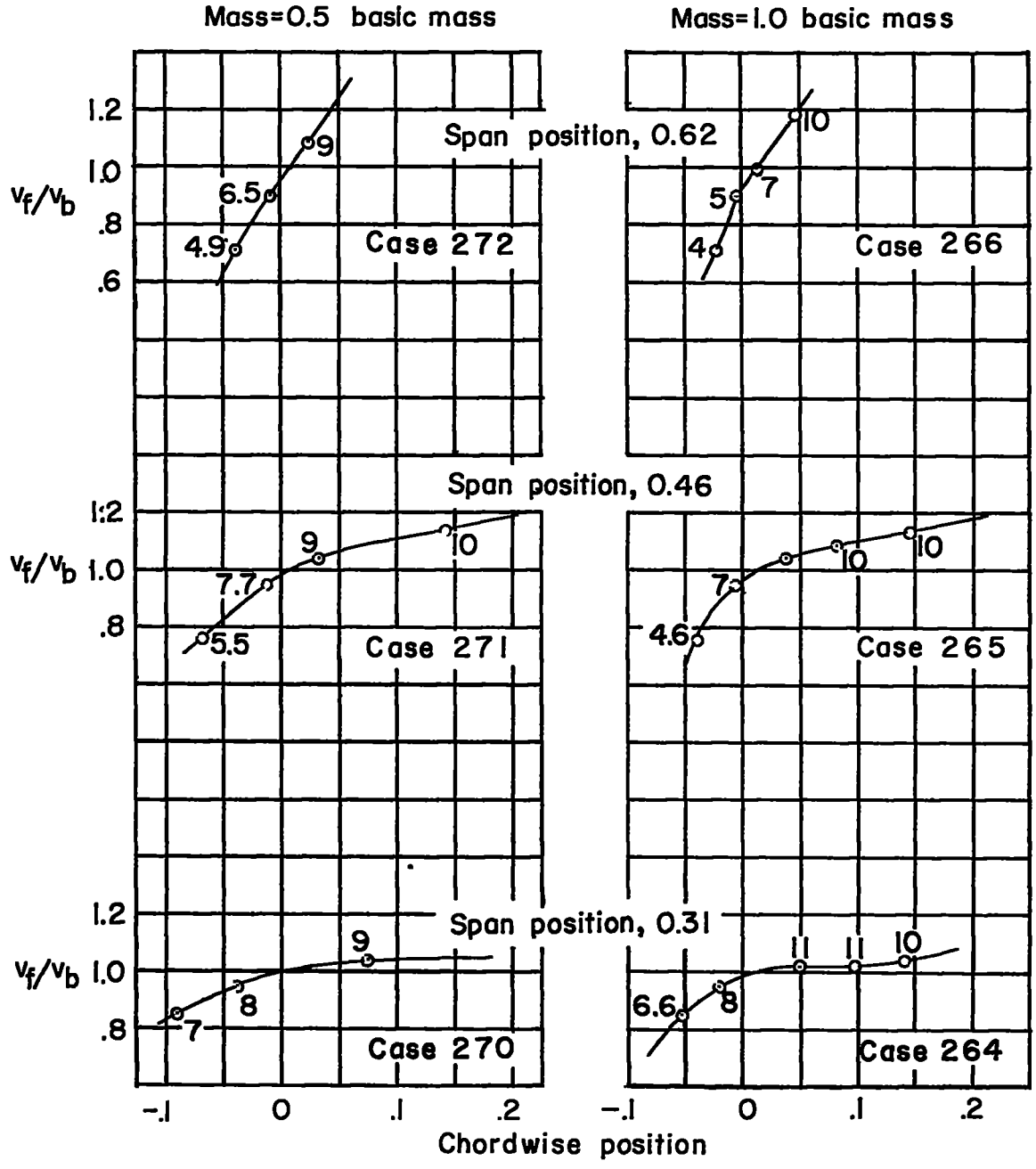

(h) Concluded.

Figure 18.- Continued.

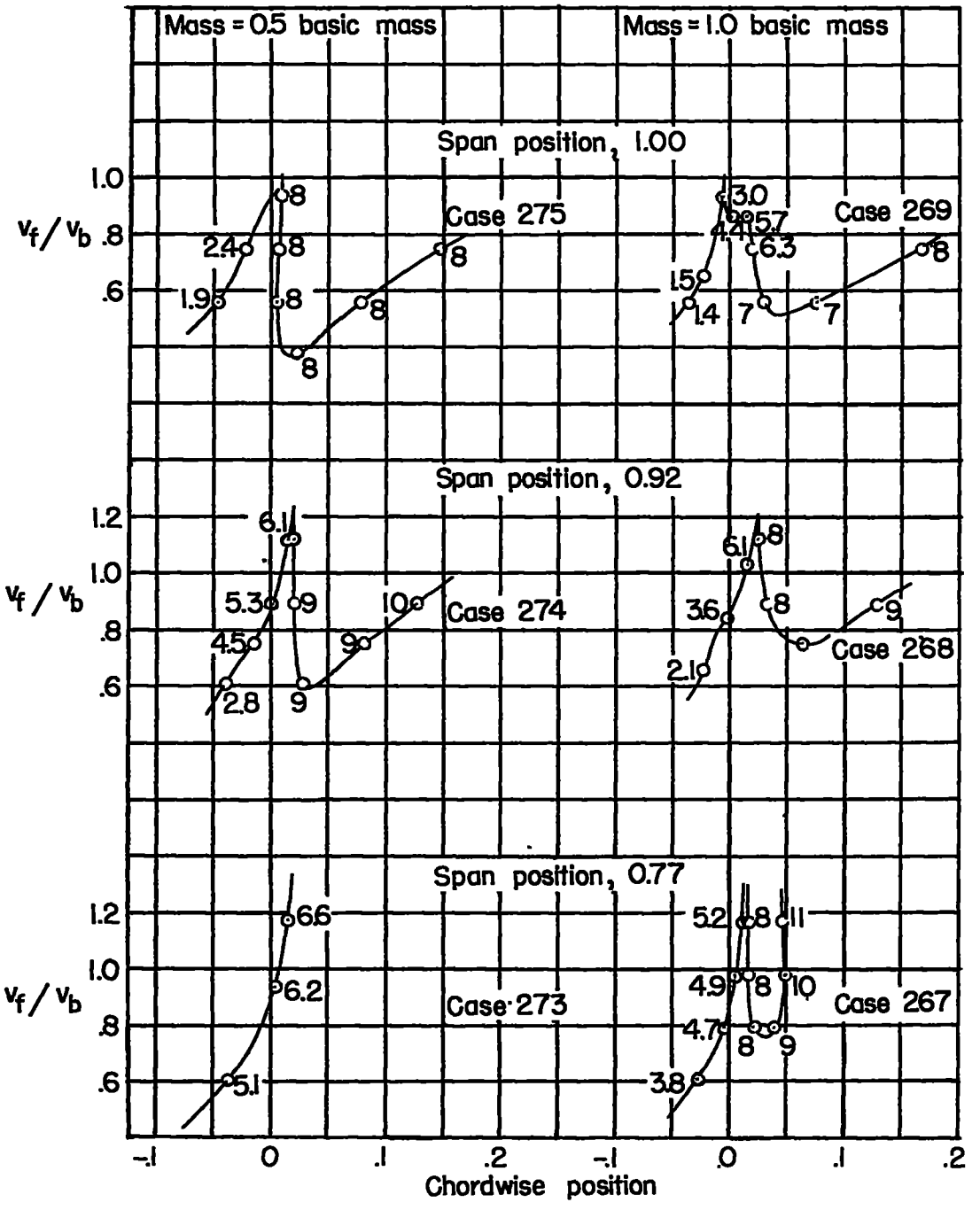

(i) Bomber B; $\Lambda = 0^{\circ}$; antisymmetric.

Figure 18.- Continued.

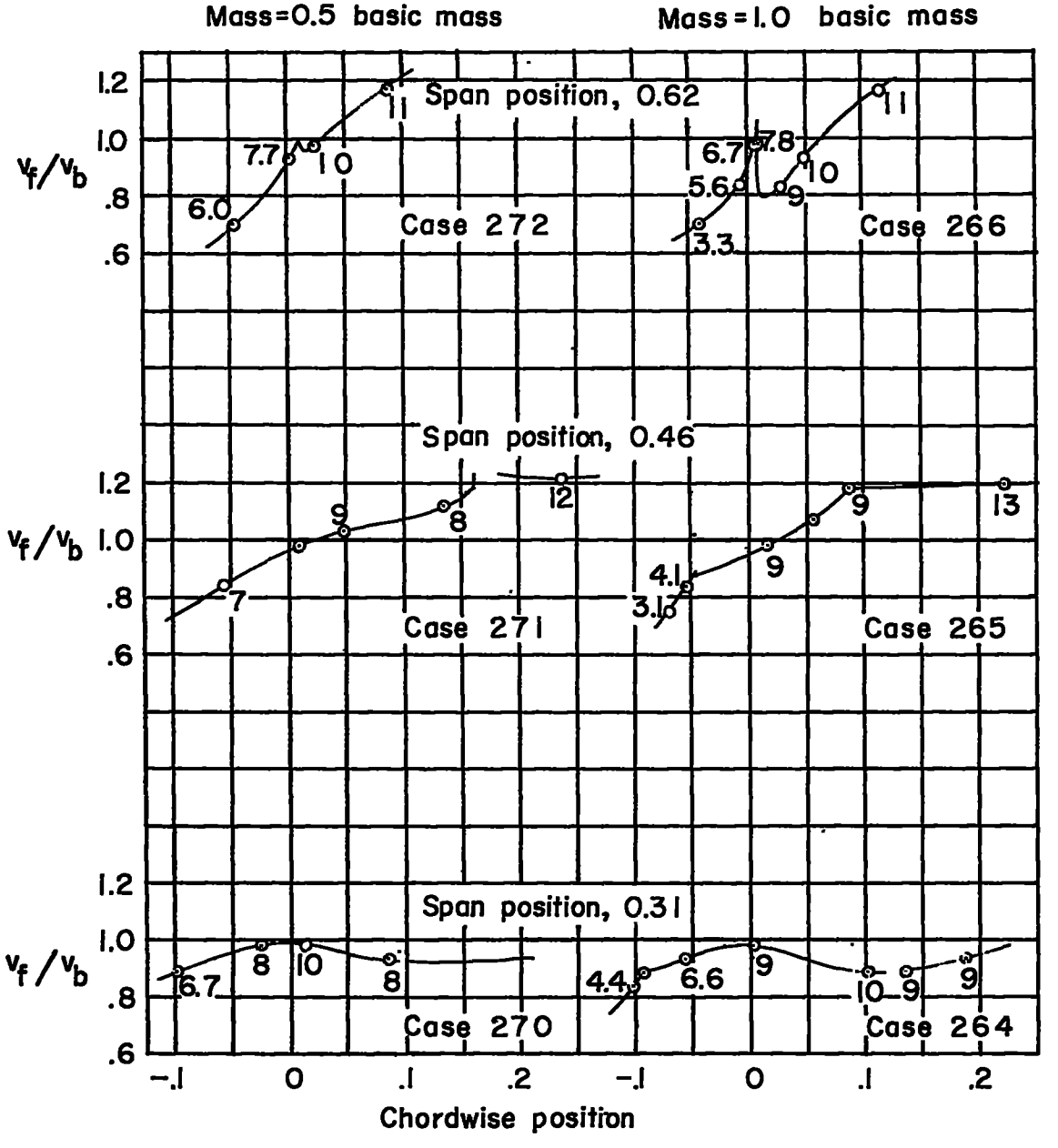

(i) Concluded.

Figure 18.- Continued.

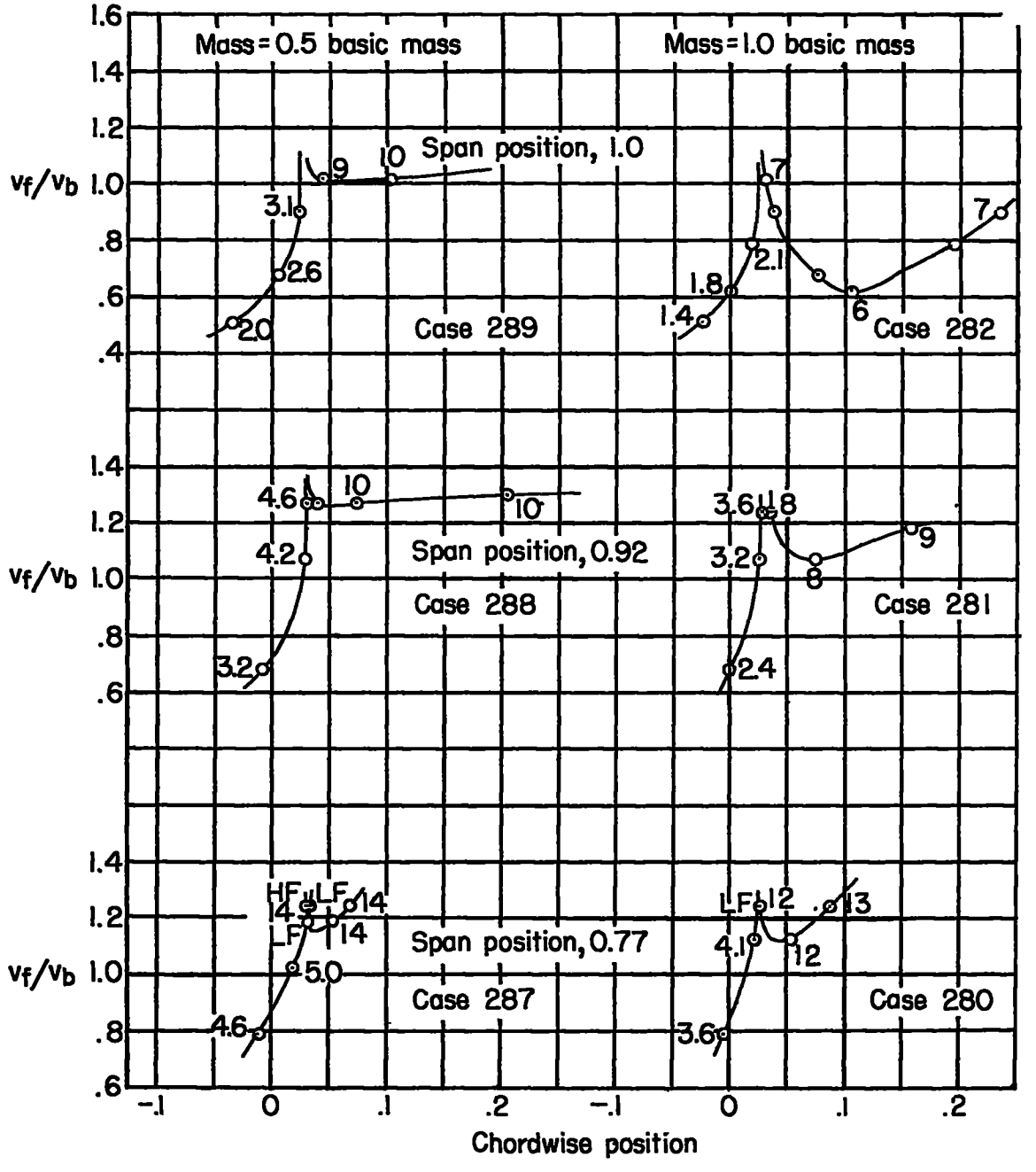

(j) Bomber B; $\Lambda = 30^\circ$; symmetric. LF, low frequency; HF, high frequency.

Figure 18.- Continued.

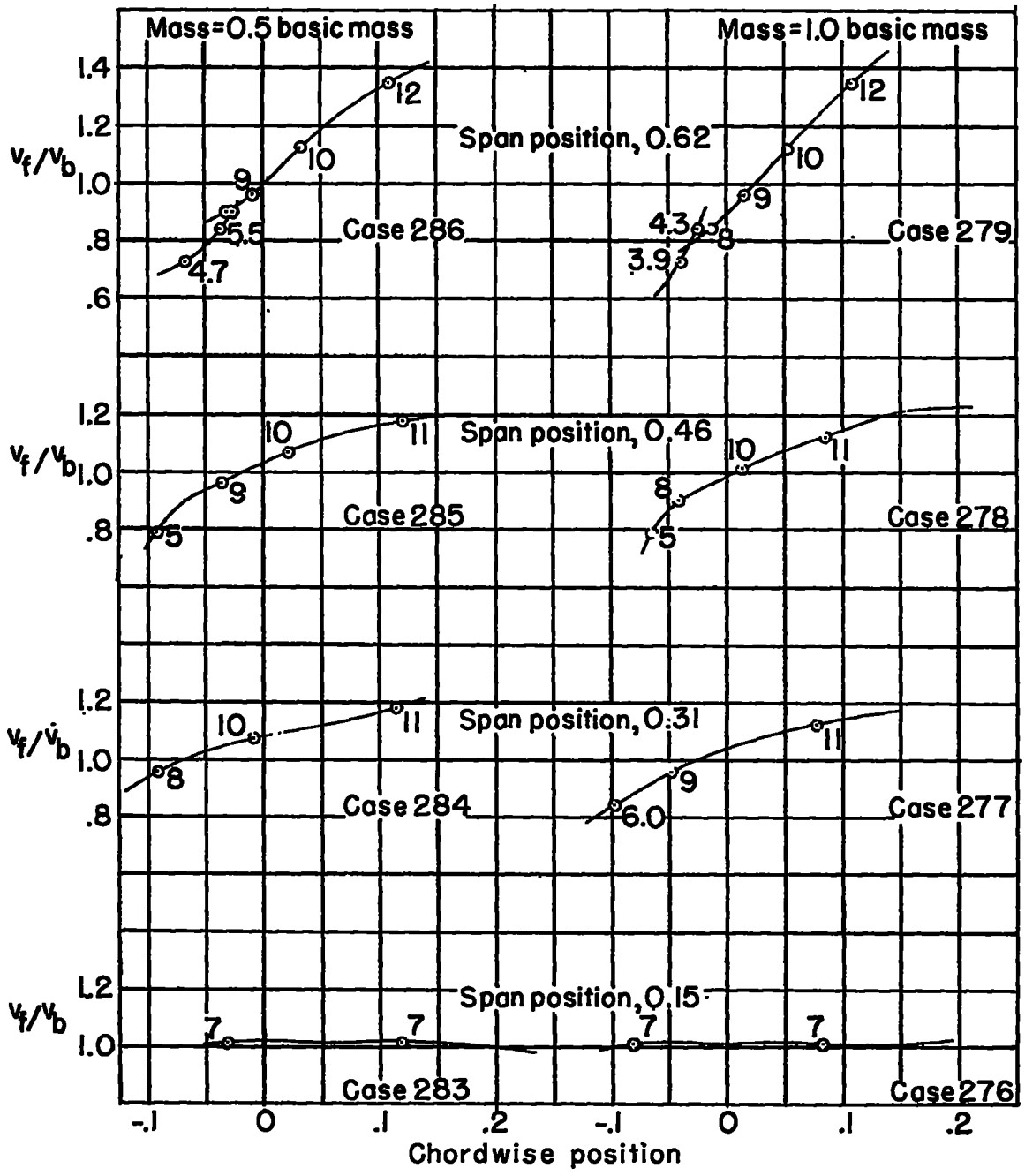

(j) Concluded.

Figure 18.- Continued.

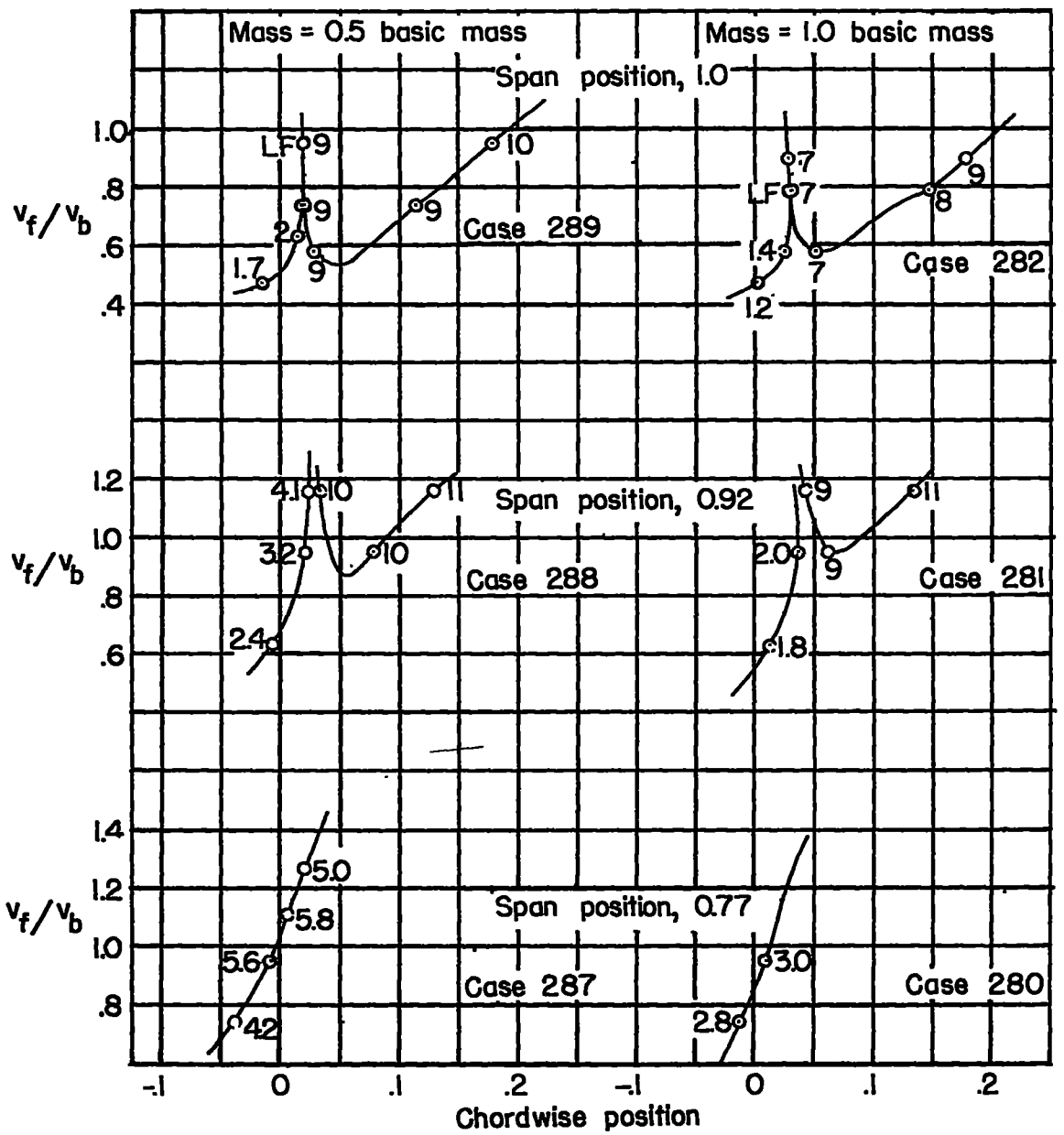

(k) Bomber B; $\Lambda = 30^{\circ}$; antisymmetric. LF, low frequency.

Figure 18.- Continued.

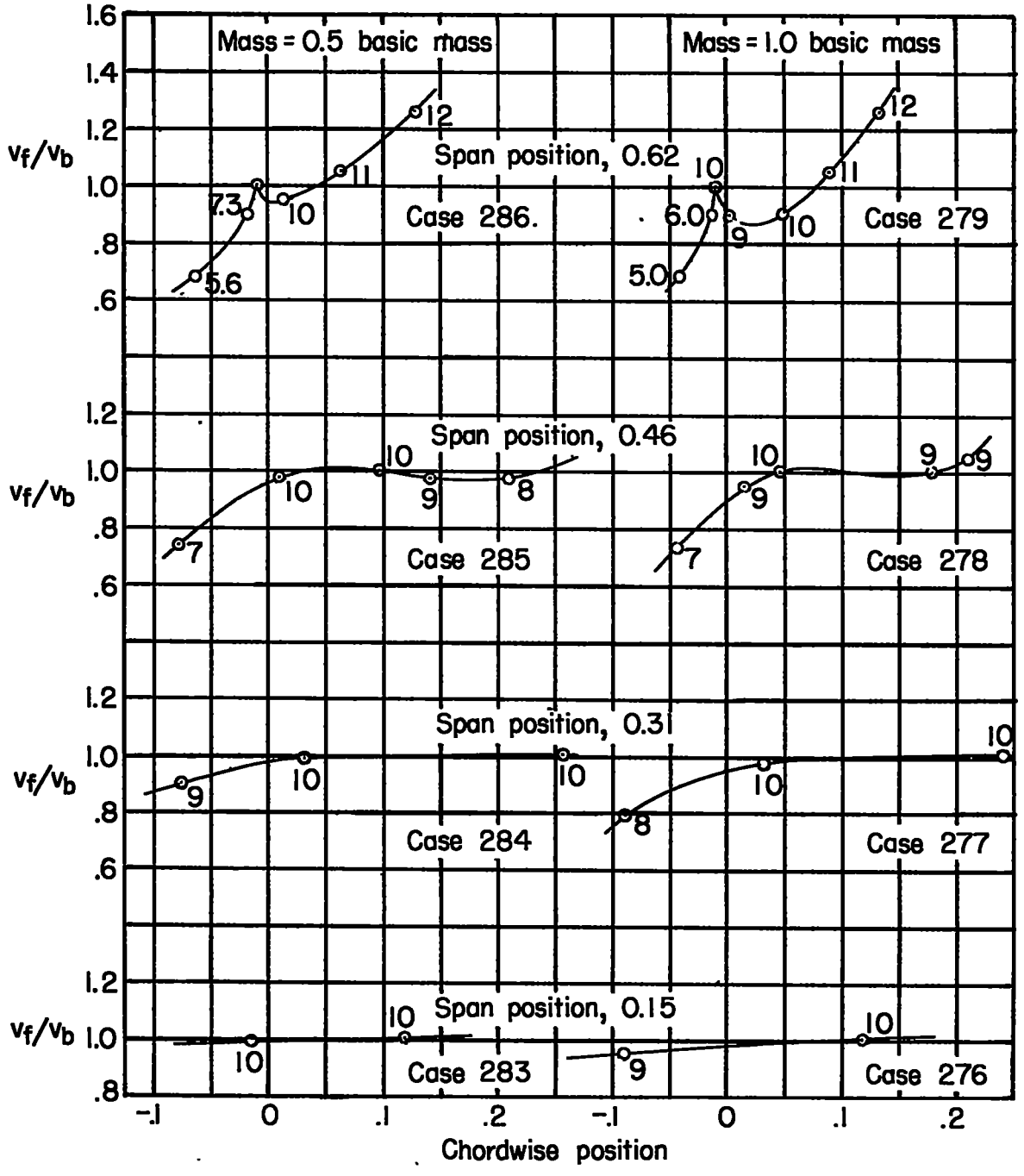

(k) Concluded.

Figure 18.- Concluded.

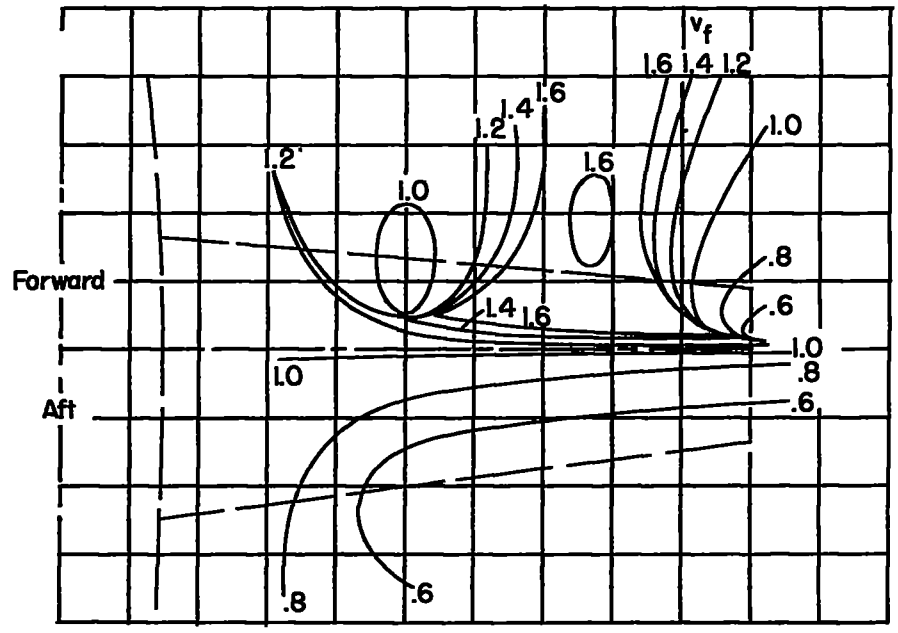

(a) Fighter A; $\Lambda = 0^\circ$; symmetric; radius of gyration, 6 inches; $1.0v_f$ = 989 miles per hour.

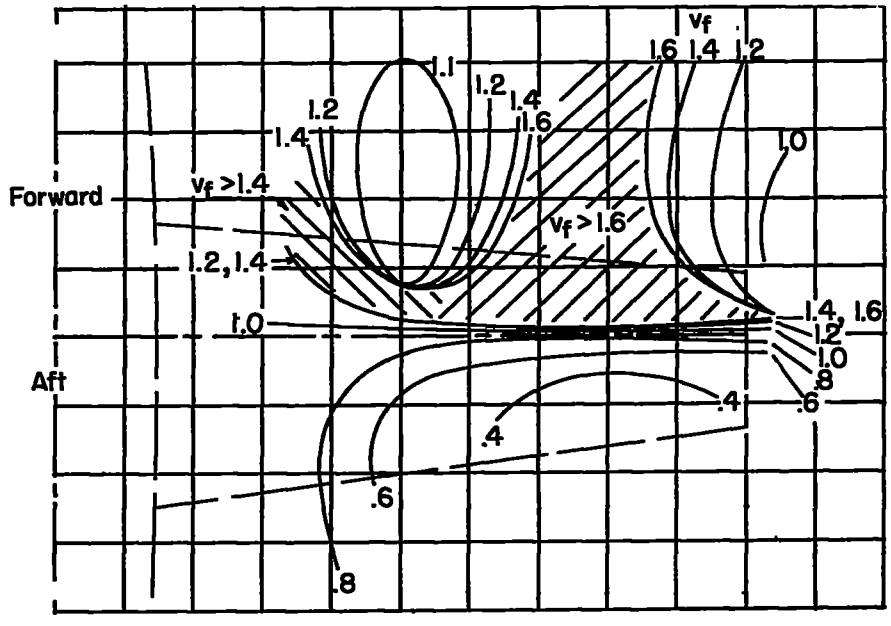

(b) Fighter A; $\Lambda = 0^\circ$; symmetric; radius of gyration, 30 inches; $1.0v_f$ = 989 miles per hour.

Figure 19.- Contours of constant flutter speed with concentrated mass.

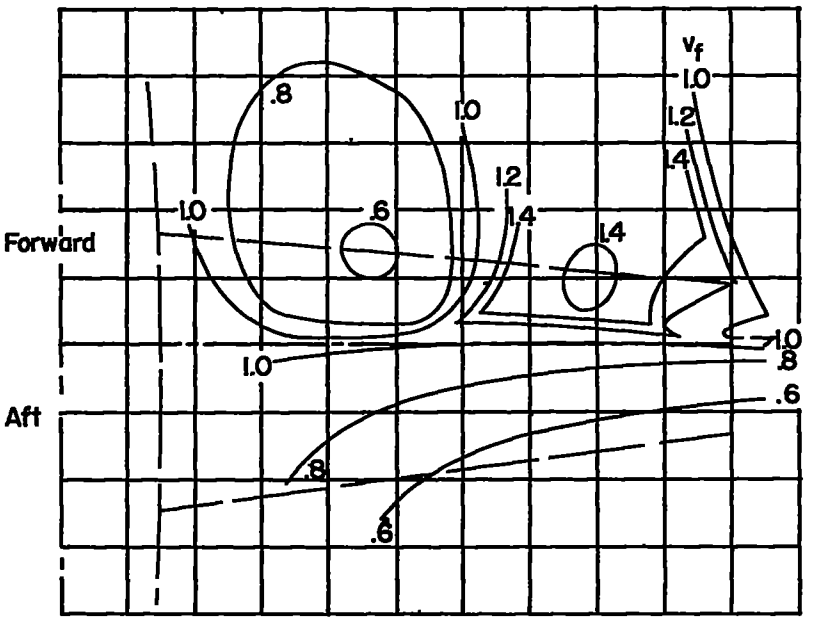

(c) Fighter A; $\Lambda = 0^{\circ}$; antisymmetric; radius of gyration, 6 inches; $1.0v_f$ = 1,091 miles per hour.

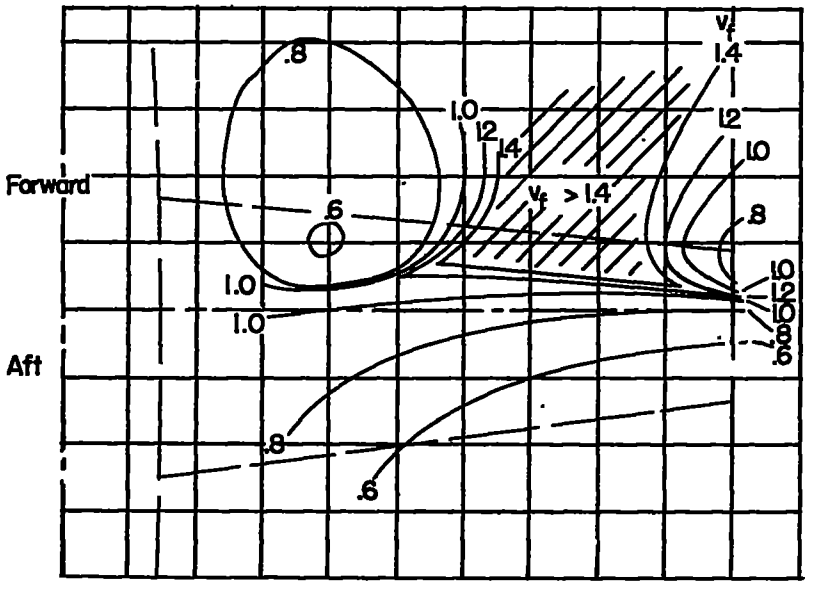

(d) Fighter A; $\Lambda = 0^{\circ}$; antisymmetric; radius of gyration, 30 inches; $1.0v_f$ = 1,091 miles per hour.

Figure 19.- Continued.

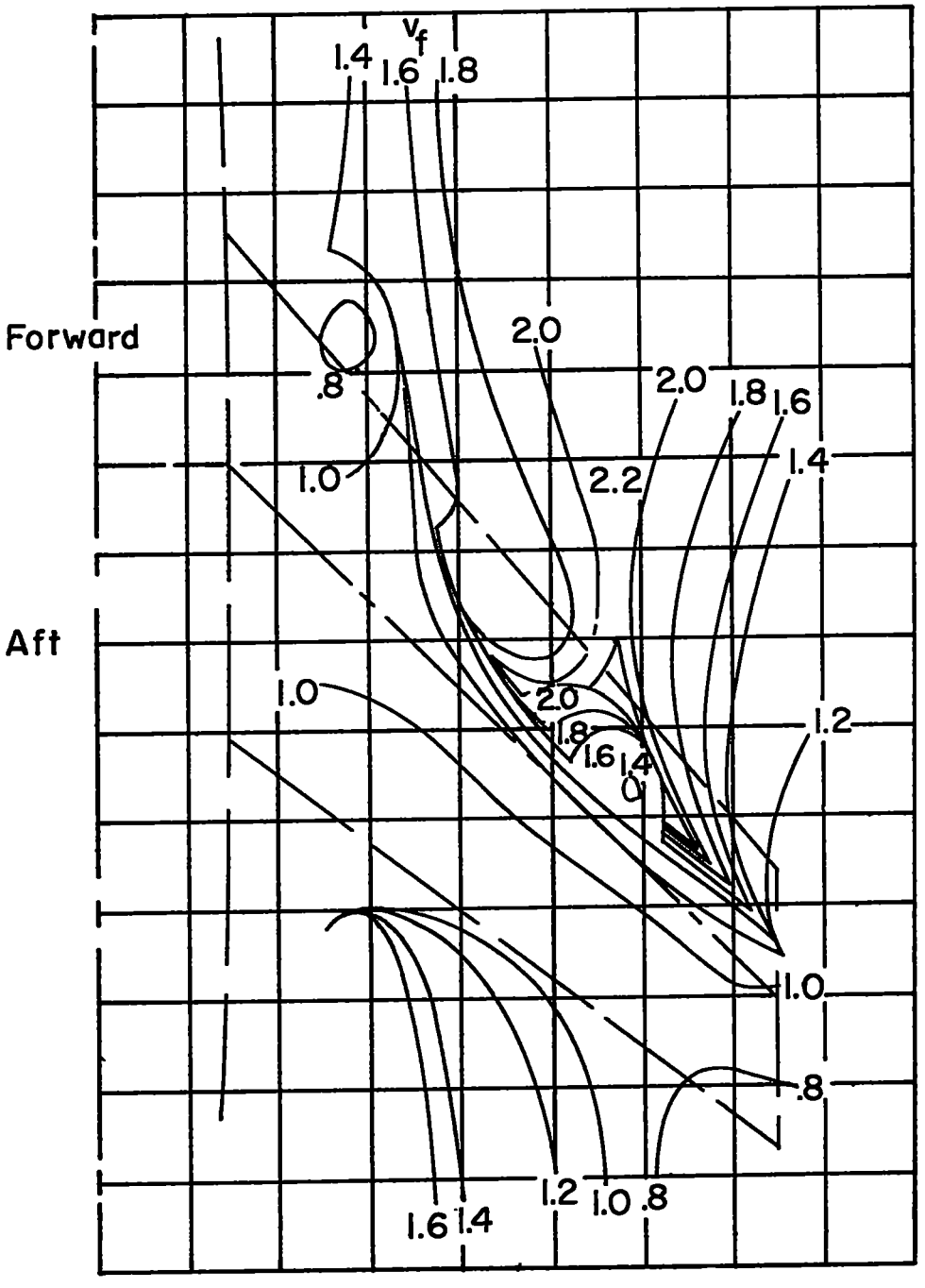

(e) Fighter A; $\Lambda = 45^\circ$; symmetric; radius of gyration, 6 inches; $1.0v_f$ = 1,028 miles per hour.

Figure 19.- Continued.

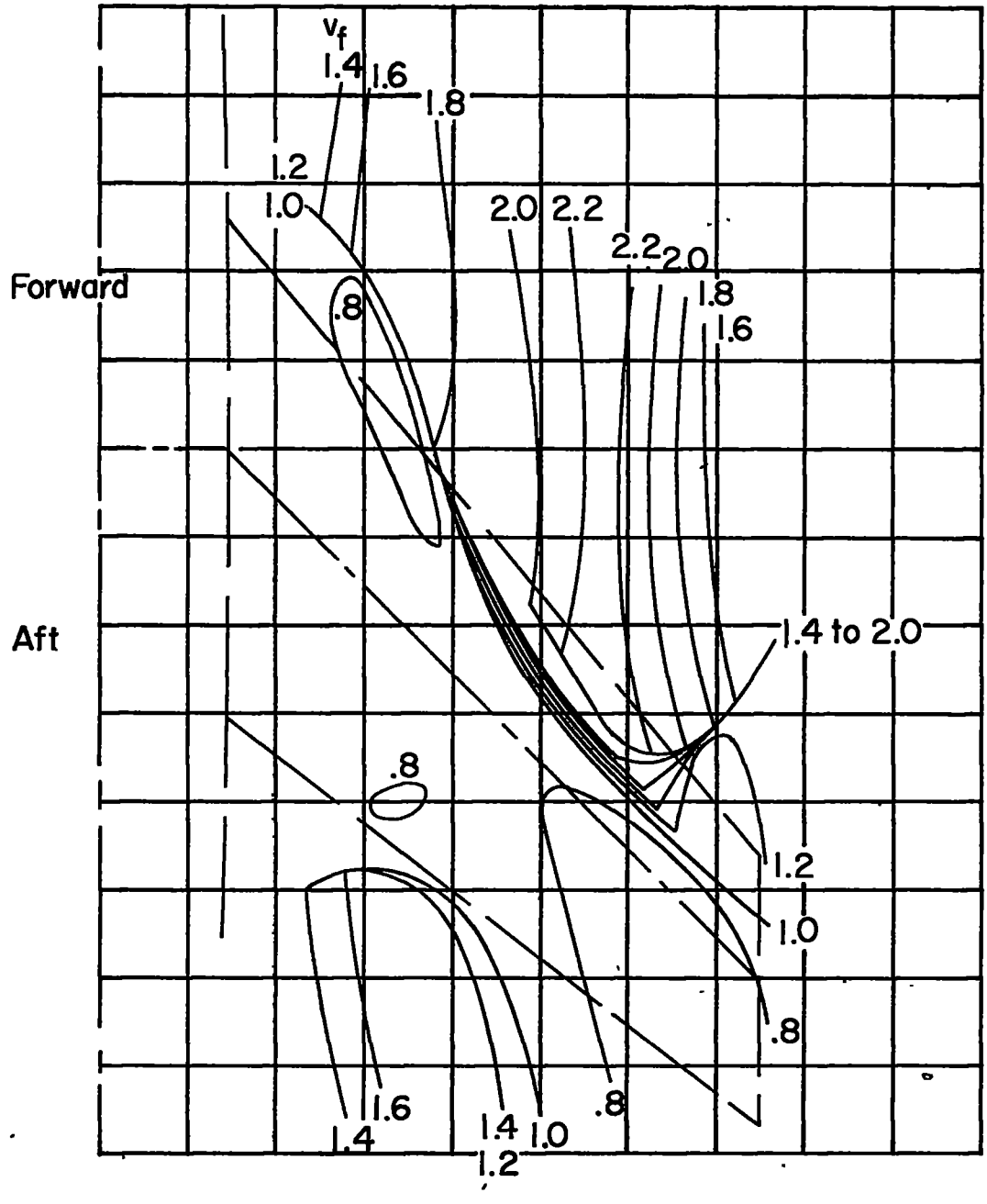

(f) Fighter A; $\Lambda = 45^{\circ}$; symmetric; radius of gyration, 30 inches; $1.0V_f$ = 1,028 miles per hour.

Figure 19.- Continued.

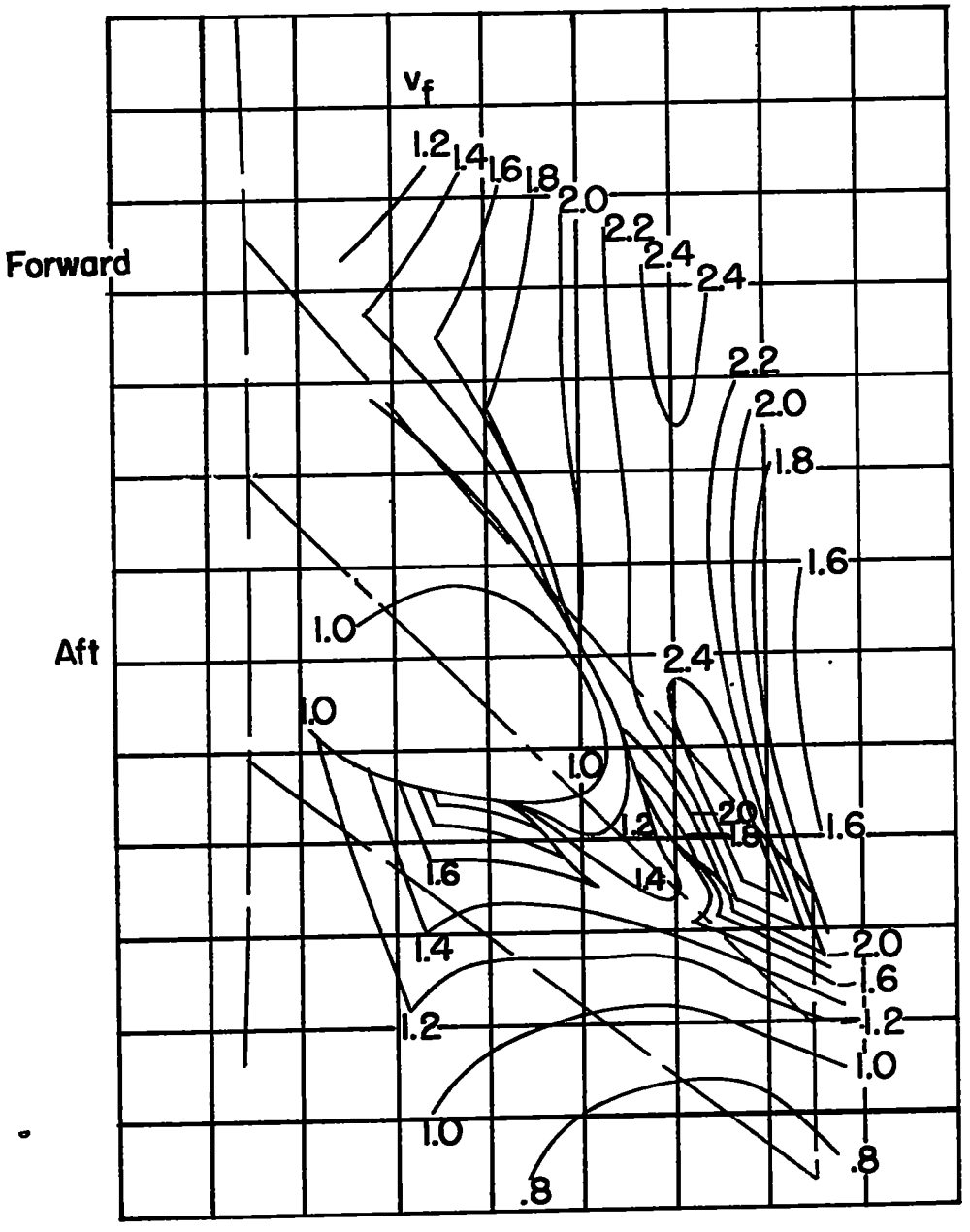

(g) Fighter A; $\Lambda = 45°$; antisymmetric; radius of gyration, 6 inches; $1.0v_f$ = 881 miles per hour.

Figure 19.- Continued.

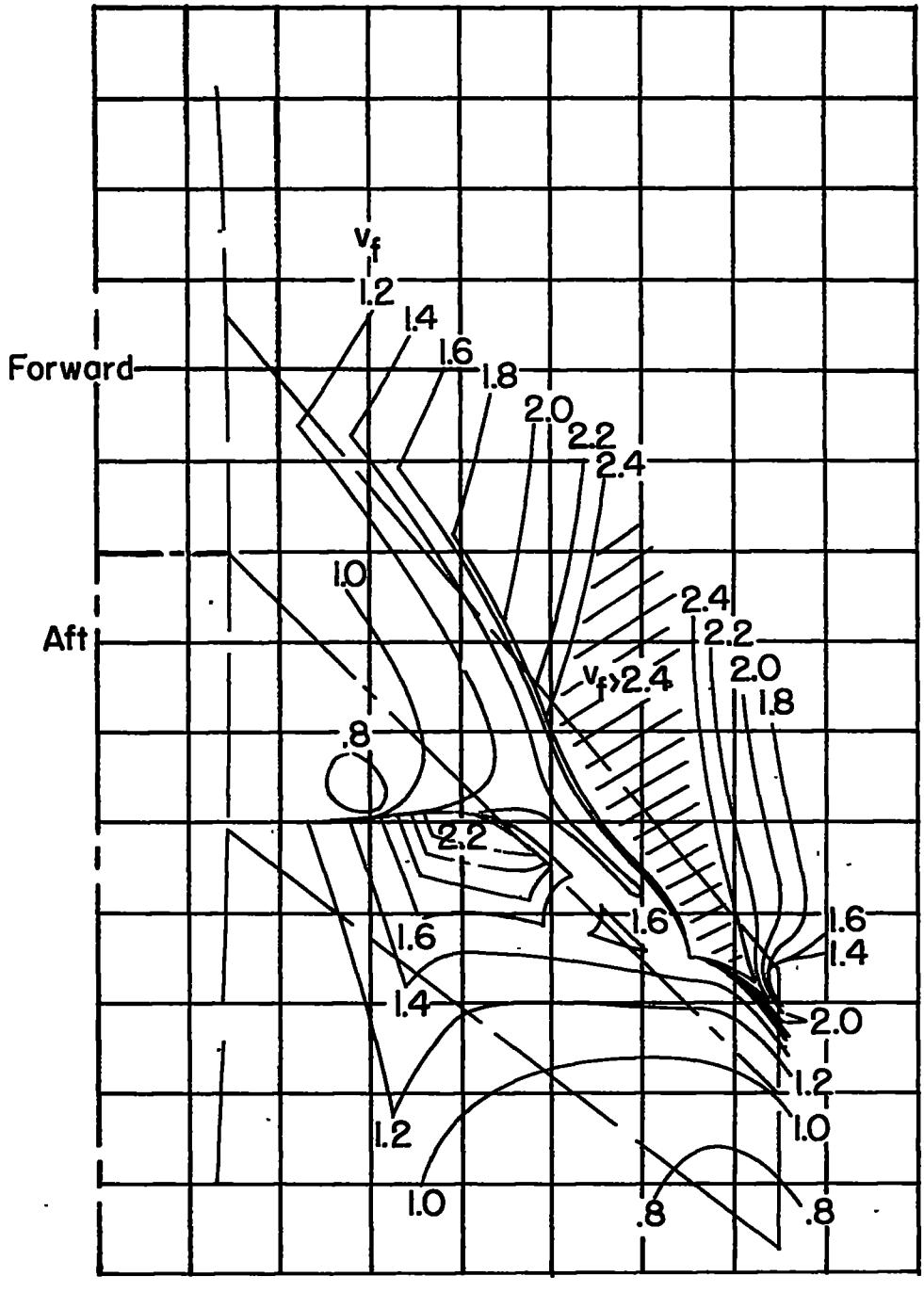

(h) Fighter A; $\Lambda = 45^\circ$; antisymmetric; radius of gyration, 30 inches; $1.0v_f$ = 881 miles per hour.

Figure 19.- Continued.

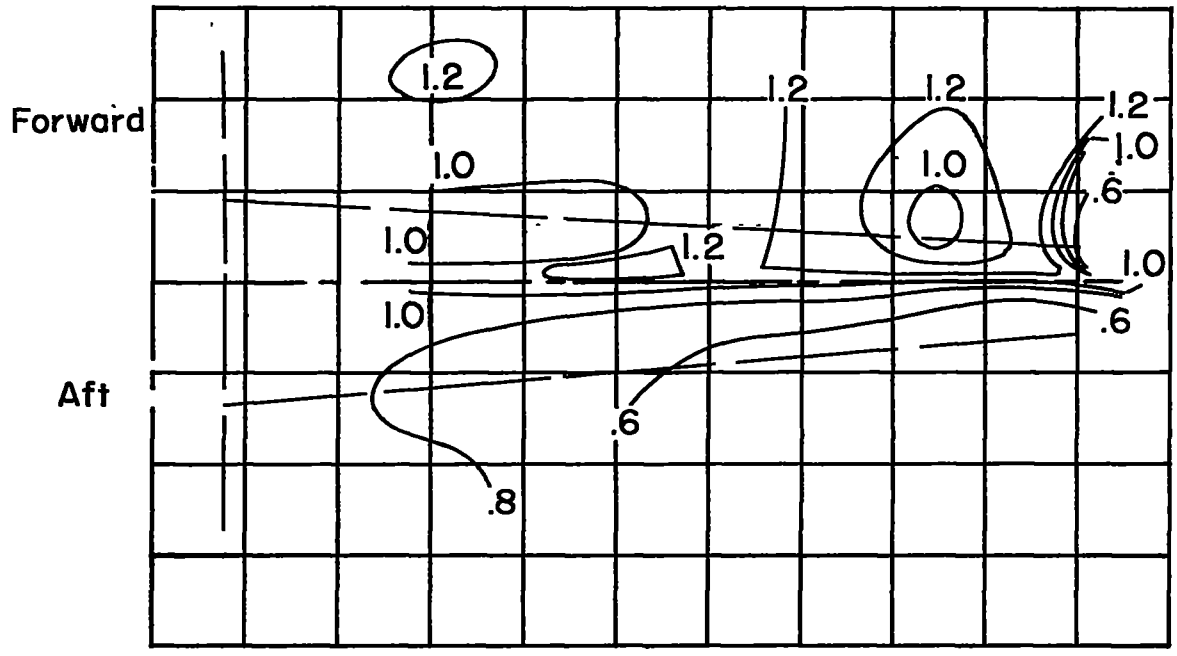

(i) Bomber A; symmetric; $1.0v_f$ = 818 miles per hour.

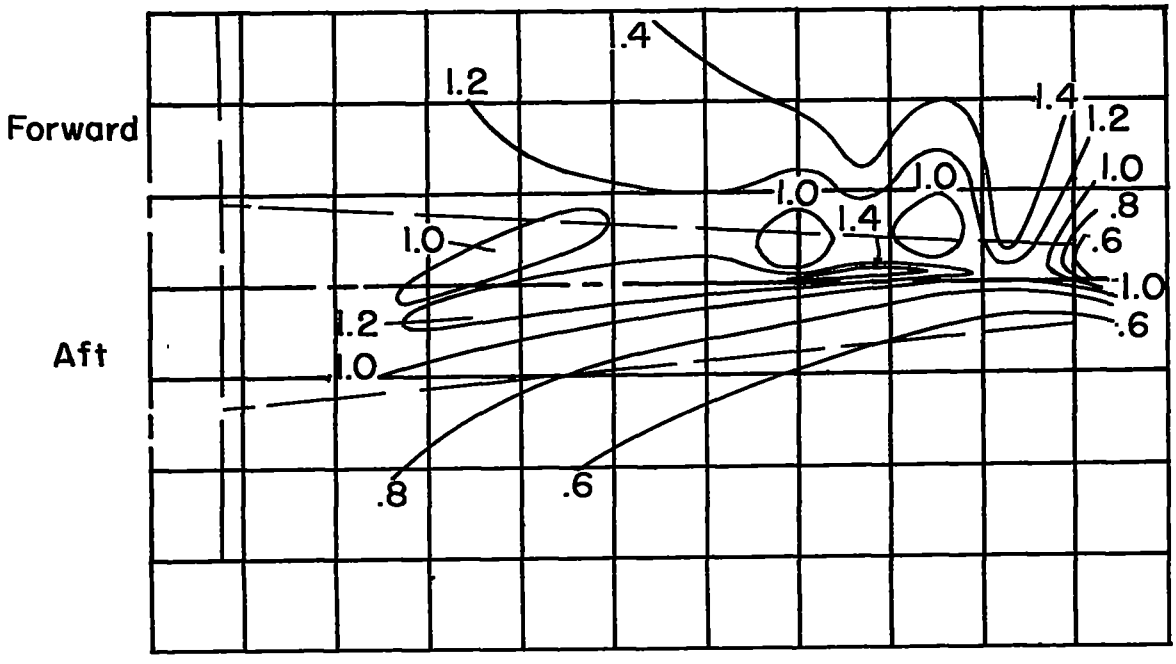

(j) Bomber A; antisymmetric; $1.0v_f$ = 886 miles per hour.

Figure 19.- Continued.

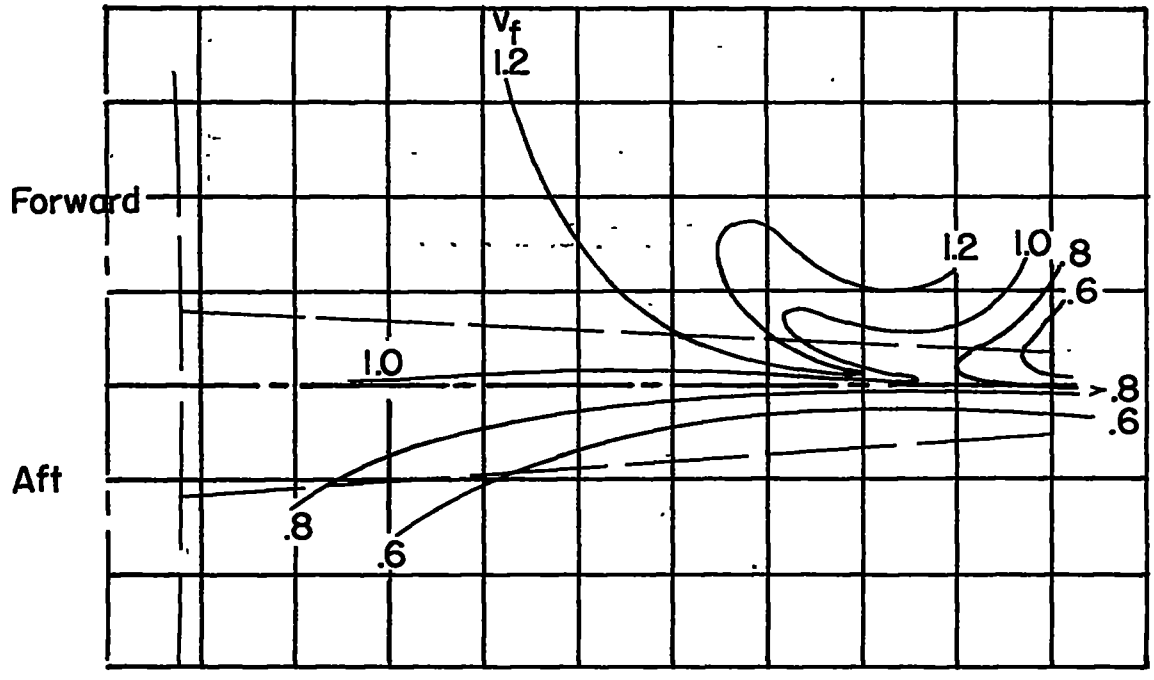

(k) Bomber B; symmetric; $1.0v_f$ = 1,216 miles per hour.

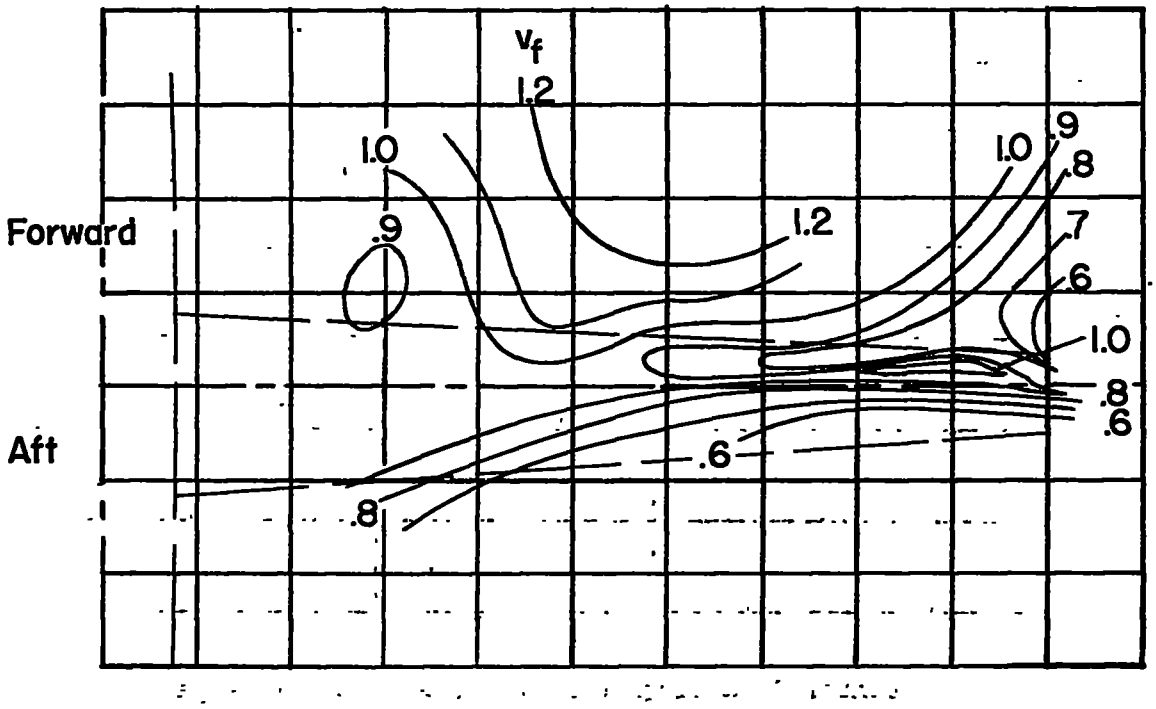

(l) Bomber B; antisymmetric; $1.0v_f$ = 1,216 miles per hour.

Figure 19.- Continued.

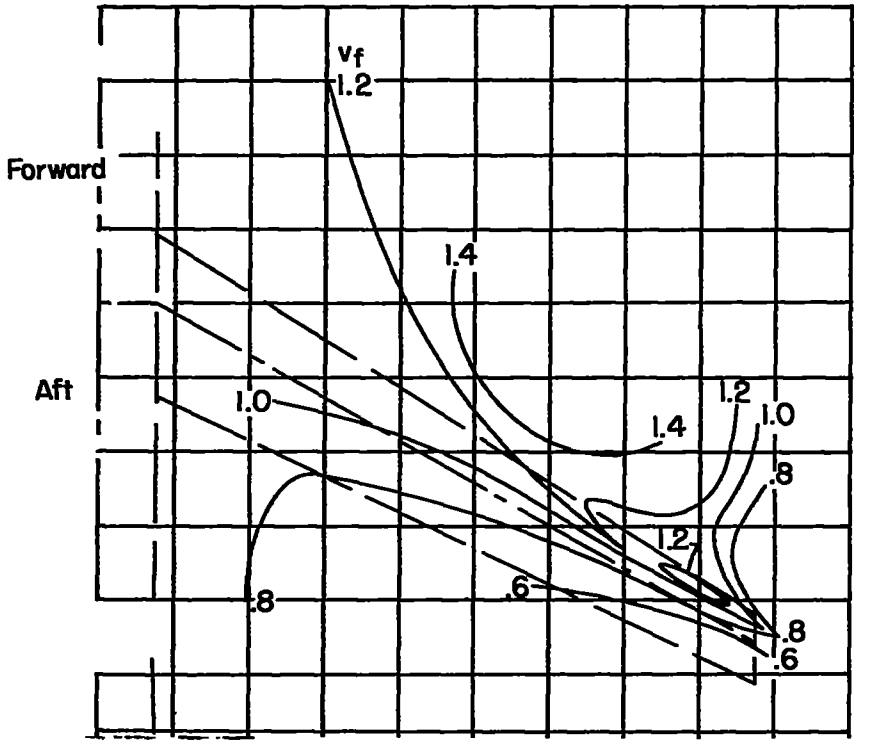

(m) Bomber B; symmetric; $1.0v_f$ = 1,165 miles per hour.

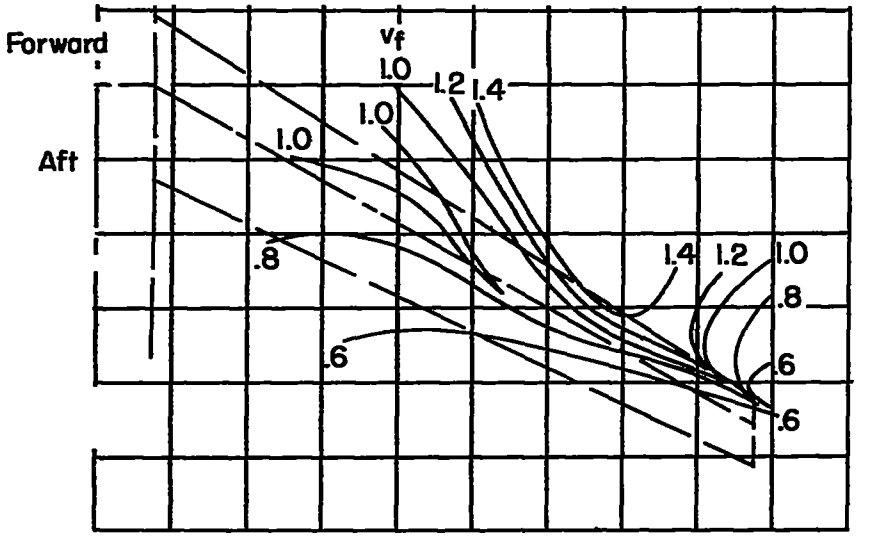

(n) Bomber B; antisymmetric; $1.0v_f$ = 1,244 miles per hour.

Figure 19.- Concluded.

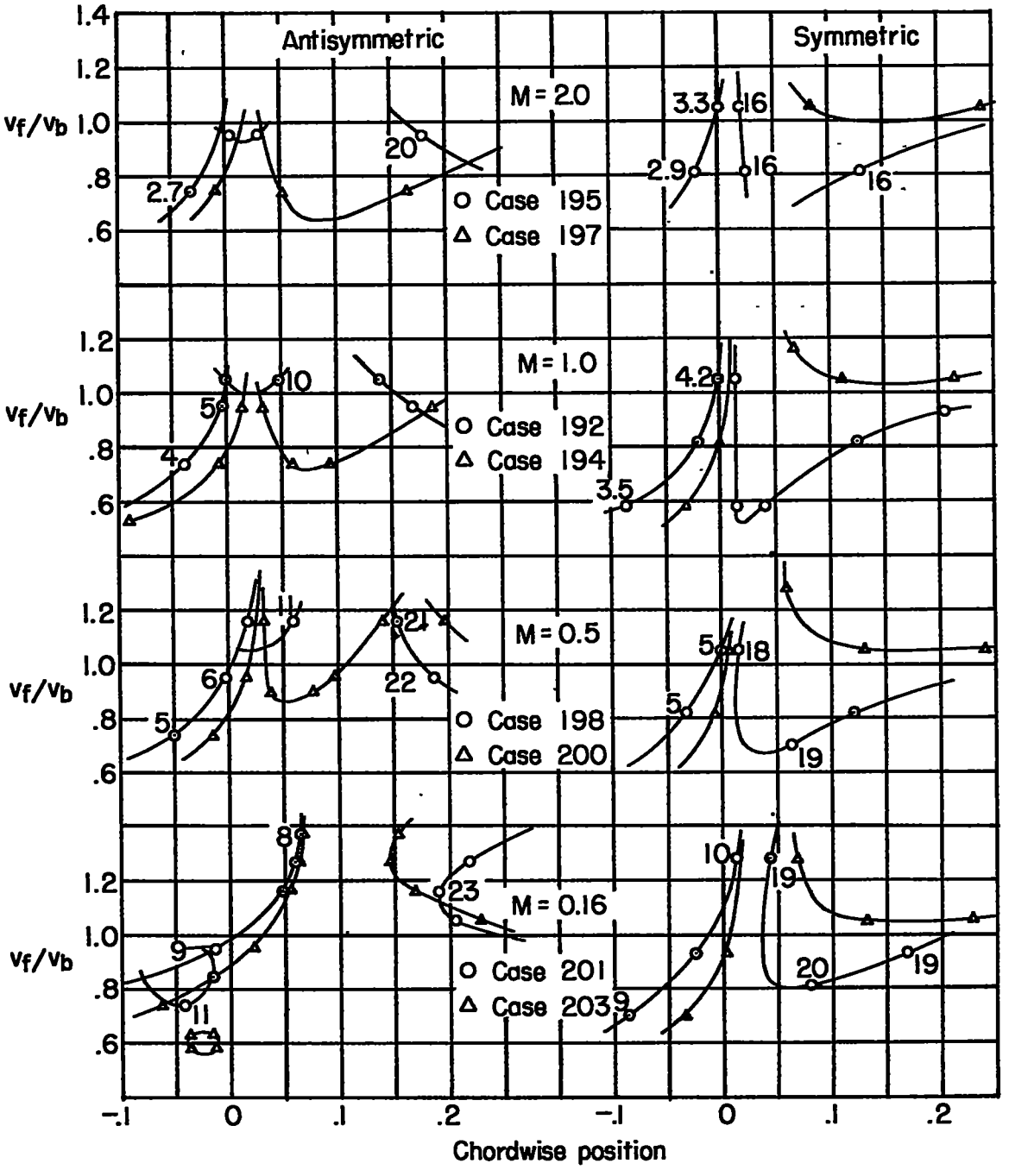

(a) Concentrated mass at tip.

Figure 20.- Effect of size of concentrated mass on flutter characteristics, Fighter A, $\Lambda = 0^{\circ}$.

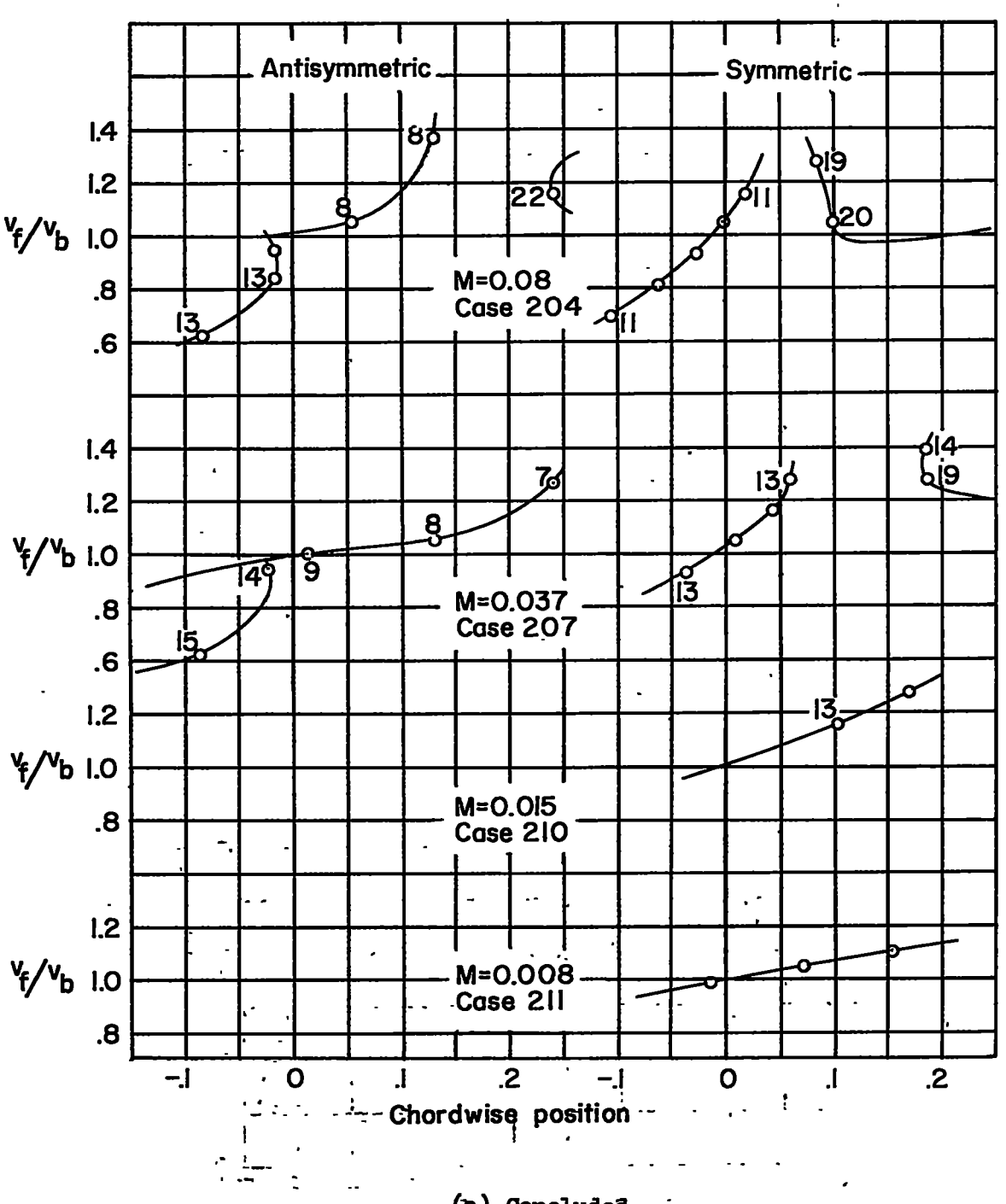

(a) Concluded.

Figure 20.- Continued.

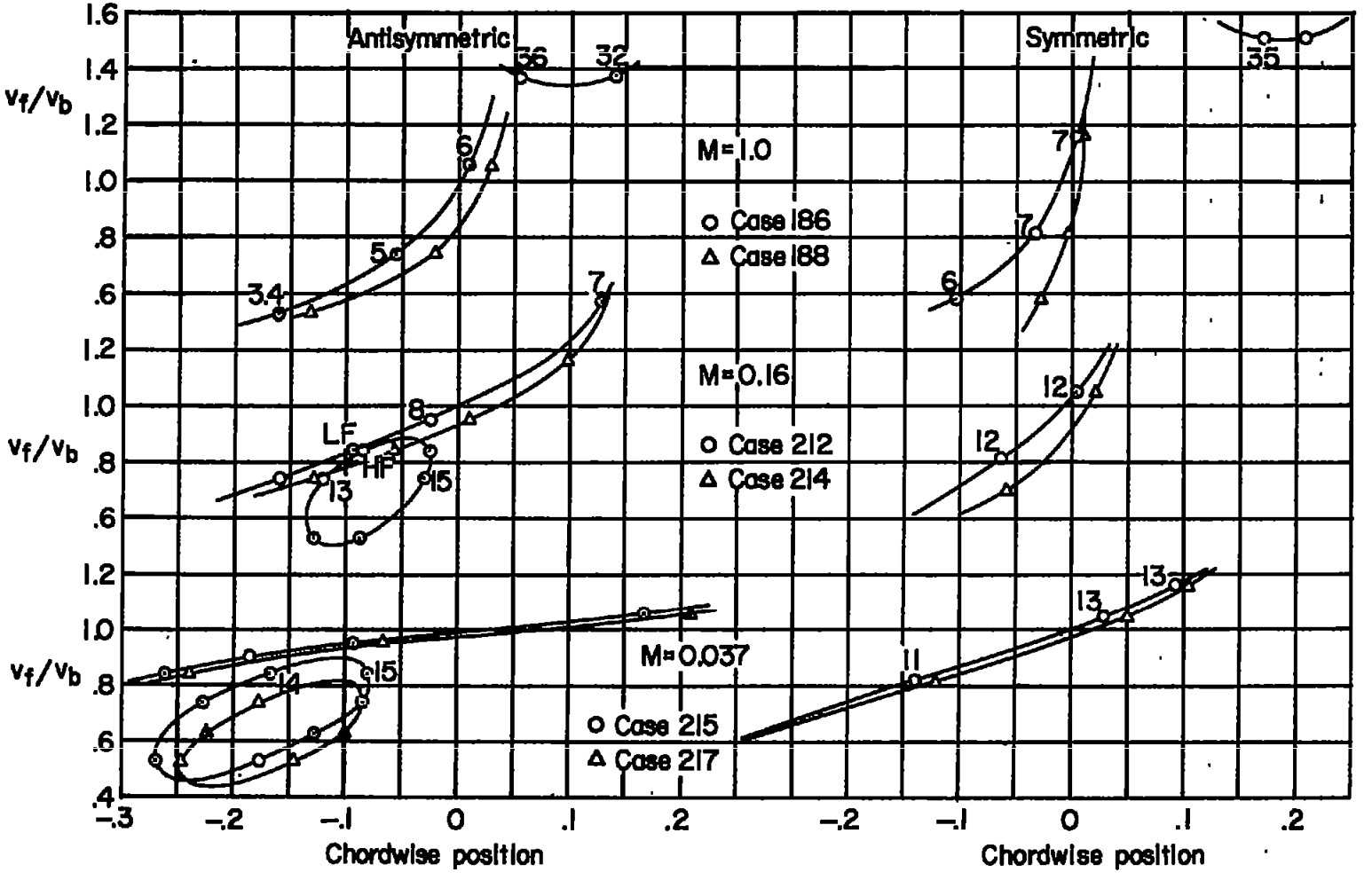

(b) Concentrated mass at 0.79-span position.

Figure 20.- Concluded.

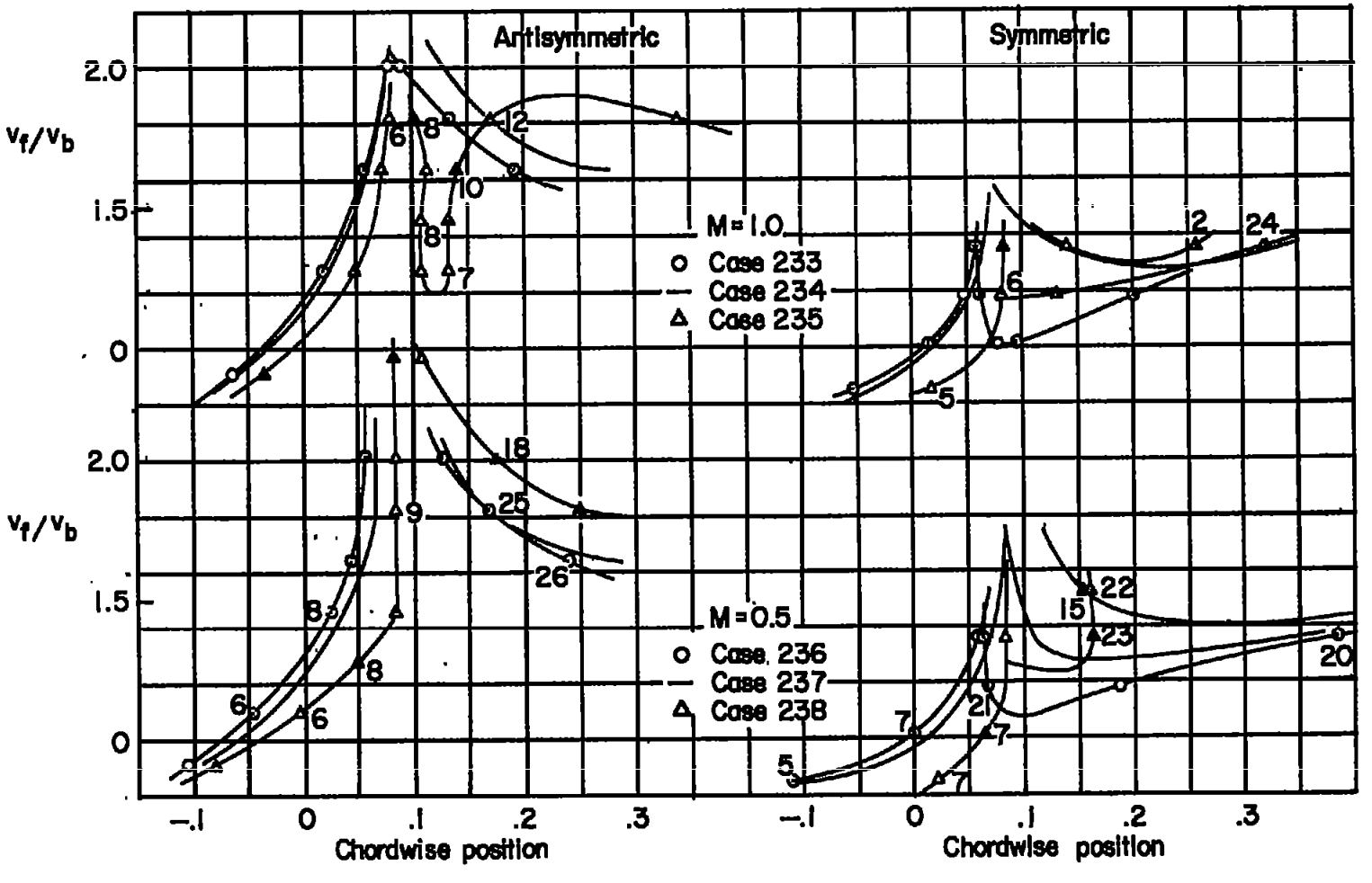

(a) Basic mass and 0.5 basic mass at tip.

Figure 21.- Comparison of characteristics for basic mass and 0.5 basic mass. Fighter A, $\Lambda = 45°$.

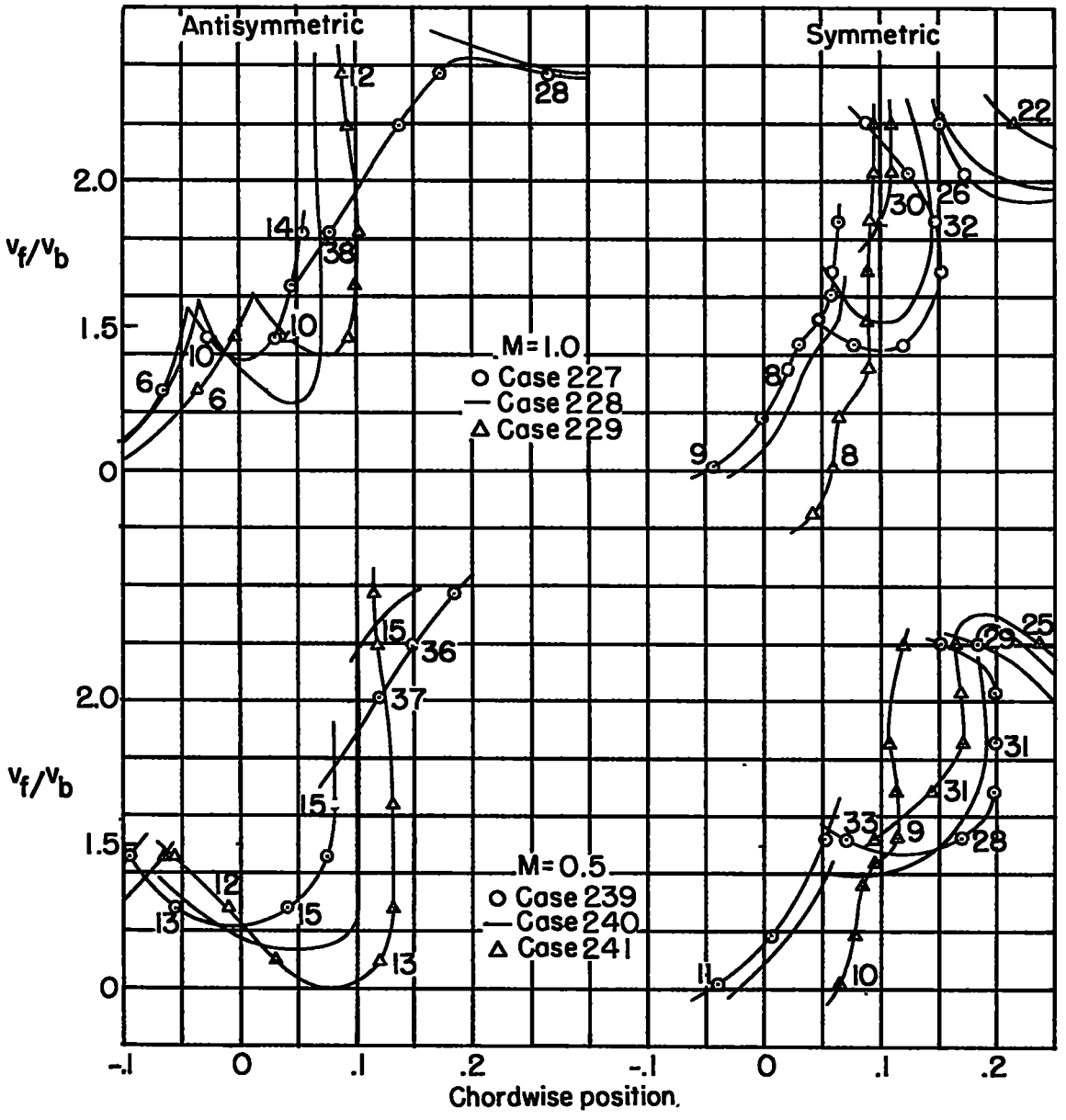

(b) Basic mass and 0.5 basic mass at 0.79-span position.

Figure 21.- Concluded.

NACA - Langley Field, Va.